

THE UNIVERSITY OF CALGARY

Adaptation of the Muscularis Propria to
Massive Intestinal Resection

by

Beth Colleen Chin

A DISSERTATION

SUBMITTED TO THE FACULTY OF GRADUATE STUDIES
IN PARTIAL FULFILMENT OF THE REQUIREMENTS FOR THE
DEGREE OF DOCTOR OF PHILOSOPHY

DEPARTMENT OF GASTROINTESTINAL SCIENCES

CALGARY, ALBERTA

FEBRUARY, 1996

© Beth Colleen Chin 1996

"Great Effects Come of Industry and Perseverance"

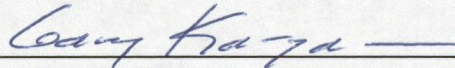
- attributed to Francis Bacon

THE UNIVERSITY OF CALGARY
FACULTY OF GRADUATE STUDIES

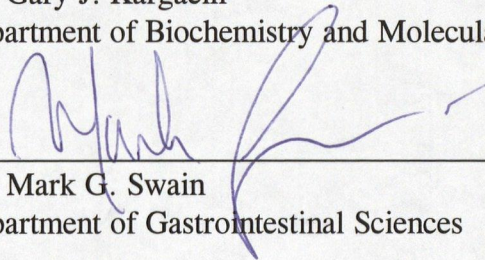
The undersigned certify that they have read, and recommend to the Faculty of Graduate Studies for acceptance, a dissertation entitled "Adaptation of the Muscularis Propria to Massive Intestinal Resection" submitted by Beth Colleen Chin in partial fulfilment of the requirements for the degree of Doctor of Philosophy.



Supervisor, Dr. R. Brent Scott
Department of Gastrointestinal Sciences



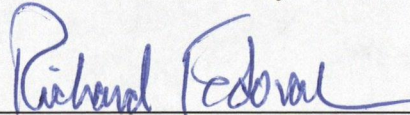
Dr. Gary J. Kargacin
Department of Biochemistry and Molecular Biology



Dr. Mark G. Swain
Department of Gastrointestinal Sciences



Dr. Michael P. Walsh
Department of Biochemistry and Molecular Biology



Dr. Richard N. Fedorak
Department of Medicine
University of Alberta

FEB 27, 1996

Date

ABSTRACT

Massive intestinal resection (removal of $> 1/3$ the total bowel length) commonly complicates management of a variety of clinical conditions. To date, the potential for adaptation of the muscularis propria of the remnant bowel has not been considered. To address this question, surgical removal of 75% of the small intestine of the rat was compared to the sham-operation of transection and anastomosis (no bowel removed).

The model was characterized with respect to food intake, weight gain, gross morphological and histological alterations of the smooth muscle layer, as well as basal and active contractility of the circular and longitudinal muscle layers. Contractile stimuli included bethanechol, serotonin, KCl, and electrical field stimulation. To explore the mechanism of altered contractility, experiments involving blockade of extracellular calcium flux were conducted and receptor binding assays performed. To assess the functional consequence of altered *in vitro* contractility, gastrointestinal transit studies were conducted.

Resection was associated with a significant increase in food intake, but no change in the rate of weight gain. Intestinal circumference increased concurrent with hyperplasia of the muscularis propria. Basal stress in circular and longitudinal muscle was unaffected by resection. In longitudinal muscle, active tonic stress induced by bethanechol or KCl was unchanged, while phasic activity was significantly increased. In circular muscle, bethanechol-stimulated active tonic stress and phasic activity were significantly reduced, while contractile responses to serotonin, KCl and electrical field stimulation were unaffected or enhanced by resection. With extracellular calcium entry excluded,

contractile responses were similar between treatment groups. Resection significantly increased muscarinic receptor density (B_{max}) but did not alter affinity (K_d). Gastric emptying was unchanged but the velocity of intestinal transit was significantly reduced post-resection.

In conclusion, the muscularis propria of the remnant bowel after massive intestinal resection adapts by increasing circumference and mass, due to hyperplasia. The circular muscle layer exhibits depressed contractile responses to bethanechol stimulation despite an increase in muscarinic receptor density. While circular and longitudinal muscle layers have independent responses *in vitro*, the co-ordinated outcome *in vivo* is a reduction in velocity of intestinal transit, an adaptation known to enhance nutrient absorption.

ACKNOWLEDGEMENTS

I would like to thank my supervisor, Dr. R. Brent Scott, for his intellectual guidance, encouragement and unwavering support throughout my doctoral studies. I am also greatly appreciative of his efforts spent in the critical reading of this dissertation. To the other members of my supervisory committee, Dr. Mark G. Swain, Dr. Norman C.W. Wong and Dr. Michael P. Walsh, I would like to extend my sincerest gratitude for their time, efforts and invaluable tutelage.

I would also like to acknowledge the advice, support and efforts of Quyen Lam and Daimen T.M. Tan.

Studentships from the Medical Research Council of Canada, and the Alberta Heritage Foundation for Medical Research are gratefully acknowledged.

DEDICATION

TO MY FAMILY

for their love, understanding support and never-ending patience

John L. Wallace

Alexandra E. Wallace

M. Evelyn Wallace

Rita I. Chin

TABLE OF CONTENTS

TITLE PAGE	i
APPROVAL PAGE	ii
ABSTRACT	iii
ACKNOWLEDGEMENTS	v
DEDICATION	vi
TABLE OF CONTENTS	vii
LIST OF FIGURES	xvii
LIST OF TABLES	xx
LIST OF ABBREVIATIONS	xxi
 CHAPTER ONE: INTRODUCTION AND LITERATURE REVIEW.....	1
1.1. The intestine.....	2
1.2. Contractions and motor patterns of the small intestine	2
1.2.1. Fasting pattern	5
1.2.2. Fed pattern.....	6
1.3. Control of smooth muscle motor function	7
1.3.1. Neurogenic control	7
1.3.2. Hormonal control.....	9
1.3.3. Smooth muscle control	11
1.4. Intestinal transit and absorption.....	12
1.5. Massive intestinal resection.....	14

1.5.1. Clinical aspects.....	14
1.5.2. Short bowel syndrome.....	15
1.6. Adaptation of smooth muscle.....	16
1.7. Potential mechanisms	19
1.8. Specifics of the model	23
1.8.1. Extent and location of resection.....	23
1.8.2. Choice of tissue for study	24
1.8.3. Analysis of longitudinal and circular muscle layers.....	25
 CHAPTER TWO: HYPOTHESES AND EXPERIMENTAL APPROACHES.....	 27
 CHAPTER THREE: MATERIALS AND METHODS.....	 30
3.1. Materials	31
3.1.1. Chemical reagents and isotopes.....	31
3.1.2. Equipment.....	32
3.2. Animal model	32
3.2.1. Animals.....	32
3.2.2. Surgery	33
3.3. Characterization of the model.....	36
3.3.1. Body weight and food intake	36
3.3.2. Intestinal length and jejunal circumference	36
3.3.3. Tissue wet weight, total protein and DNA content.....	38

3.3.4. Histological measurements.....	39
3.4. Longitudinal muscle contractility	40
3.4.1. Experimental design.....	40
3.4.2. Basal stress in response to stretch	41
3.4.3. Length-active stress response and determination of optimal length	41
3.4.4. Concentration-response to bethanechol.....	42
3.4.5. Concentration-response to KCl.....	42
3.4.6. Normalization of contractile responses	44
3.5. Circular muscle contractility	45
3.5.1. Experimental design.....	45
3.5.2. Basal stress in response to stretch	46
3.5.3. Length-active stress response and determination of optimal length	46
3.5.4. Concentration-response to bethanechol.....	46
3.5.5. Concentration-response to serotonin	47
3.5.6. Concentration-response to KCl.....	48
3.5.7. Electrical field stimulation	48
3.5.8. Normalization of contractile responses	49
3.6. Gastrointestinal transit.....	49
3.7. Contractile protein immunoassays.....	51
3.7.1. Experimental design.....	51

3.7.2. Tissue preparation.....	52
3.7.3. Protein assay.....	53
3.7.4. Immunoassays.....	54
3.8. Extracellular calcium	55
3.9. Muscarinic receptors.....	56
3.9.1. Smooth muscle cell isolation	56
3.9.2. ³ H-QNB binding assay.....	57
3.10. Statistical analyses	58
 CHAPTER FOUR: RESULTS I - CHARACTERIZATION OF THE MODEL	 59
4.1. Body weight and food intake	60
4.2. Intestinal adaptation.....	64
4.2.1. Intestinal length, circumference and wet weight.....	64
4.2.2. Histological assessment.....	69
4.2.3. Biochemical assessment	69
4.3. Summary of morphological studies	77
 CHAPTER FIVE: RESULTS II - LONGITUDINAL SMOOTH MUSCLE	
CONTRACTILITY	78
5.1. Morphological adaptation	79
5.2. Length-basal stress response.....	81
5.3. Active tonic contractile responses	84

5.3.1. Length-active stress response and optimal length.....	84
5.3.2. Concentration-tonic stress response to bethanechol	84
5.3.3. Concentration-tonic stress response to KCl.....	90
5.4. Active phasic contractile activity	93
5.4.1. Basal and bethanechol-stimulated phasic frequency	93
5.4.2. Basal and bethanechol-stimulated phasic amplitude	93
5.4.3. Tetrodotoxin and phasic contractility	97
5.5. Summary of longitudinal muscle contractility.....	100

CHAPTER SIX: RESULTS III - CIRCULAR SMOOTH MUSCLE

CONTRACTILITY	101
6.1. Morphological adaptation.....	102
6.2. Length-basal stress response.....	102
6.3. Active tonic contractile response	107
6.3.1. Length-active stress response and optimal length.....	107
6.3.2. Concentration-tonic stress response to bethanechol	107
6.3.3. Concentration-tonic stress response to serotonin	111
6.3.4. Concentration-tonic stress response to KCl.....	111
6.3.5. Electrical field stimulation and tonic stress	111
6.3.6. Tetrodotoxin, bethanechol and tonic stress	115
6.4. Active phasic contractile activity	118
6.4.1. Basal and bethanechol-stimulated phasic frequency	118

6.4.2. Basal and bethanechol-stimulated phasic amplitude	118
6.4.3. Serotonin-stimulated phasic amplitude	118
6.4.4. Electrical field stimulation and phasic amplitude	124
6.4.5. Tetrodotoxin, bethanechol and phasic contractility	124
6.5. Summary of circular muscle contractility	131
 CHAPTER SEVEN: RESULTS IV - GASTROINTESTINAL TRANSIT.....	132
7.1. Fasted transit	133
7.2. Fed transit.....	133
7.3 Summary of the effect of resection on gastrointestinal transit.....	139
 CHAPTER EIGHT: RESULTS V - STRATEGIES TO EXPLORE	
MECHANISM	140
8.1. Relevance of contractile protein function	141
8.1.1. Contractile protein immunoassay	142
8.2. Influence of extracellular calcium	145
8.2.1. Extracellular calcium and bethanechol-stimulated tonic stress	145
8.2.2. Extracellular calcium and EF-stimulated tonic stress	149
8.2.3. Extracellular calcium and bethanechol-stimulated phasic amplitude	151

8.2.4. Extracellular calcium and EF-stimulated phasic amplitude	151
8.3. Muscarinic cholinergic receptors	155
8.4. Summary of excluded potential mechanisms	158
 CHAPTER NINE: DISCUSSION.....	159
9.1. Morphological alterations of the residual bowel following massive intestinal resection	160
9.1.1. Intestinal length, circumference and wet weight.....	160
9.1.2. Hypertrophy versus hyperplasia	161
9.1.3. Model design for subsequent studies.....	162
9.2. Longitudinal muscle contractility.....	163
9.2.1. Basal stress in response to stretch	163
9.2.2. Changes in contractility are distinct from circular muscle	163
9.2.3. Functional relevance	165
9.3. Circular muscle contractility	166
9.3.1. Basal stress in response to stretch	166
9.3.2. Functional relevance of depressed contractility in response to bethanechol	167
9.3.3. Source of the altered stress response.....	168
9.3.4. Source of the alterations in phasic contractility	169
9.3.5. Relevance of the stress response to serotonin	170

9.4. Potential mechanisms of adaptation	171
9.4.1. Contractile machinery of smooth muscle.....	171
9.4.2. Extracellular calcium and stress	172
9.4.3. Extracellular calcium and phasic amplitude	173
9.4.4. Interpretation of binding studies	174
9.5. Alterations <i>in vivo</i> - gastrointestinal transit.....	176
9.6. Summary and conclusions	177
 CHAPTER TEN: FUTURE PERSPECTIVES	180
 CHAPTER ELEVEN: BIBLIOGRAPHY	185
 CHAPTER TWELVE: APPENDICES	197
 Appendix I. The effect of time on the phasic frequency of bethanechol-stimulated longitudinal muscle from the sham-operated group	198
 Appendix II. The effect of time on the phasic frequency of bethanechol-stimulated longitudinal muscle from the resected group	199

Appendix III.	The effect of time on the phasic amplitude of bethanechol-stimulated longitudinal muscle from the sham-operated group.....	200
Appendix IV.	The effect of time on the phasic amplitude of bethanechol-stimulated longitudinal muscle from the resected group.....	201
Appendix V.	The effect of time on the tonic stress response of bethanechol-stimulated circular muscle from the sham-operated group.....	202
Appendix VI.	The effect of time on the tonic stress response of bethanechol-stimulated circular muscle from the resected group.....	203
Appendix VII.	The effect of time on the phasic frequency of bethanechol-stimulated circular muscle from the sham-operated group.....	204
Appendix VIII.	The effect of time on the phasic frequency of bethanechol-stimulated circular muscle from the resected group.....	205
Appendix IX.	The effect of time on the phasic amplitude of bethanechol-stimulated circular muscle from the sham-operated group.....	206

Appendix X. The effect of time on the phasic amplitude of bethanechol-stimulated circular muscle from the resected group	207
Appendix XI. Manuscripts.....	208

LIST OF FIGURES

CHAPTER THREE

Figure 3.1. Outline of surgical protocol	35
Figure 3.2. Schematic diagram of contractile parameters.....	43

CHAPTER FOUR

Figure 4.1. Body weight	61
Figure 4.2. Daily food intake	62
Figure 4.3. Jejunal circumference.....	66
Figure 4.4. Wet weight per unit length of full thickness jejunum and muscularis propria alone.....	67
Figure 4.5. Depth of individual muscle layers.....	72
Figure 4.6. Ratio of total protein to DNA content.....	76

CHAPTER FIVE

Figure 5.1. Representative tracings of jejunal longitudinal muscle contractile activity.....	80
Figure 5.2. Length-basal stress response	83
Figure 5.3. Schematic diagram of active tonic stress.....	86
Figure 5.4. Day 10 concentration-tonic stress response to bethanechol.....	87
Figure 5.5. Schematic diagram of phasic frequency and amplitude.....	94

Figure 5.6. Frequency of phasic contractile activity.....	95
Figure 5.7. Amplitude of phasic contractile activity.....	96
Figure 5.8. The effect of tetrodotoxin on phasic contractile frequency	98
Figure 5.9. The effect of tetrodotoxin on phasic contractile amplitude	99

CHAPTER SIX

Figure 6.1. Representative tracings of jejunal circular muscle contractile activity	103
Figure 6.2. Length-basal stress response	106
Figure 6.3. Schematic diagram of active tonic stress.....	109
Figure 6.4. Concentration-tonic stress response to bethanechol.....	110
Figure 6.5. Concentration-tonic stress response to serotonin	112
Figure 6.6. Electrical field stimulation and tonic stress.....	114
Figure 6.7. The effect of tetrodotoxin on the tonic stress response of bethanechol-stimulated circular muscle.....	116
Figure 6.8. Schematic diagram of phasic frequency and amplitude.....	120
Figure 6.9. Frequency of phasic contractile activity.....	121
Figure 6.10. Amplitude of phasic contractile activity	122
Figure 6.11. Serotonin-stimulated contractile amplitude.....	123
Figure 6.12. Electrical field stimulation and phasic amplitude	125
Figure 6.13. The effect of tetrodotoxin on phasic contractile frequency within treatment groups	126

Figure 6.14. The effect of tetrodotoxin on phasic contractile frequency between treatment groups	128
-----------------------------------------------------------------------------------------------------------	-----

Figure 6.15. The effect of tetrodotoxin on phasic contractile amplitude.....	129
------------------------------------------------------------------------------	-----

CHAPTER SEVEN

Figure 7.1. Distribution of ^{51}Cr in fasted rats.....	135
------------------------------------------------------------------	-----

Figure 7.2. Velocity of intestinal transit in fasted rats.....	136
----------------------------------------------------------------	-----

Figure 7.3. Distribution of ^{51}Cr in fed rats.....	137
---------------------------------------------------------------	-----

Figure 7.4. Velocity of intestinal transit in fed rats.....	138
-------------------------------------------------------------	-----

CHAPTER EIGHT

Figure 8.1. Representative standard curve of chicken gizzard actin.....	143
-------------------------------------------------------------------------	-----

Figure 8.2. Representative standard curve of rat abdominal aorta.....	144
-----------------------------------------------------------------------	-----

Figure 8.3. Schematic diagram of active tonic stress and phasic amplitude.....	146
--------------------------------------------------------------------------------	-----

Figure 8.4. Extracellular calcium and bethanechol-stimulated tonic stress.....	147
--------------------------------------------------------------------------------	-----

Figure 8.5. Extracellular calcium and EF-stimulated tonic stress.....	150
-----------------------------------------------------------------------	-----

Figure 8.6. Extracellular calcium and bethanechol-stimulated phasic amplitude.....	152
---------------------------------------------------------------------------------------	-----

Figure 8.7. Extracellular calcium and EF-stimulated phasic amplitude.....	154
---------------------------------------------------------------------------	-----

Figure 8.8. Specific binding of ^3H -QNB.....	156
--------------------------------------------------------	-----

LIST OF TABLES

CHAPTER FOUR

Table 4.1. Total protein and DNA content	74
------------------------------------------------	----

CHAPTER FIVE

Table 5.1. Basal stress "m" parameter values.....	82
Table 5.2. Day 20, 30 and 40 concentration-tonic stress responses to bethanechol.....	88
Table 5.3. Concentration-tonic stress responses to KCl.....	91

CHAPTER SIX

Table 6.1. Basal stress "m" parameter values.....	104
Table 6.2. Concentration-tonic stress response to KCl.....	113

LIST OF ABBREVIATIONS

B_{\max}	receptor density
CCK	cholecystokinin
^{51}Cr	$\text{Na}_2^{51}\text{CrO}_4$
dpm	disintegrations per minute
EC_{50}	half maximal effective concentration
EFS	electrical field stimulation
EDTA	ethylenediaminetetraacetic acid
EGTA	ethyleneglycol-(β -aminoethyl ether)-N, N, N', N'-tetraacetic acid
fmol	femtomoles
h	hour
HEPES	N-2-hydroxyethylpiperazine-N'-2-ethanesulphonic acid
5-HT	5-hydroxytryptamine (serotonin)
^3H -QNB	1-quinuclidinyl[phenyl-4- ^3H]benzilate
L_i	initial length
L_o	optimal length
msec	milliseconds
min	minutes
μm	micrometer

OPD	o-phenylenediamine
PBS	phosphate buffered saline
sec	second
SEM	standard error of the mean
S_m	maximal stress
TCA	trichloroacetic acid
TTX	tetrodotoxin
Tween 20	polyoxyethylene-sorbitan monolaurate
YE	<i>Yersinia enterocolitica</i>

CHAPTER ONE

INTRODUCTION

1.1. THE INTESTINE

The intestine is a long, convoluted tube whose primary function is the absorption of materials from the gut lumen. In the small intestine, such materials include nutrients, electrolytes, vitamins, bile acids and water, whereas in the large intestine, water, short-chain fatty acids, the by-products of undigested carbohydrate fermentation by the colonic microflora, and bile acid metabolites, derived from the bacterial degradation of bile acids not absorbed in the ileum, constitute the main absorbable elements (Granger et al., 1985).

While it is the specific job of the mucosa to extract nutrients and other essential materials from the luminal contents, it is important that the chyme be exposed and re-exposed to as much of the mucosal surface as possible to achieve maximal absorption. Chyme does not flow passively, but must be propelled along the length of the gut. Through the specialized motor functions of the muscle wall of the intestine, chyme is moved along the length of the intestine, in general, at a rate of approximately 1-4 cm per min (Granger et al., 1985). In addition, within a given segment of the small intestine, integrative patterns of contractile activity mix the chyme and increase its contact time with the mucosa, thereby enhancing the absorptive process. Thus, efficient absorption of luminal contents requires the co-ordinated actions of all layers of the bowel wall.

1.2. CONTRACTIONS AND MOTOR PATTERNS OF THE SMALL INTESTINE

The smooth muscle of the intestine consists of spindle-shaped cells arranged in sheet-like fashion to form an inner circular and an outer longitudinal muscle layer. The

cells of the two muscle layers are oriented at 90° to each other and thus, the planes of their contractions are also 90° relative to one other. Contraction of the circular muscle layer, which is of greater importance in the mixing and propulsive actions of the intestine, results in the occlusion of the gut lumen. In contrast, contraction of the longitudinal muscle layer serves to shorten the intestine.

The integration of contractile events in both muscle layers and over a given segment of intestine produces a motor pattern. Such motor patterns are linked to the intrinsic electrical activity of smooth muscle cells, specifically, slow waves and spike bursts. The former are regularly occurring oscillations in the resting membrane potential of the cell. Slow waves repeat at a constant frequency within a specific segment of the small bowel, with the frequency being highest in the duodenum and upper jejunum, at 12 cycles per min, and gradually declining in step-wise fashion down the length of the gut to 8-9 cycles per min in the ileum in man (Read, 1983). There appear to be two hypotheses regarding the mechanism of initiation of the slow wave frequency, although the two may not be mutually exclusive. There is a growing body of evidence to suggest that pacemaker activity in the intestine arises from a metabolically regulated intracellular event in the interstitial cells of Cajal and associated smooth muscle cells (Huizinga, 1991). Granger et al. (1985) have summarized the more commonly held view that pacemaker activity is the role of the smooth muscle cell. According to this hypothesis, smooth muscle cells with the highest intrinsic slow wave frequencies, those in the duodenum and proximal jejunum, serve as pacemaker oscillators that impose their frequency on adjacent

cells of lower intrinsic frequency. This communication is achieved through electrical coupling, and continues aborally until intrinsic frequency of the distal segment becomes too low to be influenced by the higher frequency pacemaker cells. Cells with the highest intrinsic frequency in this next intestinal segment in turn become new pacemaker oscillators, imposing their slow wave frequency on cells located more distally. In this manner, segments of intestine are established in which the slow wave frequency is constant. Between adjacent segments of differing slow wave frequencies, there exists a short segment of bowel, the transition zone, which shifts its own frequency between that of the upper and lower segments. The presence of a gradient in slow wave frequency along the length of the intestine contributes to aboral propulsion of luminal contents from a region of higher to a region of lower potential contractile frequency. Within a given segment, where the slow wave frequency is constant, aboral propagation is achieved because the slow waves do not occur simultaneously throughout the segment *i.e.*, proximal to distal phase lag. Overall, it is the slow wave frequency which determines the timing and rate of propagation of smooth muscle contractions.

Whether or not a contraction occurs is dependent upon the generation of spike bursts, which are sudden, rapid depolarizations of smooth muscle membrane superimposed upon the slow wave cycle at its point of maximal depolarization (Read, 1983). Spike bursts do not necessarily accompany each cycle of the slow wave, but their occurrence always results in contraction, such that one spike burst precedes one

contraction (Oigaard and Dorph, 1974). The generation of spike bursts depends upon neurohumoral excitation or release of inhibition.

1.2.1. Fasting pattern

The myoelectric activity of the small intestine in the interdigestive period was originally described by Szurszewski as "a caudad band of large-amplitude action potentials starting in the duodenum and traversing the small bowel" (1969). In their original analysis of this fasting pattern, Code and Marlett (1975) identified four phases of activity, although it is currently held that the interdigestive pattern, known as the migrating motor or myoelectric complex, consists of three phases. Phase I is a quiescent period, characterized by little or no contractile activity. In phase II, contractions are irregular and sporadic, while in phase III, the most active of the three, regular phasic contractions occur at a maximal rate determined by the local slow wave frequency (Bueno and Fioramonti, 1993). The intense contractile activity during phase III effectively propels luminal contents in an aboral direction. Since the migrating myoelectric complex propagates the length of the small intestine, it "sweeps" ahead of it any undigested material left in the intestinal lumen from the last feeding period, while concomitantly preventing the colonization of the lower small intestine by the orad emigration of bacteria in the proximal colon (Granger et al., 1985). At the onset of feeding, this fasting pattern is immediately replaced with the post-prandial motor pattern.

1.2.2. Fed pattern

The motor pattern induced by feeding resembles that of phase II of the migrating myoelectric complex, *i.e.*, intermittent and apparently irregular contractions (Bueno et al., 1975). Two types of contractions occur post-prandially, rhythmic segmentation and peristalsis. Segmental contractions occur over short distances (<2 cm), and reflect alternating regions of contraction and relaxation, such that chyme is propelled orally and aborally within a given segment of the intestine (Granger et al., 1985). This back and forth movement serves to mix the chyme, continually re-exposing it to mucosal digestive and absorptive surfaces. In the case of peristaltic contractions, luminal contents are moved aborally by the co-ordinated actions of circular and longitudinal smooth muscle. Distension of the gut by a luminal bolus causes a reflex relaxation of circular muscle, and a concomitant contraction of longitudinal muscle in the region of the intestine aboral to the bolus. The subsequent increase in luminal diameter reduces intraluminal pressure. Conversely, in the region oral to the bolus, circular muscle contracts and longitudinal muscle relaxes, thereby increasing intraluminal pressure. The net effect of these contractile events is the propulsion of the bolus aborally, down the pressure gradient into the dilated intestinal segment (Wood, 1994; Granger et al., 1985). Under normal circumstances, peristalsis occurs over relatively short distances. Effective aboral propulsion is the result of numerous overlapping runs of short, propulsive peristaltic rushes.

1.3. CONTROL OF SMOOTH MUSCLE MOTOR FUNCTION

To generate the complex motor patterns of the interdigestive and post-prandial periods requires the integration of numerous contractile events into a temporally and spatially co-ordinated arrangement. Such control of smooth muscle motor function arises from the interaction of neurogenic, hormonal and myogenic events.

1.3.1. Neurogenic control

While intestinal smooth muscle function can be modulated by the central nervous system, it is the enteric nervous system, and primarily the myenteric plexus, which organizes and co-ordinates fasting and fed intestinal motor activity. The level of control exerted by the enteric nervous system has been likened to a collection of sensory, motor and integrative circuits (Wood, 1994), contained within overlapping segments that are replicated along the length of the intestine (Wingate, 1993), and in close proximity to their effector organs. Sensory signals are received and processed by integrative circuits which in turn relay motor signals that determine the timing and sequence of excitatory and inhibitory output to enteric muscle (Wood, 1994). The presence of both excitatory and inhibitory neurons within the enteric nervous system permits the development of integrated, patterned motor responses over the length of the intestinal tract.

For example, peristaltic propulsion is a stereotyped sequence of muscle behaviour that is initiated by a basic reflex circuit of enteric neurons. A comprehensive description of the neuronal events involved has been eloquently provided by Wood (1994). In brief,

the aboral propulsion of luminal contents requires the activation of both excitatory and inhibitory pathways. As previously stated, relative to the location of the bolus, the distal receiving segment is relaxed, while the proximal propulsive segment is contracted. In order to achieve this configuration, excitatory and inhibitory interneurons are activated by signals from stretch receptors in the intestinal segment occupied by the bolus. The excitatory interneurons extend distally, branch and simultaneously activate two types of motor neurons (in direct communication with smooth muscle); excitatory signals are sent to the longitudinal muscle (contraction) and inhibitory to circular muscle (relaxation). In the proximal segment the circuitry is reversed. The activation of inhibitory interneurons by signals from stretch receptors sends two sets of signals. One branch turns off excitatory motor neurons to the longitudinal muscle (relaxation) while the other turns off inhibitory motor neurons to the circular muscle (disinhibition = contraction). Additional accessory circuits, comprised of excitatory motor neurons similarly activated by stretch receptors, augment the strength of the propulsive event by directly stimulating the circular muscle of the proximal segment. In order to achieve synchrony in the propulsive event, numerous such reflex circuits must be activated simultaneously around the circumference of a given length of intestine. It is the role of enteric driver circuits, aided by the syncytial properties of intestinal smooth muscle, to accomplish this task. Since the basic peristaltic circuit is repeated along the length of the intestine, additional control mechanisms are required to determine the distance of propagation. This control is provided by synaptic gates, which connect the basic circuit blocks. When the gates are

open, peristalsis propagates over long distances, and conversely, when the gates are closed, peristalsis does not propagate beyond the length of the activated circuit block. Thus, control of intestinal smooth muscle by the enteric nervous system exists at multiple levels. The complexity of the system, which consists of three functional types of neurons, sensory neurons, interneurons and motor neurons, allows for the precise and synchronized co-ordination of smooth muscle motor activity.

1.3.2. Hormonal control

In addition to neurogenic control, smooth muscle motor function may be regulated hormonally, although specific roles remain unclear. Numerous studies have assessed potentially relevant hormones with respect to their abilities to induce either the fasting or fed motor patterns. A tabulated comparison of these studies has been made by Bueno and Fioramonti (1993). In a variety of animal models, motilin, somatostatin and pancreatic polypeptide have all been shown to induce phase III of the migrating motor complex in the stomach and/or the duodenum following their exogenous administration. However, in the studies in which fed pattern was concurrently assessed, only one of five was able to demonstrate suppression of the fed pattern (Bueno et al., 1982). The ability of insulin, pancreatic polypeptide, somatostatin, glucagon, secretin, motilin, gastrin, cholecystokinins CCK₃₃ and CCK₈, and neurotensin to disrupt the fasting pattern and initiate a fed motor pattern has been assessed in numerous studies and summarized by Bueno and Fioramonti (1993). With the exception of pancreatic polypeptide, all

hormones which were systemically infused were able to disrupt the interdigestive pattern. However, only insulin (Pascaud et al., 1982) and CCK₃₃, CCK₈ (Weisbrodt et al., 1976; Mukhopadhyay et al., 1977; Wingate et al., 1978) were able to additionally initiate and maintain a fed motor pattern. While these hormones were able to produce alterations in motor patterns, inconsistencies with other aspects of normal intestinal physiology question their role in the control of motor function. In the dog, ingestion of fat produces a clear disruption in the migrating motor complex but this is not associated with increases in the plasma levels of insulin; conversely, when plasma insulin levels are elevated following glucose ingestion or intravenous infusion, no disruption of the fasting motor pattern is observed (Eeckhout et al., 1978). In the case of CCK, its infusion leads to disruption of duodenal fasting patterns and is associated with a persistent elevation in plasma motilin levels; however, in the same study, this disagrees with the finding that plasma motilin levels were shown to be reduced following normal meal ingestion (Lee et al., 1980). Furthermore, contractions induced by CCK infusion do not resemble those normally observed after a meal (Wingate, 1978). Thus, while no single hormone can be ascribed a conclusive role, it remains possible that the actions of several hormones, through their modulatory effects on enteric neural circuits, control certain aspects of smooth muscle motor function.

1.3.3. Smooth muscle control

The third element affecting motor function is the structure and function of the smooth muscle itself. Contraction of smooth muscle cells is achieved through the sliding interactions of myosin and actin filaments. The events leading to muscle contraction have been extensively reviewed (Rembold, 1992; Walsh, 1991). Briefly, this process begins, in most instances, with the binding of an agonist to its receptor on the sarcolemma, which is coupled to a G-protein. The subsequent activation of phosphatidylinositol-specific phospholipase C via the G-protein results in phosphoinositide turnover; specifically, the generation of inositol 1,4,5-trisphosphate (IP_3) and 1,2-diacylglycerol (DAG) from phosphatidylinositol 4,5-bisphosphate. IP_3 and DAG are themselves second messengers. The water soluble IP_3 moiety travels to the sarcoplasmic reticulum, where it binds to IP_3 receptors and results in the release of Ca^{2+} from this intracellular store. The Ca^{2+} thus released binds to calmodulin. The complex of $(Ca^{2+})_4$ -calmodulin binds to myosin light chain kinase (MLCK), rendering the kinase active. Phosphorylation of myosin light chain by MLCK in turn activates the actin-activated myosin Mg^{2+} ATPase. The result is cycling of actin and myosin cross bridges leading to fibre shortening, and tension development. The removal of Ca^{2+} from the cytosol, via Ca^{2+} pumps in the sarcoplasmic reticulum and sarcolemma, and additionally a Na^+/Ca^{2+} exchanger in the sarcolemma, begins the process of relaxation. With respect to intestinal smooth muscle, calcium mobilization as described above is thought to occur primarily in circular smooth muscle. In contrast, agonist stimulation of longitudinal smooth muscle results primarily in calcium

influx from extracellular sources, which may in turn initiate Ca^{2+} -induced Ca^{2+} release from the intracellular store (Kuemmerle et al., 1994; Murthy et al., 1992). To add to the complexity of the contractile process, it appears that within the smooth muscle cell itself, there are additional pathways involving calponin and/or caldesmon, which are capable of modulating contractile protein interactions and, consequently, tension development (Walsh, 1994). Since smooth muscle cells themselves form the structural units of contraction, any factor(s) which affect the mechanics of contractility, *i.e.*, from receptor stimulation to contraction, will in turn affect patterned motor activity.

1.4. INTESTINAL TRANSIT AND ABSORPTION

Ultimately, the desired outcome of patterned motor activity is to achieve a rate of propulsion that permits the optimal digestion and maximal absorption of luminal contents.

If motor activity is altered such that contact time with the mucosa is reduced, *e.g.*, in conditions such as irritable bowel syndrome, Celiac disease and secretory diarrhea in which abnormally propulsive forms of motor activity occur (Read, 1986), then transit time will be shortened, and may be accompanied by malabsorption and diarrhea. In such cases of rapid transit, the nutrient load reaching the ileum is greatly elevated when compared to conditions of normal motility. In studies assessing the effects of fat malabsorption in the intestine, lipid infused directly into the ileum was shown to decrease the rate of gastric emptying of a liquid meal (Spiller et al., 1984; Holgate and Read, 1985) and improve intestinal absorption (Holgate and Read, 1985). This protocol

mimics, in part, the increased nutrient load presented to more distal gut regions in association with increased rate of transit. The retardation of gastric emptying by the presence of lipid in the ileum is known as the ileal brake (Spiller et al., 1984) and demonstrates the existence of feedback mechanisms which allow the organism to compensate for alterations in proximal gut function (*e.g.*, mucosal disease or resection causing decreased absorption, unusually rapid transit as a result of primary or secondary motor disease).

The factors which affect the flow of chyme through the intestine are numerous and interdependent. As explained by Weems (1987), the enteric nervous system, the intestinal musculature, the contractile state and geometry of the intestine, the physical conditions of luminal contents such as viscosity and density, as well as its chemical composition, all interact and combine to determine the mechanics of fluid flow within a given intestinal segment. The complexity of the system is further increased when it is considered that adjacent intestinal segments, each affected by the above-mentioned parameters in a site-specific manner, must also be coupled to one another hydraulically, electrically, mechanically and neurally, in order to achieve aboral propulsion of chyme (Weems, 1987). Thus, while certain indices of motility can be measured, *e.g.*, transit time, myoelectric activity, intraluminal pressures, it remains extremely difficult to assess all the variables which affect fluid flow through the intestine.

1.5. MASSIVE INTESTINAL RESECTION

1.5.1. Clinical aspects

Numerous clinical conditions, congenital or acquired, exist for which treatment requires the surgical removal of a large segment or segments of either small or large intestine, or in some cases both. While Crohn's disease has been cited as the most common condition for which massive ($>1/3$ the total bowel length) resection is performed in adult patients, other maladies necessitating resection include ulcerative colitis, ischemia, irradiation, volvulus, adhesions, diverticular disease (Nightingale and Lennard-Jones, 1993). In contrast, pediatric patients most commonly require surgical resections of bowel due to congenital disorders such as volvulus, atresias, gastroschisis and, less commonly, as a result of inflammatory diseases such as necrotizing enterocolitis, inflammatory bowel disease and vascular insufficiency (Bohane et al., 1979; Wilmore, 1972; Vanderhoof, 1992). Several factors can contribute to the severity of the disease and include the extent of resection, the site of resection, the underlying intestinal disease necessitating resection, the presence or absence of the ileocecal valve, the functional status of the remaining digestive organs, and the adaptive capacity of the residual intestine to the re-introduction of oral nutrition (Thompson, 1994; Wilmore, 1972). In rats (Nygaard, 1966a), dogs (Flint, 1921) and humans (Wilmore, 1972; Touloukian and Walker-Smith, 1983; Thompson et al., 1991) this adaptive response and survival are reduced when the extent and location of resection is sufficient to impair absorption and, therefore, nutritional status.

1.5.2. Short Bowel Syndrome

A complication of a sufficiently large surgical resection is Short Bowel Syndrome, which is defined as malabsorption due to bowel resection (Vanderhoof, 1992). Malabsorption results from the loss of absorptive surface area and a decrease in transit time which further reduces the contact time of chyme with the mucosa (Read, 1986). Clinical symptoms or conditions associated with Short Bowel Syndrome include: weight loss, steatorrhea, diarrhea, nutritional deficiency states, bacterial overgrowth, parenteral nutrition-induced cholestatic liver disease, renal stones, gallstones and problems related to catheters implanted for intravenous nutritional support (Nightingale and Lennard-Jones, 1993; Vanderhoof, 1992). Thus, while surgery can cure the original disease it may also result in serious, debilitating consequences, not the least of which is a life-long dependence on total parenteral nutrition. Clinical management following surgery involves an initial period of enteral and/or total parenteral nutritional support (Vanderhoof, 1992) until complex adaptive changes in the remnant bowel permit the gradual progression to oral bolus feeding.

Since the primary clinical difficulty in short bowel syndrome is one of malabsorption, the major portion of research efforts in this area has concentrated on elucidating the adaptive changes in mucosal surface area and function. Less well described are the adaptive changes occurring in intestinal smooth muscle structure, contractility and motility following intestinal resection. Yet, there is some morphological evidence to suggest that adaptation involving the smooth muscle layer does occur post-

resection. Furthermore, the clinical observation that the diarrhea and malabsorption initially associated with surgical Short Bowel Syndrome gradually wane over time (and for some time after mucosal adaptation has occurred) suggests that there are adaptive changes occurring in the residual smooth muscle structure and contractility (Quigley, 1993).

1.6. ADAPTATION OF SMOOTH MUSCLE

With regard to the morphological characteristics of the residual bowel post-resection, previous evaluation of the adaptive response has demonstrated changes in intestinal diameter and length. It is well established that a significant increase in luminal diameter/external circumference occurs following massive intestinal resection (Dowling and Booth, 1967; Nygaard, 1967a; Wilmore et al., 1971). With respect to intestinal length, studies using animal models have yielded inconsistent results regarding significant increases in the length of the remnant bowel (Nygaard, 1967a; Loran and Althausen, 1958; Flint, 1921; Clatworthy, 1952). In the human, it appears that the potential for adaptive increases in intestinal length may be greater in pre-term than full-term newborn infants (Touloukian and Walker-Smith, 1983), while such increases do not characterize the adaptive response of adults (Bristol and Williamson, 1985; Dowling 1982).

As previously stated, studies involving the adaptive response of the mucosa following intestinal resection have dominated research efforts in this area. Structural, functional and cytokinetic changes of the mucosa have all been documented (Williamson,

1978; Johnson, 1988) and include the following characteristics: hyperplasia (Dowling and Booth, 1967; Porus, 1965; Weser and Hernandez, 1971), alterations in villus/crypt morphology (Nygaard, 1967a; Hanson et al., 1977b) and changes in mucosal transport (Gouttebel et al., 1989; Schulzke et al., 1992; Weinstein et al., 1969).

Examination of the changes occurring in the muscularis propria following intestinal resection have led some authors to report that the thickness of the individual muscle layers increases post-resection ((Nygaard, 1967a; Hanson et al., 1977b), but a more consistent observation is the increase in muscle weight per cm intestinal length (Nygaard, 1967a; Hanson, 1977a; Nemeth et al., 1981; Wittman et al., 1986). This response has been loosely described in the literature as "hypertrophic" based on qualitative, macroscopic observations (Wittman et al, 1986). While it has been suggested that the more accurate term is hyperplasia (Nygaard, 1967a; Hanson et al., 1977a), this awaits quantitative confirmation. Furthermore, how this structural adaptation affects contractile function is not yet clear.

Quite apart from the morphological adaptive responses, the functional effects on intestinal transit of resection and jejuno-ileal bypass (surgically similar to resection) have been assessed. Post-surgery, there is an initial period of increased transit in the rat (Nygaard, 1967b; Nemeth et al., 1983) and the dog (Quigley et al., 1993). However, with increasing post-surgical time intestinal transit decreased, such that as early as two weeks post-surgery in one rat model, transit time had returned to control levels (Nygaard, 1967b). Similarly, duodenal to cecal transit time increased by 40% over the course of a

three month study in a canine model of 75% resection (Quigley et al., 1993). Interestingly, in the latter study, electromyographic studies revealed no accompanying changes in the frequency or periodicity of the interdigestive motor pattern, the migrating motor complex. In contrast, throughout the length of the intestinal remnant, both the fasting and fed motor patterns exhibited repetitive clusters of rhythmic activity, a pattern resembling the normal motor response of the distal ileum of control animals (Quigley et al., 1993). Resection had no effect on the presence or time of onset of a fed motor response (Quigley, 1993). However, it was not determined whether resection affected the time of re-appearance of the fasting motor pattern. The authors suggest that such alterations in motor patterns may contribute to the initial and adaptive clinical manifestations observed following massive resection. While it is clear that significant adaptive increases in intestinal transit time occurred over the three month study period, the alterations in motor pattern may not have been causally related, since the repetitive cluster activity was observed at the first time point studied, two weeks post-surgery, and did not exhibit any alteration in its incidence over the remainder of the study period (Quigley, 1993). Thus, while adaptive increases in transit time post-resection have been documented, it remains to be determined whether adaptation encompasses alteration in the contractile function of intestinal smooth muscle itself.

1.7. POTENTIAL MECHANISMS

While the potential for adaptation of intestinal smooth muscle after massive intestinal resection has yet to be fully explored, the literature would suggest that intestinal muscle may exhibit significant and varied alterations in both structure and function in response to external stimuli. For example, smooth muscle contractility, intestinal motor activity and transit have been studied in two models of intestinal infection/inflammation: one induced by the bacterium *Yersinia enterocolitica*, the other by the nematode *Trichinella spiralis*. In the former model, there was no change in the depth of the circular or longitudinal muscle layers and a decrease in the ability of longitudinal muscle to generate tonic tension in response to the nicotinic/muscarinic receptor agonist, carbachol, concomitant with altered motility and increased intestinal transit (Scott et al., 1989). In the *Trichinella* model, infection was associated with marked thickening of the muscularis propria, an increased ability to develop tonic tension in response to carbachol (Marzio et al., 1990), altered motility (Palmer et al., 1984) and increased transit (Castro et al., 1977). In a model of immune complex-induced colitis, colonic circular smooth muscle has been shown to exhibit decreased contractility in response to both receptor- and non-receptor-mediated activation (Cohen et al., 1986).

If contractile activity is indeed altered in the remnant bowel, several potential factors might contribute to the altered response. Certainly, non-muscle parameters, such as connective tissue content (reflecting tissue elasticity), neuronal pathways and neurotransmitter content, and hormonal regulation could be altered post-resection.

Potential changes related to smooth muscle itself might include the number and/or affinity of membrane receptors, signal transduction pathways, calcium source and its availability during excitation-contraction coupling, as well as synthesis and/or expression of contractile proteins.

While any number of the previously mentioned parameters may be modified, it is not unreasonable to begin to address this complex question by assessing whether the fundamental units of contraction, namely actin and myosin, are themselves altered. Six isoforms of actin have been identified (Vandekerckhove and Weber, 1978), four of which are associated with muscle. These isoactins include α -skeletal, α -cardiac, α -vascular and γ -enteric. All actin isoforms are regulated in a developmental and tissue-specific manner (McHugh et al., 1991; Fatigati and Murphy, 1984) with γ -enteric isoactin being the predominant isoform of the adult gastrointestinal tract (Vandekerckhove and Weber, 1981). Myosin is a hexamer consisting of two heavy chains, two regulatory (able to be phosphorylated) light chains, and two essential light chains (Rovner et al., 1986; Helper et al., 1988). Support for the hypothesis that an alteration in intestinal muscle contractility may be the result of changes in the contractile proteins actin and myosin comes from research involving cardiac muscle. It is now well established that in the early stages following pressure-induced overload and hypertrophy of cardiac muscle, the tissue responds by turning off expression of certain "adult" genes and re-activates expression of a set of "fetal" genes (Schneider et al., 1991). Affected genes include β -tropomyosin

(Izumo et al., 1988) and fibronectin (Villarreal and Dillmann, 1992), as well as actin and myosin heavy chain. Specifically, α -cardiac actin expression switches to α -vascular isoactin, the earliest α -actin mRNA expressed during cardiac myogenesis (Black et al., 1991), and the α isoform of myosin heavy chain is replaced with the β isoform, which is normally expressed during the time of fetal development (Lompre et al., 1979; Schiaffino et al., 1989). It is assumed that the induction of the fetal genetic programme confers some advantage to the stressed, hypertrophied heart. Indeed, the up-regulated β isoform of myosin heavy chain, when compared to its α counterpart, has a lower rate of actin-activated ATPase (3-5 fold less), and results in a more energy efficient contraction at the expense of contractile speed (Schwartz et al., 1981; Alpert and Mulieri, 1982; Mercadier et al., 1981). It may be that under the conditions of "stress" imposed by removal of a large segment of intestine, similar switches in the isoforms of the contractile proteins occur.

With regard to the gastrointestinal tract, studies of contractile protein content have been conducted in a surgical model of jejuno-ileal bypass, which, as previously stated, is surgically similar to resection. In the rat bypass model, a length of small bowel is removed out of continuity from the remaining intestine. The proximal and distal ends of the remaining intestine are sewn together in an end-to-end anastomosis, thereby creating a length of remnant bowel similar to surgical resection. This portion of the small intestine is referred to as the "in continuity" segment. The removed length of intestine is sewn

closed at its oral end, and its aboral end attached elsewhere in the intestine, in a side-to-end anastomosis, thus forming the "bypassed" segment. Using this model, Bowers et al. (1986) removed 70% of the jejuno-ileal portion of the intestine, leaving 7 cm of proximal jejunum anastomosed to 15 cm of distal ileum. The bypassed segment was attached to the side of the distal colon. It was determined that the ratio of actomyosin content : total protein was not different for in continuity tissues compared to sham surgical controls, in spite of their ability to generate increased stress (Bowers et al., 1986). The authors suggest that the altered contractility may be associated with changes in the isoform expression of the contractile proteins. According to the same group, further suggestive evidence was obtained in a later study, in which they determined that the proportion of mRNA specific for α -actin relative to total RNA had increased significantly by 4-5 days after jejuno-ileal bypass (Lai et al., 1990). However, the RNA for these studies was obtained from the ileal longitudinal muscle layer only, while the previously described increase in stress was demonstrated in circular muscle only (Bowers et al., 1986). In fact, in studies of longitudinal muscle contractility in this model there were no differences in the active stress generated by tissues from bypass compared to sham-operated control groups (Weisbrodt et al., 1985). Furthermore, while increases were observed at the pre-translational level, this does not address any potential changes in RNA processing and/or stability, which would have made determination of concomitant protein levels a more informative measurement in this study.

Changes in the level of actin protein have been reported in a different animal model of altered muscle contractility. After feeding prairie dogs a high-cholesterol diet for a period of eight days, gallbladder smooth muscle demonstrated a proportionate increase in γ -enteric isoactin protein concurrent with a decrease in α -vascular isoactin protein (Li et al., 1990). It is speculated that these alterations are associated with the previously documented reduction in gallbladder contractility observed after high-cholesterol feeding (Fridhandler et al., 1983; Li et al., 1987).

1.8. SPECIFICS OF THE MODEL

In the studies to be described herein, a rat model of 75% resection of the mid-intestine was established. The remnant bowel consisted of a proximal jejunal segment, a distal ileal segment and the ileo-cecal valve. The extent and location of the resection, and the choice of residual jejunum were selected for study based on methodological reasons.

1.8.1. Extent and location of resection

Previous studies of the enteric mucosal adaptation to surgical resection indicated that the adaptive response is proportional to the length of intestine resected (Nygaard, 1967a; Williamson, 1978; Hanson et al., 1977a). The decision to remove 75% of the small intestine was made to maximize any potential adaptive responses. The retention of equal portions of proximal jejunum and distal ileum was chosen to avoid the nutritional complications (Wilmore, 1972; Nygaard, 1966a, 1966b; Flint, 1921; Touloukian and

Walker-Smith, 1983) associated with removal of a) the specialized absorptive capacity of the terminal ileum for Vitamin B₁₂ and bile acids (Kalser et al., 1960) and b) the ileal brake (Spiller et al., 1984). Adaptation in rats occurs more slowly and to a lesser extent after a 75% distal resection than after a 75% proximal resection, a phenomenon that Nygaard (1967a) attributed to the more rapid transit, more severe malabsorption and the greater impact of a 75% distal resection on nutritional status. In human infants of normal birth weight, successful outcome following extensive intestinal resection is associated with retention of at least 15 cm of jejunum or ileum and the ileocecal valve, or 40 cm of small intestine without the ileocecal valve (Wilmore, 1972). These measurements constitute from 5 to 13 % of total intestinal length (Touloukian and Walker-Smith, 1983). Thus, while the 75% resection performed in the present studies is indeed massive, it is expected that the residual 25% of small intestine, which includes the ileo-cecal region and a portion of distal ileum, creates a model in which the intestinal adaptation to resection can be studied uncomplicated by malabsorption leading to poor growth and malnutrition.

1.8.2. Choice of tissue for study

Studies of mucosal adaptation post-resection have shown that the magnitude of the response was greatest in the distal compared to the proximal portion of the residual small bowel (Touloukian and Walker-Smith, 1983). This differential responsiveness is a function of the proportional increase in luminal nutrient load found in the ileum compared to the jejunum (Dowling and Booth, 1967; Altmann and Leblond, 1970; Tepperman et

al., 1942). To look at the response to resection independent of large increases in luminal nutrient load, the muscularis propria from the jejunum was selected. In this way, any changes observed would reflect the potential for adaptive change in an intestinal segment already exposed to the volume and nutrient load of that animal's normal caloric intake. To minimize the contributing effect of the surgical anastomosis on the assessment of the adaptive response to resection (Nygaard, 1967a), all structural and biochemical measurements were performed on jejunal tissue obtained greater than 5 cm away from the anastomotic site.

1.8.3. Analysis of longitudinal and circular muscle layers

While increased isometric force is developed by jejunal longitudinal muscle six days after infection with the nematode *Trichinella spiralis* (Vermillion and Collins, 1988), the tension developed by circular muscle from the same model has been shown to be significantly decreased (Crosthwaite et al., 1990). Similar discrepancies in the contractile response of the two muscle layers have been demonstrated in tissues obtained from patients with Crohn's disease. Stimulation of longitudinal muscle with carbachol resulted in a significant increase in maximal force without affecting the EC_{50} . Conversely, in circular muscle from Crohn's patients, the EC_{50} was significantly reduced while maximal force remained unchanged (Vermillion et al., 1993). Thus, the effect of massive intestinal resection on contractile events of the residual bowel must include both the

circular and longitudinal muscle layers, given the independent and, seemingly, opposite nature of their respective contractile responses.

CHAPTER TWO

HYPOTHESES AND EXPERIMENTAL APPROACHES

Following massive intestinal resection, there is an adaptation of the remnant bowel. While it has been established that numerous morphological and functional alterations in the mucosal layer of the residual gut occur, little has been done to characterize the adaptive response of the muscularis propria. Thus, initial studies were designed to address this issue, with the result that two major hypotheses followed. The initial and subsequent hypotheses are listed in bold face type below, accompanied by a brief description of the experimental approaches utilized to test them:

1) **The muscularis propria undergoes a morphological adaptation in response to massive intestinal resection.** Initial studies involved characterization of the model, including measurement of intestinal circumference, tissue wet weight per unit length of gut, tissue depth of the individual circular and longitudinal muscle layers, as well as histological examination of the muscle layers. Total protein and DNA content per unit length of bowel were measured to assess whether tissue mass was increased post-resection. Having demonstrated an increase in tissue mass, the ratio of total protein : DNA content per unit gut length determined whether this response was hypertrophic or hyperplastic in nature.

2) **The structural alterations of the muscularis propria are not accompanied by enhanced contractile function (increased stress).** Without a compensatory increase in the ability to develop tonic stress, an increase in luminal diameter (known to occur post-resection) will lead to a reduction in the ability to develop luminal pressure, as stated

by the Lamé approximation (Weems, 1987):

$$\text{pressure gradient across the gut wall} = \frac{\text{stress}}{\text{internal radius}} \times \text{wall thickness}$$

This relationship and the fact that transit has been shown to gradually slow post-resection in the dog (Quigley and Thompson, 1993) and in a rat model of jejuno-ileal bypass (Nemeth et al., 1981), suggests that luminal pressure remains decreased following resection. Morphological data (to be presented) provide additional support for the hypothesis that the reduced ability to develop luminal pressure (predicted from the documented adaptive increase in luminal radius, absence of a change in wall thickness, and the Lamé approximation) will not be compensated for by an increase in circular smooth muscle contractility. To assess contractile function, intestinal tissues were isolated and stimulated *in vitro* using several contractile stimuli. Tonic and phasic contractile responses were assessed.

3) The changes in contractile function of circular smooth muscle post-resection are the result of alteration(s) at the level of the muscarinic receptor, the source of calcium utilized for excitation-contraction coupling, or the contractile protein machinery itself. Muscarinic receptor density and binding affinity were assessed by receptor binding assay. Contractile responses were measured under conditions which excluded extracellular calcium entry. Immunoassays were developed to measure the relative abundance of myosin heavy chain, α -vascular isoactin, γ -enteric isoactin and total muscle actin.

CHAPTER THREE

MATERIALS AND METHODS

3.1. MATERIALS

3.1.1. Chemical reagents and isotopes

All surgical supplies were purchased from Davis + Geck, Cyanamid Canada Inc., Willowdale, ON, Canada. Sustacal (liquid elemental diet) was obtained from Mead Johnson, Belleville, ON, Canada. All chemicals, including bethanechol (carbamyl-BETA-methylcholine chloride), serotonin (5-hydroxytryptamine), tetrodotoxin, verapamil, nifedipine, collagenase type II, chicken gizzard actin, o-phenylenediamine, EGTA, monoclonal antibody to smooth muscle myosin heavy chain and anti-mouse IgG peroxidase conjugate were purchased from the Sigma Chemical Co., St. Louis, MO, USA. Dounce tissue grinders were obtained from Wheaton Scientific, Millville, NJ, USA. Spectra/Mesh polypropylene filters (pore sizes 200 and 500 μm) were obtained from Spectrum, Houston, TX, USA. Betamax scintillation cocktail and disodium chromate, $\text{Na}_2^{51}\text{CrO}_4$ (^{51}Cr), were purchased from ICN Biomedicals Inc., Costa Mesa, CA, USA. NCS-II Tissue Solubilizer and 1-quinuclidinyl[phenyl-4- ^3H]benzilate, ^3H -QNB, were purchased from Amersham, Oakville, ON, Canada. Monoclonal antibodies to γ -enteric isoactin, α -vascular isoactin and total muscle actin were kindly donated by Dr. J. Lessard, University of Cincinnati, Cincinnati, OH, USA but can be purchased commercially from ICN Biomedicals, Costa Mesa, CA, USA. DC Protein Assay Kit was purchased from Bio-Rad, Mississauga, ON, Canada. Immunoassay plates were obtained from VWR Canlab, Edmonton, AB, Canada.

3.1.2. Equipment

Ocular micrometer and standard image-splitting micrometer with a Leitz-Wetzlar microscope, Germany were used in the histological studies. Isometric force transducers (Model 50-7905) and transducer amplifiers (model 50-7970) were purchased from Harvard Apparatus Ltd., Kent, UK. Bioelectrical amplifiers (Model 8811A) and eight-channel chart recorder (Model 7858A) were obtained from Hewlett Packard, Mississauga, ON, Canada. Electrical field stimulation was generated using a Grass S88 stimulator, Grass Instruments, Quincy, MA, USA. The platform shaker used to agitate samples for the binding studies was an AROS 160 Adjustable Reciprocating Orbital Shaker, Barnstead/Thermolyne Corporation, Dubuque, IO, USA. ^3H -QNB samples were spun in a Microspin 24S centrifuge from Sorvall Instruments, DuPont and counted in a Beckman LS 9800 beta counter. A Wallac Wizard 1480 gamma counter was used to measure ^{51}Cr radioactivity. Immunoassay plates were read using a UVmax kinetic microplate reader purchased from Molecular Devices Corporation, Menlo Park, CA, USA.

3.2. ANIMAL MODEL

3.2.1. Animals

Sprague-Dawley rats (Life and Environmental Sciences Animal Resource Centre, University of Calgary) of either sex weighing 160-180 g were used in the present experiments. All experimental procedures were approved by the Animal Care Committee

of the University of Calgary Faculty of Medicine under the guidelines of the Canadian Council on Animal Care.

3.2.2. Surgery

In early experiments, surgery was performed on animals anesthetized with a mixture of xylazine and ketamine-hydrochloride (4 mg and 78 mg per kg body weight, respectively) given intramuscularly. In later studies, anaesthesia was induced with halothane. Animals were prepared with proviodine, draped and, following a midline abdominal incision, the intestine was exteriorized. Its length from the ligament of Treitz to the ileocecal valve was measured by parallel placement of a previously measured and marked segment of umbilical braid. The validity and accuracy of this technique has been previously evaluated (Nygaard, 1967a). Taking this length as 100%, a resection of 75% of the mid-jejuno-ileum was performed such that 12.5% of proximal jejunum and 12.5% of distal ileum remained. These two segments were joined by a primary end-to-end anastomosis using a single layer of 7-0 silk with interrupted technique. To ensure patency of the lumen and integrity of the anastomosis 1 ml of sterile saline was injected (25 gauge needle) through the jejunal wall at a site near the anastomosis. Additional interrupted sutures were made to correct any overt blockage or leakage. The intestinal remnant was returned to the abdominal cavity. The musculature of the abdominal wall was closed with interrupted sutures of 3-0 dextron and the skin incision closed with interrupted sutures of 3-0 silk. Prior to closure, 5 ml of sterile saline were injected into the peritoneum. As

Figure 3.1. illustrates, sham-operated rats were subjected to transection and re-anastomosis of the proximal jejunum such that, similar to resected rats, 12.5% of the total jejuno-ileal length lay between the ligament of Treitz and the anastomosis. In the initial studies involving characterization of the model, a third untreated group of rats was maintained.

Rats were housed individually in stainless steel, mesh-bottom cages kept in a temperature and humidity controlled environment with a 12 hour light/dark cycle. Commencing 24 hours after surgery and continuing for 2 days, rats were fed an elemental liquid diet, Sustacal, *ad libitum*. Thereafter animals received rat chow *ad libitum*.

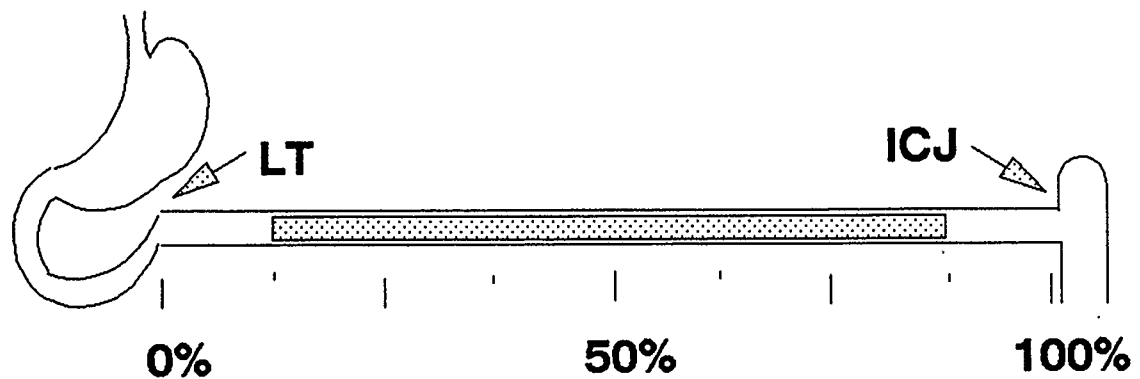


Figure 3.1. Outline of surgical protocol. Resection involved removal of 75% of the mid-jejuno-ileum, followed by a primary end-to-end anastomosis of the remnant bowel. The sham operation consisted of transection and anastomosis of the proximal jejunum such that no intestine was removed. The site of transection of the proximal jejunum was comparable to that of the resected group. The residual proximal jejunum (≥ 3 cm orad to the anastomosis) was used for all experimental studies. LT, ligament of Treitz; ICJ, ileo-cecal junction.

3.3. CHARACTERIZATION OF THE MODEL

3.3.1 Body weight and food intake

A group of untreated control animals was sacrificed on day 0, and groups of unoperated control, resected and sham-resected animals were sacrificed on days 10, 20, 30 and 40 post-operatively (n=14 in each group, on each day). Rats were sacrificed by light anaesthetization with diethyl ether followed by cervical dislocation. In each group, the daily food intake and weight of individual animals was recorded.

3.3.2 Intestinal length and jejunal circumference

A laparotomy was performed at the time of sacrifice. Animals from either surgical group in which stricture at the anastomotic site was suspected on the basis of a visible difference in diameter of the bowel proximal as compared to distal to the anastomosis, were excluded from this and future studies. Total intestinal length was measured by running a length of umbilical braid with cm markings parallel to the course of the gut. Once recorded, the intestine between the ligament of Treitz and the ileocecal valve was removed and cleared of feces by gently flushing with normal saline. This length of bowel was then placed in oxygenated ice-cold Krebs solution for twenty minutes, during which time the initially observed spontaneous, slow muscle contractions diminished in frequency and finally ceased. The composition of the Krebs buffer was (mM): NaCl 120.3, KCl 5.9, CaCl₂ 2.5, MgCl₂ 1.2, NaHCO₃ 15.4, NaH₂PO₄ 1.2, and glucose 11.5.

Since measurement of circumference and wall thickness will vary with the degree of stretch and motor activity, preliminary experiments were performed in four animals to validate a simple measure of external circumference against a physiological standard. After twenty minutes in oxygenated ice-cold Krebs, the proximal four cm of jejunum was opened longitudinally and the external circumference measured by laying a 1.8 g plastic ruler across the width of the opened gut at three locations 1 cm apart along its length. The physiological standard against which the former method could be validated consisted of three 0.5 cm width rings of tissue that were suspended transversely between the base of a 20 ml tissue bath and an isometric force transducer and bathed in Krebs solution. Temperature was maintained at 37°C and the bath was bubbled continuously with 95% O₂ - 5% CO₂. Mechanical activity detected by the isometric force transducer was amplified by a transducer amplifier, input to a bioelectric amplifier and recorded on an 8-channel chart recorder. Segments were allowed to stabilize in the tissue bath for one hour and then stretched until muscle tension began to increase with any further increase in muscle length (the initial length, L_i). At this point the external diameter of the ring was measured and multiplied by 3.14 to obtain the circumference beyond which any further stretch was associated with an increase in tension. Using multivariate least-squares regression analysis and the statistical package Systat, intestinal circumference was modelled as the sum of the classification variable rat, the measurement technique and the interaction term (rat * measurement) (Mendenhall, 1968).

$$\text{Circumference} = \text{rat} + \text{measurement technique} + (\text{rat} * \text{measurement}) + \text{constant}$$

While the mean external circumference of the opened gut on ice was significantly (3-fold) less than that of the tissue rings stretched to L_i at 37°C , the very high correlation ($r = 0.98$) between the measure of external circumference of opened gut on ice and that calculated from the diameter of a tissue ring stretched to L_i and at 37°C validated the former technique.

In all subsequent experiments, all rats were treated in the following manner. Isolated intestine was left in oxygenated iced Krebs solution for 20 min and then transferred to a petri dish containing iced Krebs solution. Eight cm of small intestine starting from the ligament of Treitz and extending towards the anastomotic margin was opened longitudinally and the external circumference measured with a ruler.

3.3.3. Tissue wet weight, total protein and DNA content

After measuring jejunal circumference, the proximal 3 cm of opened bowel, now contracted and immobile in ice-cold Krebs, was stapled to cardboard and placed in formalin for fixation prior to histological assessment (see section 3.3.4). The distal 5 cm of tissue was gently patted dry and weighed. Then the mucosa and as much of the submucosa as possible were scraped from the muscularis propria using a glass slide, and the muscularis propria weighed. The muscularis propria was then homogenized in 2.5 mM EDTA using a Dounce tissue grinder, and subsequently assayed for total protein and

DNA content. The protocols of Lowry et al. (1951) and Schmid et al. (1963) were used to measure total tissue protein and DNA content, respectively.

3.3.4. Histological measurements

Formalin-fixed tissues were embedded in paraffin, thick sectioned (3-4 μm), and stained with hematoxylin and eosin. The total tissue depth, *i.e.*, serosa to villus tip, depth of the muscularis propria, and of the circular and longitudinal muscle layers individually, were measured using an ocular micrometer and standard image-splitting micrometer at 250 X power. In addition, photomicrographs were taken of each tissue section under oil immersion at 1000 X power. For reference, photomicrographs were also taken of a hemocytometer grid. The number of cross-sectioned circular smooth muscle cells per unit area, including all whole cells within the grid and all partial cells adjacent to the bottom and left margins of the grid, was determined by comparing the photographs of the tissue to those of the grid. Cell counts were performed in a blinded manner by two independent observers. The two separate sets of counts were highly correlated ($r=0.97$), were not significantly different and the mean of the two sets was calculated.

The effectiveness of the scraping technique for the removal of mucosa and submucosa was assessed in preliminary experiments using scraped and intact jejunal tissue samples ($n=8$ rats per group). Tissues were prepared for histological assessment as described above. The thickness of the residual submucosa, circular and longitudinal muscle layers were determined. In addition, the number of nuclei in the residual

submucosa, and the number of smooth muscle nuclei in the circular and longitudinal muscle were counted per linear mm of the tissue sections.

3.4. LONGITUDINAL MUSCLE CONTRACTILITY

3.4.1. Experimental design

For this and all subsequent sets of experiments two treatment groups were studied, namely, sham-operated and resected. Experiments were performed on days 10, 20, 30 and 40 post-operatively with 7 rats per treatment group per time point.

At the appropriate time post-surgery, rats were lightly anesthetized with diethyl ether, then sacrificed by cervical dislocation. The small intestine from the ligament of Treitz to a point distal to the anastomosis was quickly removed. The jejunum was then divided into two segments: a ring 1 cm in length from which circumference was measured as previously described (section 3.3.2), and the balance was used for contractility studies. For the latter experiments, the tissue was placed in warmed, oxygenated Krebs solution, opened longitudinally at the mesenteric attachment, and pinned out flat. A 0.5 x 2.0 cm longitudinally oriented segment of proximal bowel was obtained from the anti-mesenteric wall, and suspended between the base of a 20 ml tissue bath and an isometric force transducer. Tissues were bathed in Krebs solution, the composition of which was (mM): NaCl 120.3, KCl 5.9, CaCl₂ 2.5, MgCl₂ 1.2, NaHCO₃ 15.4, NaH₂PO₄ 1.2, and glucose, 11.5. Temperature was maintained at 37°C and the bath continuously bubbled with 95% O₂ - 5% CO₂. Mechanical activity of the

longitudinal muscle was detected by isometric force transducers, enhanced by a transducer amplifier, relayed to a bioelectric amplifier and recorded on an 8-channel chart recorder.

3.4.2. Basal stress in response to stretch

Basal stress developed in response to stretch, or the length-tension relationship, was determined for tissues from both treatment groups. After hanging, tissues were left to stabilize in the tissue bath for 1 h and then slowly stretched until muscle tension began to increase with any further increase in muscle length. From this initial length (L_i), the muscle strip was progressively stretched to 110, 120, 130, 140, 150 and 160 % of L_i . After each incremental stretch, the muscle was allowed to reach a stable basal tension which was recorded.

3.4.3. Length-active stress response and determination of optimal length

After basal tension was recorded at each incremental stretch (110, 120, 130, 140, 150 and 160 % of L_i), the muscle strips were contracted maximally with 10^{-4} M bethanechol, a muscarinic receptor agonist. The bethanechol-stimulated muscle tension was measured as the difference between the stable level of resting tension and the peak tension recorded after bethanechol administration. From these experiments, optimal muscle length (L_o), the muscle length at which peak active tension was developed in

response to a standard stimulus (10^{-4} M bethanechol), was determined. All subsequent experiments assessing active stress were performed with tissues equilibrated at L_0 .

3.4.4. Concentration-response to bethanechol

The concentration-response to bethanechol was determined over the range of 10^{-9} - 10^{-4} M. Bethanechol was added to tissue baths in a non-cumulative manner with two washes and a 20 min equilibration period between successive concentrations. Analysis of the contractile response included measurement of the following parameters, which are illustrated in Figure 3.2.: maximal tonic tension, maximal frequency and maximal amplitude of phasic activity before and after bethanechol stimulation. Parameters which were significantly changed by resection were re-assessed in the presence of 10^{-6} M tetrodotoxin (TTX) to determine whether these alterations were myogenic in origin.

3.4.5. Concentration-response to KCl

The maximal tonic stress in response to graded concentrations of KCl, namely 5.9 to 80 mM, was established in a non-cumulative manner. Tissues were washed twice with normal Krebs buffer and left 20 min to equilibrate between successive exposures. The increase in ionic strength of each challenge solution due to KCl was balanced by an appropriate decrease in NaCl. In all other respects, the composition of the Krebs buffer was normal.

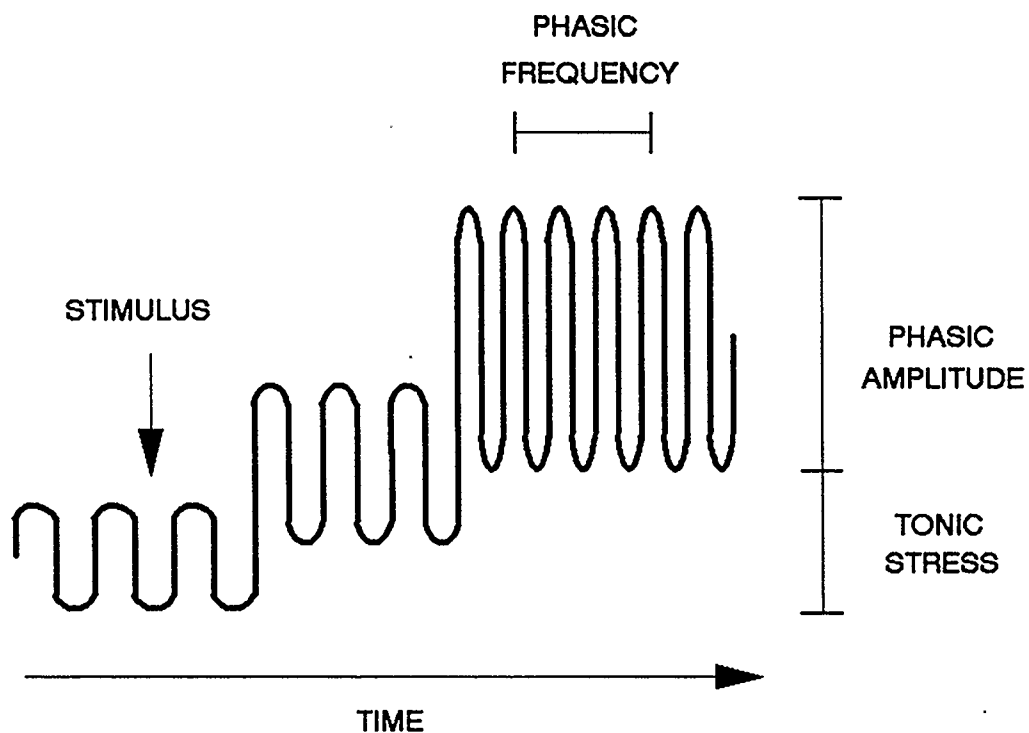


Figure 3.2. Schematic diagram of contractile parameters. The components tonic stress, phasic frequency and phasic amplitude are used to describe the *in vitro* contractile activity of muscular tissue.

3.4.6. Normalization of contractile responses

All basal and active contractile responses were normalized to tissue cross-sectional area. At the end of each experiment jejunal tissue strips were removed from the tissue baths, scraped free of mucosa using a glass slide, and lightly blotted. Tissue dry weights were recorded.

On each post-operative day (10, 20, 30, and 40), a second segment of jejunum not used in the contractility studies was obtained from each rat and its length measured. The luminal surface was scraped free of mucosa and, after light blotting, tissue wet weight was recorded. By comparing the ratios of wet tissue weight/tissue length : dry tissue weight/tissue length, a dry weight to wet weight conversion factor was determined for each rat.

The area of muscle (mm^2) for each tissue was then determined using the following equation:

$$\text{muscle area (mm}^2\text{)} = \frac{\text{mass of the dry muscle strip (mg)} \times \text{wet weight conversion factor}}{\text{length of the muscle strip (mm)} \times \text{density (mg mm}^{-3}\text{)}}$$

where the density of smooth muscle was assumed to be 1.05 mg mm^{-3} . For each tissue, the fractional thickness of the wet muscle strip attributable to the longitudinal smooth muscle layer was determined histologically.

Using these data and the following formula, all calculations have been corrected such that tension has been normalized to the cross-sectional area of longitudinal smooth muscle alone and expressed as stress, in units of mNewtons mm⁻²:

$$\text{stress (mNewtons mm}^{-2}\text{)} = \frac{\text{tension (g)} \times 9.8 \text{ mN/g}}{\text{muscle area (mm}^2\text{)}}$$

3.5. CIRCULAR MUSCLE CONTRACTILITY

3.5.1. Experimental design

Rats were subjected to either massive intestinal resection or a sham-operation. Body weight was measured twice weekly. Experiments were performed on days 10, 20, 30 and 40 post-surgery, with six rats per treatment group per time point.

At the appropriate time post-surgery, rats were lightly anesthetized with diethyl ether, then sacrificed by cervical dislocation. The small intestine from the ligament of Treitz to a point distal to the anastomosis was quickly removed and immediately placed in warmed, oxygenated Krebs solution. After discarding the first centimetre, two 1 cm long rings of proximal jejunum were removed and suspended transversely between the base of a 20 ml tissue bath and an isometric force transducer. Tissues were bathed in normal Krebs buffer (composition as per section 3.4.1.). Temperature was maintained at 37°C and the bath was continuously bubbled with 95% O₂ - 5% CO₂. Mechanical activity of

the circular muscle was detected by isometric force transducers, enhanced by a transducer amplifier, relayed to a bioelectric amplifier and recorded on an 8-channel chart recorder.

3.5.2. Basal stress in response to stretch

Following measurement of the initial length (L_i) of the jejunal tissue rings, basal length-tension relationships were determined as described previously (section 3.4.2.). In these experiments, circular muscle tissues were progressively stretched to 120, 140, 150, 160, 170 and 180 % of L_i .

3.5.3. Length-active stress response and determination of optimal length

From experiments performed in similar fashion to those described in section 3.4.3., it was possible to determine the optimal muscle length (L_o) for circular smooth muscle contraction. L_o was defined as that muscle length which permitted the development of maximal active stress following stimulation with 10^{-4} M bethanechol. All subsequent experiments were performed with tissues equilibrated at L_o .

3.5.4. Concentration-response to bethanechol

The concentration-response to the muscarinic receptor agonist, bethanechol, was determined over the range of 10^{-9} - 10^{-4} M. Bethanechol was added to tissue baths in a non-cumulative manner with two washes and a 20 min equilibration period between successive concentrations. Analysis of the contractile response included measurement of

the following parameters: maximal tonic tension, maximal frequency and maximal amplitude of phasic activity before and after bethanechol stimulation, and the length of time taken after stimulation to reach maximal tonic tension. As noted earlier, Figure 3.2. provides a schematic representation of these contractile parameters.

In another series of experiments, the same parameters were measured first in the absence and then presence of 10^{-6} M TTX, to determine whether significant alterations in contractility could be attributed to myogenic changes. Two concentrations of bethanechol were chosen, specifically, EC_{50} (the concentration at which half maximal stress is generated) and 10^{-4} M (a concentration which evoked maximal stress). Between successive stimulations, tissues were washed twice with Krebs solution and allowed to equilibrate for 30 min. When TTX was present, it was added immediately after washing and the tissues were allowed a 30 min exposure period before being stimulated with bethanechol.

3.5.5. Concentration-response to serotonin

All experiments were conducted with tissues equilibrated to L_0 and with 10^{-6} M TTX in the tissue baths. After the addition of TTX, tissues were left to equilibrate for 30 min. The maximal tonic stress and maximal amplitude of phasic activity of sham-operated and resected tissues was determined over the concentration range of 10^{-9} to 10^{-4} M serotonin (5-HT).

3.5.6. Concentration-response to KCl

The response to graded concentrations of KCl, 5.9 to 80 mM, was established in a non-cumulative manner. Tissues were washed twice with normal Krebs buffer and left 20 min to equilibrate between successive exposures. The increase in ionic strength of each challenge solution due to KCl was balanced by an appropriate decrease in NaCl. Maximal tonic stress was determined.

3.5.7. Electrical field stimulation

The contractile response to non-receptor mediated stimulation was measured by subjecting tissues from both treatment groups to electrical field stimulation (EFS). Tissues were collected as described above, but were suspended such that ring electrodes were positioned both above and below at 90° to the plane of the jejunal tissue ring. EFS consisted of an 80 volt charge delivered as 10 pulses per sec, 10 msec per pulse with no delay over a 10 sec period. Maximal tonic and phasic (amplitude) stress were determined.

Prior to EFS, the response to 10^{-4} M bethanechol was taken as a reference measure. After EFS, tissues were left to equilibrate in normal Krebs buffer for 20 min and then exposed to 10^{-6} M nifedipine. After a further 30 min equilibration period, tissues were again subjected to EFS.

3.5.8. Normalization of contractile responses

Basal and active contractile responses were normalized to tissue cross-sectional area. At the end of each experiment jejunal rings were removed from the tissue baths, opened, scraped free of mucosa using a glass slide, and lightly blotted. Tissue wet weights were recorded. The cross-sectional area (mm^2) of each tissue was determined using the following equation:

$$\text{cross-sectional area (mm}^2\text{)} = \frac{\text{mass of the wet muscle strip (mg)}}{\text{length of the muscle ring (mm)} \times \text{density (mg mm}^{-3}\text{)}}$$

where the density of the smooth muscle was assumed to be 1.05 mg mm^{-3} . From the earlier studies involving characterization of the rat model of resection, the fractional thickness of the wet muscle strip attributable to the circular smooth muscle alone had been determined histologically. Combining these data, all calculations have been corrected such that tension (g) is normalized to the cross-sectional area of circular smooth muscle alone and expressed as stress, in units of mNewtons mm^{-2} . The formula for the conversion of tension to stress has been previously stated in section 3.4.6.

3.6. GASTROINTESTINAL TRANSIT

Fasting gastrointestinal transit experiments were conducted on day 14 post-surgery. Following an overnight fast, sham-operated ($n=7$) and resected ($n=8$) rats were

administered 1 ml of saline containing 10 uCi (1 Ci = 37 GBq) of $\text{Na}_2^{51}\text{CrO}_4$ (^{51}Cr) by orogastric gavage. After 30 min all rats were sacrificed by an overdose of diethyl ether. Using 3-0 silk, the following points were tied off *in situ*: the distal end of the esophagus, the pylorus, the ileocecal junction, the junction between the cecum and ascending colon and the distal end of the distal colon. The gastrointestinal tract was then cut free of the mesentery and carefully removed from the peritoneum. After measuring the total gut length, the small intestine was tied off into segments of equal length. The stomach, each individual intestinal segment, the cecum, the remaining colon, and a blood sample drawn by cardiac puncture were then measured for radioactivity. For each treatment group, the distribution of ^{51}Cr throughout the gastrointestinal tract, as well as the geometric centre of ^{51}Cr distribution were determined. The latter parameter, which identifies a segment number and thus, has no units, was calculated in the following manner:

$$\text{Geometric centre} = \frac{\text{the sum of } [(\text{counts per segment} \times \text{segment number})]}{\text{total counts}}$$

Since the resected group had 75% of their small intestine removed at surgery, the length of the residual intestine and, therefore, the number of segments used to calculate geometric centre was inherently different between sham-operated and resected rats. For this reason, a direct comparison of the geometric centre for each treatment group was not a valid approach. Instead, the data were normalized by converting to a common measure,

specifically, velocity of transit, with units of cm min^{-1} . The following equation was used to derive this parameter:

$$\text{Velocity (cm min}^{-1}\text{)} = \frac{\text{geometric centre of distribution of } ^{51}\text{Cr} \times \frac{\text{intestinal length (cm)}}{\text{\# of intestinal segments}}}{30 \text{ min}}$$

Fed gastrointestinal transit was also determined. In these experiments, 6 ml of a liquid elemental diet (Sustacal) containing 2.14 μCi of $\text{Na}_2^{51}\text{CrO}_4$ were instilled into sham-operated and resected rats by orogastric gavage. All animals had been subjected to an overnight fast. In all other respects, the protocol and data analyses were identical to that of the fasting gastrointestinal transit experiments described in the preceding paragraph.

3.7. CONTRACTILE PROTEIN IMMUNOASSAY

3.7.1. Experimental design

As stated in the chapter entitled "Hypotheses and Experimental Approaches", any alterations in contractile function which occur post-resection may be the result of changes in the abundance or isoform expression of the contractile proteins actin and myosin. To this end, immunoassays for the detection of γ -enteric and α -vascular isoactins, total muscle actin and myosin heavy chain were developed. However, for technical reasons (circular and longitudinal muscle layers are more easily separated in the rabbit compared

to the rat), the model used to develop these assays was not that of massive intestinal resection in the rat, but one of *Yersinia enterocolitica* (YE) infection in the rabbit. Although these two models are obviously different, a feature common to both is an alteration in intestinal smooth muscle contractile function post-treatment (Scott and Tan, 1992). While initial experiments were ongoing in the rat model of massive resection, intestinal tissue samples were obtained from the rabbit model of YE infection to develop the immunoassays necessary to measure contractile protein content. Once established, the intent was to utilize these methodologies in the rat model of massive resection.

Briefly, the YE model consisted of three groups of New Zealand white rabbits (600 - 1000 g): untreated control, infected and pair-fed (to assess the separate effect of undernutrition associated with YE infection). Both the untreated control and pair-fed groups were sham-inoculated.

3.7.2. Tissue preparation

Six days post-inoculation animals were sacrificed by an overdose of sodium pentobarbital administered by intracardiac injection. A segment of distal ileum, previously shown to be the site of maximally altered contractility (Scott and Tan, 1992), was quickly removed and placed in ice-cold normal Krebs buffer. Tissues were opened and pinned out, mucosal side down, in wax dishes containing cold Krebs. With the aid of a dissecting microscope and fine forceps (Dumont #5), the longitudinal muscle layer was

gently peeled away from the remaining ileal tissue. Following measurement of wet weights, tissues were stored at -70°C .

At a later date, individual longitudinal muscle tissues were first minced and then homogenized by hand in a solution of 0.5 M Tris-Cl pH 6.8, 0.5 M dithiothreitol, 5% sodium dodecyl sulfate, and 10% glycerol, at a concentration of 100 mg wet weight tissue/ml buffer. All samples were stored at -70°C for later assay.

3.7.3. Protein assay

Total protein was determined in the following manner. 650 μl of ice-cold 10% trichloroacetic acid (TCA) was added to 50 μl of original sample and left on ice for 30 min. Samples were spun in a microcentrifuge at 14,000 rpm for 15 min. The supernatant was then removed and the protein pellet washed with ice-cold 70% ethanol. Following a 3 min spin in the microcentrifuge, the supernatant was again removed and the pellets left to air dry for 60 min at room temperature. Pellets were then resuspended in 50 μl of 1N NaOH. Since this was the original sample volume no dilution was made during the TCA precipitation procedure. Total protein was then determined using a BioRad DC protein assay kit. Bovine gamma globulin, which was used to generate the standard curve for the total protein assay, was also TCA-precipitated in the same manner as the study samples.

3.7.4. Immunoassays

Immunoassays for the measurement of myosin heavy chain, γ -enteric isoactin, α -vascular isoactin and total muscle actin were performed on the original samples. 50 μ l of sample, appropriately diluted in carbonate buffer (15 mM Na_2CO_3 , 35 mM NaHCO_3 ; pH 9.6), was delivered to each of three wells in a 96-well plate. Homogenization buffer, diluted in similar fashion as the treatment samples, was added to 6 - 12 wells to determine background levels. Plates were then incubated for 48-72 hours at 4°C to allow the samples/buffer to coat the wells. Using a plate washer, samples/buffer were removed from the wells and the wells washed six times with phosphate buffered saline (PBS) + 0.05% Tween 20 solution. This washing procedure was repeated after each incubation throughout the immunoassay. Non-specific binding sites were blocked with 4% BSA in PBS + 0.05% Tween 20 (30 min, room temperature). Each sample was then incubated with a single primary monoclonal antibody (1.5 h, room temperature), followed by a secondary IgG antibody peroxidase conjugate (1 h, room temperature). Colour development was achieved by the addition of 50 μ l of freshly prepared o-phenylenediamine solution (0.1 M citric acid, 0.2 M Na_2HPO_4 , 15 mg OPD, 15 μ l 30% H_2O_2) to each well. After 15 - 20 min the peroxidase reaction was terminated by the addition of 25 μ l of 2.5 M H_2SO_4 to each well. Optical density was measured at 490 nm. Within a given assay all samples were measured at the same dilution and in triplicate. The average background optical density for each plate was subtracted from all sample data.

Commercially available chicken gizzard actin was used to generate the standard curve for the γ -enteric isoactin assay, thus enabling quantification of this actin isoform. The data for α -vascular isoactin, total muscle actin and myosin heavy chain are expressed as their absolute optical densities. In all cases the level of contractile protein present in a given sample is expressed relative to its total protein content.

3.8. EXTRACELLULAR CALCIUM

Prior to manipulation of extracellular calcium flux, the contractile response, *i.e.*, maximal tonic and phasic (amplitude) stress response to 10^{-4} M bethanechol in normal Krebs buffer, was determined for rings of circular muscle from the proximal jejunum of sham-operated and resected rats. Tissues were washed twice in normal Krebs buffer. This was then replaced with either Krebs buffer containing 0 Ca^{2+} + 2 mM EGTA (0 Ca^{2+} buffer), or normal Krebs buffer containing 10^{-6} M verapamil. After a 30 min equilibration period, tissues were again stimulated with 10^{-4} M bethanechol and the contractile response measured.

3.9. MUSCARINIC RECEPTORS

3.9.1. Smooth muscle cell isolation

Binding of 1-quinuclidinyl[phenyl-4-³H] benzilate (³H-QNB) was performed on isolated cells harvested from the proximal jejunum of sham-operated and resected rats. The isolation procedure is based on previously reported methods (Bitar and Makhlouf, 1982; Collins and Gardner, 1982). Ten days post-surgery rats were lightly anesthetized with diethyl ether and sacrificed by cervical dislocation. The intestine from the ligament of Treitz to a site ~1-2 cm oral to the anastomosis was removed quickly and placed in ice-cold, oxygenated incubation buffer, the composition of which was (mM): HEPES 24.5, NaCl 101, KCl 13, NaH₂PO₄ 2.5, CaCl₂ 1.8, MgCl₂ 1.2, glutamine 2, sodium pyruvate 5, sodium fumarate 5, sodium glutamate 5, glucose 11.5, bovine serum albumin (BSA) 0.1%, and trypsin inhibitor 0.1%. To remove most of the chyme from the lumen, the intestine was flushed with cold incubation buffer using a 5 ml syringe. After carefully removing the mesentery, tissues were cut open along the mesenteric border and the mucosa/submucosa removed using a glass slide. Throughout the preparation period, tissues were examined for the presence of Peyer's patches. Upon detection, patches were excised. Tissues were cut transversely into thin slices, ~1 mm in width, and incubated at 37°C for 20 min in incubation buffer containing 150 U/ml of Type II collagenase while continuously being bubbled with 100% O₂. The digest was then filtered over polypropylene mesh (pore size 500 µm) and the tissues subjected to another round of collagenase digestion. After filtering and washing twice in 10 ml of incubation buffer

containing 4% BSA, the tissues were placed at 37°C in 10 ml of fresh incubation buffer for 30 min with continuous bubbling of O₂. Isolated smooth muscle cells were then collected by gravity filtration over a 200 µm polypropylene mesh filter. Cells were counted and diluted to a concentration of 2×10^5 cells/ml.

3.9.2. ³H-QNB Binding assay

The protocol is a modification of previously reported methods by Rimele et al. (1979) and Fox-Robichaud and Collins (1986). Binding of ³H-QNB to isolated smooth muscle cells from sham-operated and resected rats was determined over a concentration range of 0.5 to 10 nM, with individual ³H-QNB concentrations assayed in triplicate. Each reaction was performed at room temperature for 45 min using 10^5 cells. In preliminary experiments it had been determined that maximal ³H-QNB binding occurs by 30 min and remains stable for a further 20 min. At the end of the reaction time, samples were spun in a microcentrifuge at 14,000 rpm for 10 min. Cell pellets were washed with 1 ml of ice-cold incubation buffer and re-spun. The original and wash supernatants were pooled and collected in individual scintillation vials. Tissue solubilizer (0.5 ml) was added to each cell pellet and the tubes incubated for 30 min at 50°C. Each dissolved pellet, as well as each of two 1 ml washes of the reaction tube using Betamax scintillation cocktail, was transferred to a single scintillation vial. To each of the pellet scintillation vials 50 µl of glacial acetic acid and a further 8 ml of scintillation cocktail were added. All supernatant and pellet scintillation vials were then mechanically shaken for 1 h at 240

cycles/min. all vials were left to dark-adapt for >36 h and subsequently counted in a β -counter.

To determine specific ^3H -QNB binding two sets of reactions were run for each treatment group. One set, for the calculation of total binding, was prepared as described above. To each reaction tube of the other set, 150 μM of atropine was added to permit calculation of non-specific binding. The amount of ^3H -QNB bound to the cell pellet was calculated by multiplying the percentage of bound dpm (determined from the pellet and supernatant dpm data) x the total fmoles of ^3H -QNB in the reaction.

3.10. STATISTICAL ANALYSES

Statistical analyses were performed using the software package Systat (Evanston, IL, USA). In cases of multiple comparisons (across treatment groups or comparison of length of time post-surgery) statistical significance of the difference between means was determined at $p < 0.05$ using a one-way or two-way analysis of variance (ANOVA) followed by Tukey's procedure for the post hoc comparison of pairs of means. Data which generated linear (food intake and weight gain) and non-linear relationships (basal length-stress, concentration-response, binding curves) were subjected to least-squares regression analyses. The details of the analyses have been previously reported (Meddings et al., 1989). The remaining data were compared using Student's t-test or paired t-test, as appropriate. Results were considered significantly different when the p-value was < 0.05 .

CHAPTER FOUR

RESULTS I

CHARACTERIZATION OF THE MODEL

4.1. BODY WEIGHT AND FOOD INTAKE

The growth of untreated control, sham-operated and resected groups up to 40 days post-surgery is shown in Figure 4.1. Mean body weights of the three treatment groups were not significantly different on day 0, increased significantly throughout the study period, and were not significantly different from each other on day 40.

Daily food intake for the untreated control and resected groups up to 40 days post-surgery is graphed in Figure 4.2. Once resected animals were allowed access to rat chow *ad libitum* on post-operative day 5, their mean daily food intake was initially significantly greater ($p < 0.05$, paired Student's t-test) than sham-operated (on days 6,7,8,10,12,14 and 17) or untreated control rats (on days 5,6,7,8,10,13,14,16,17,19 and 22). When linear regression analysis of the mean daily food intake as a function of treatment group and post-operative day was applied to the whole data set, untreated control animals had a lower initial mean daily food intake (y intercept of 27.9 g/day) and a slight increment in mean daily food intake with the passage of time (the slope of the line being positive), while resected rats had a higher initial daily food intake (y intercept of 32.3 g/day) and a slight decrease in mean daily food intake with time (the slope of the line being negative). By post-operative day 40, there was no significant difference in the daily food intake of untreated control and resected animals. Food intake of the sham-operated group was not significantly different from untreated control rats and for the sake of clarity has not been graphed.

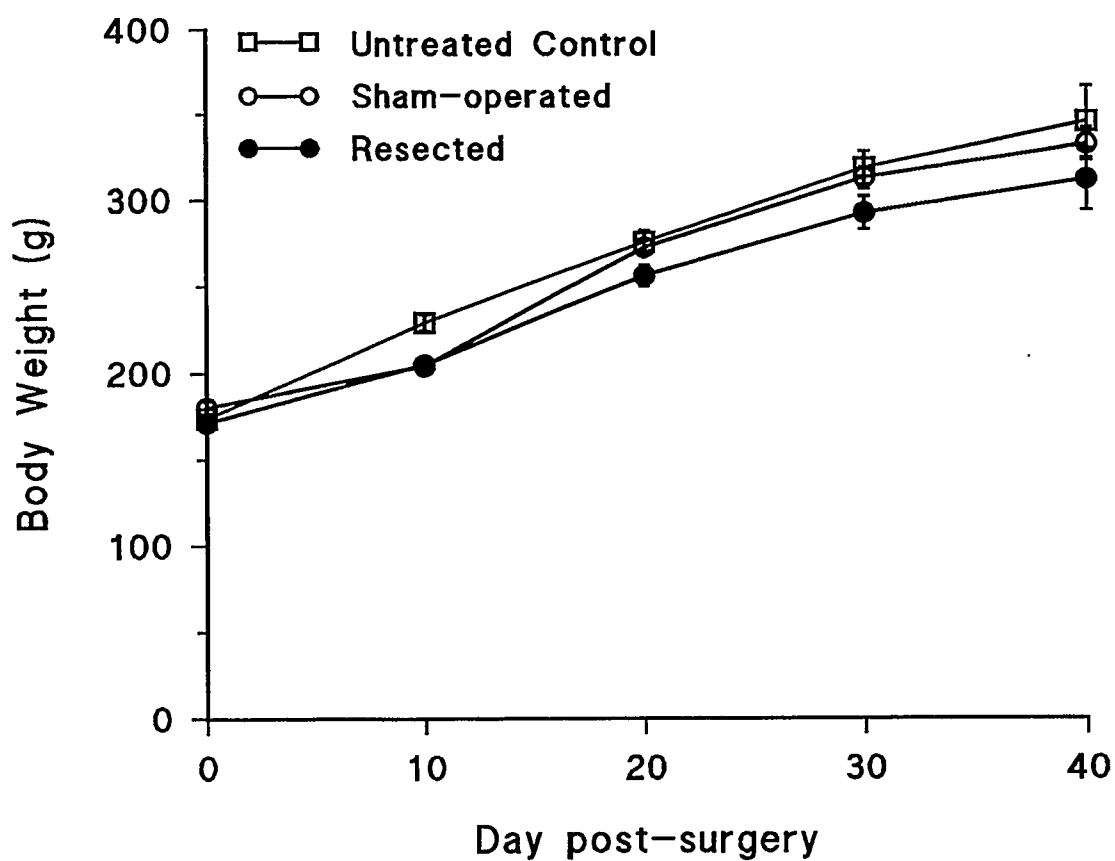
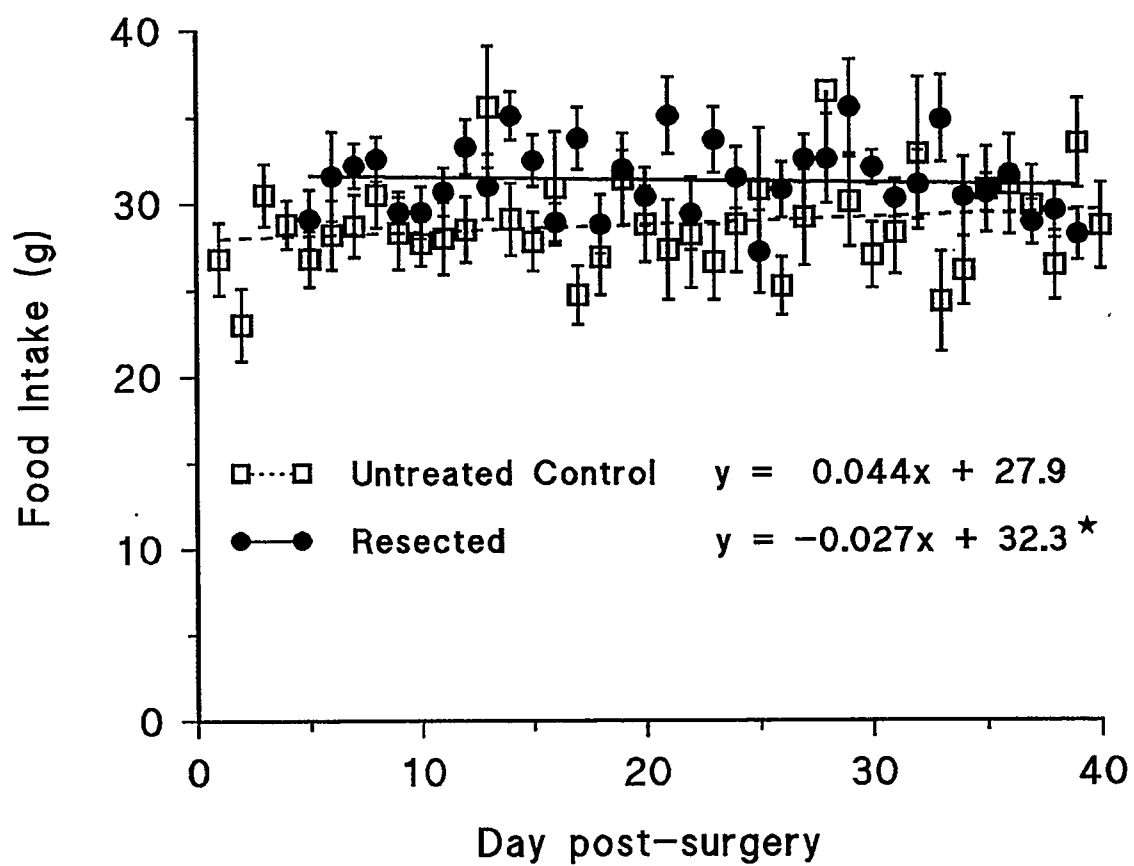


Figure 4.1. Body weight. The figure shows the mean body weight (g) of untreated control, sham-operated and resected groups on days 0, 10, 20, 30 and 40. There were no significant differences among groups. $n=14$ per treatment group.

Figure 4.2. Daily food intake. The figure shows the daily food intake (g) of untreated control and resected rats over the 40 day study period. Untreated control animals had a lower initial daily food intake, and showed a slight increase in daily food intake with time. In contrast, resected animals had a higher initial daily food intake which decreased with time. By post-operative day 40 the daily food intake of untreated control and resected animals was similar. Food intake of the sham-operated group was not significantly different from untreated control animals and is not graphed. To determine if food intake differed between the untreated control and resected groups, linear regression analysis was performed and the regression lines plotted. The y intercepts (mean daily food intake on day 0) and slopes (rate of change of food intake in g/day) are indicated in the body of the Figure and are significantly different. ★ $p < 0.001$. $n = 14$ per treatment group.



4.2. INTESTINAL ADAPTATION

4.2.1. Intestinal length, circumference and wet weight

There was no significant difference in the initial length (day 0) of the intestine between the ligament of Treitz and the ileocecal valve in the untreated control (94 ± 2.2 cm), sham-operated (94 ± 1.8 cm) or resected (96 ± 1.1 cm) groups. In resected rats, there was no statistically significant increase in the length of the residual intestine with time (16.2 ± 0.7 cm, 16.6 ± 0.3 cm, 16.8 ± 0.3 and 17.1 ± 0.3 cm on days 10, 20, 30 and 40, respectively).

In contrast, there was an adaptive increase in the jejunal circumference of the remnant bowel in resected compared to both untreated control and sham-operated groups.

As indicated in Figure 4.3 this increase reached significance on post-operative day 30 and persisted to day 40. Jejunal circumference for untreated control and sham-operated rats did not change over the course of the study period.

The wet weight per 5 cm length of full thickness jejunum is shown in the upper panel of Figure 4.4 for untreated control, sham-operated and resected animals. There was a significant increase in the wet weight per unit length in the resected as compared to the untreated control or sham-operated groups which was apparent by post-operative day 10 and persisted thereafter. To determine whether this increase was attributable to an increased mass of mucosa, or muscularis propria, or both, the mucosa was scraped from the jejunal segments and the wet weight per 5 cm of the mucosa and the muscularis propria were determined separately for each of the three treatment groups. The lower

panel of Figure 4.4 shows the wet weight per 5 cm of the muscularis propria. Both sets of data showed a significant increase by post-operative day 10, an increase which persisted thereafter.

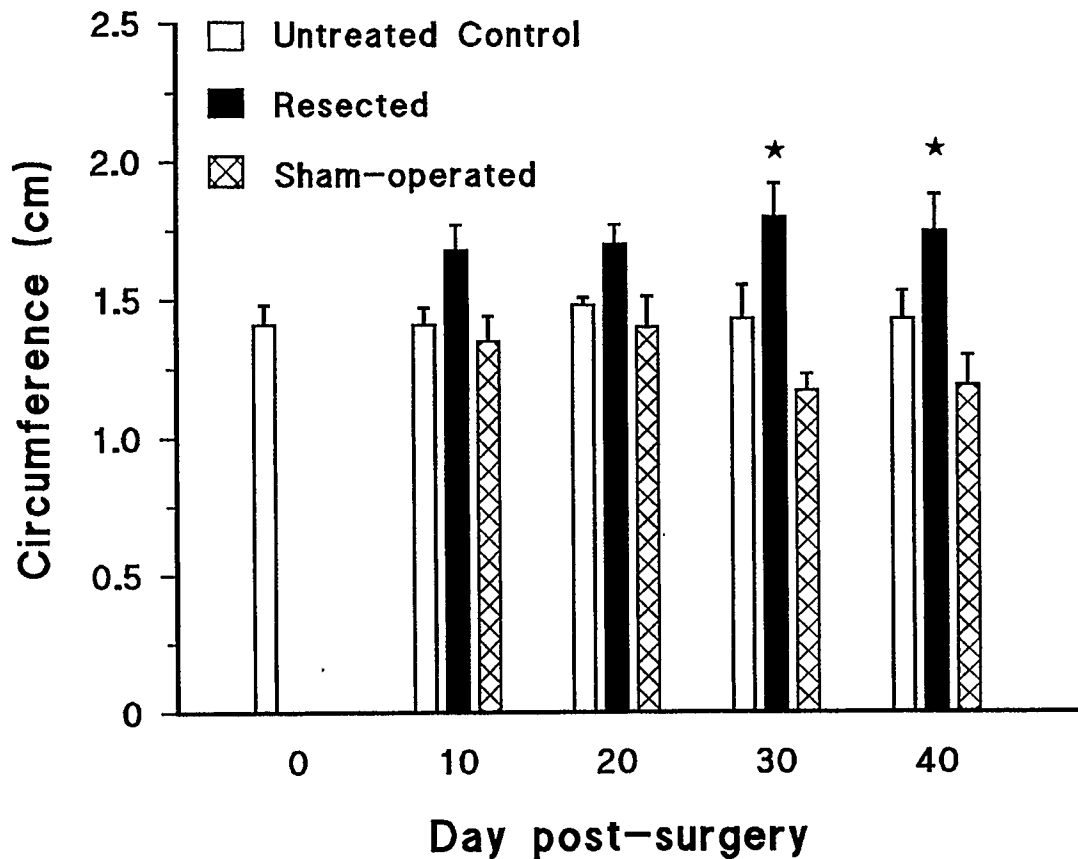
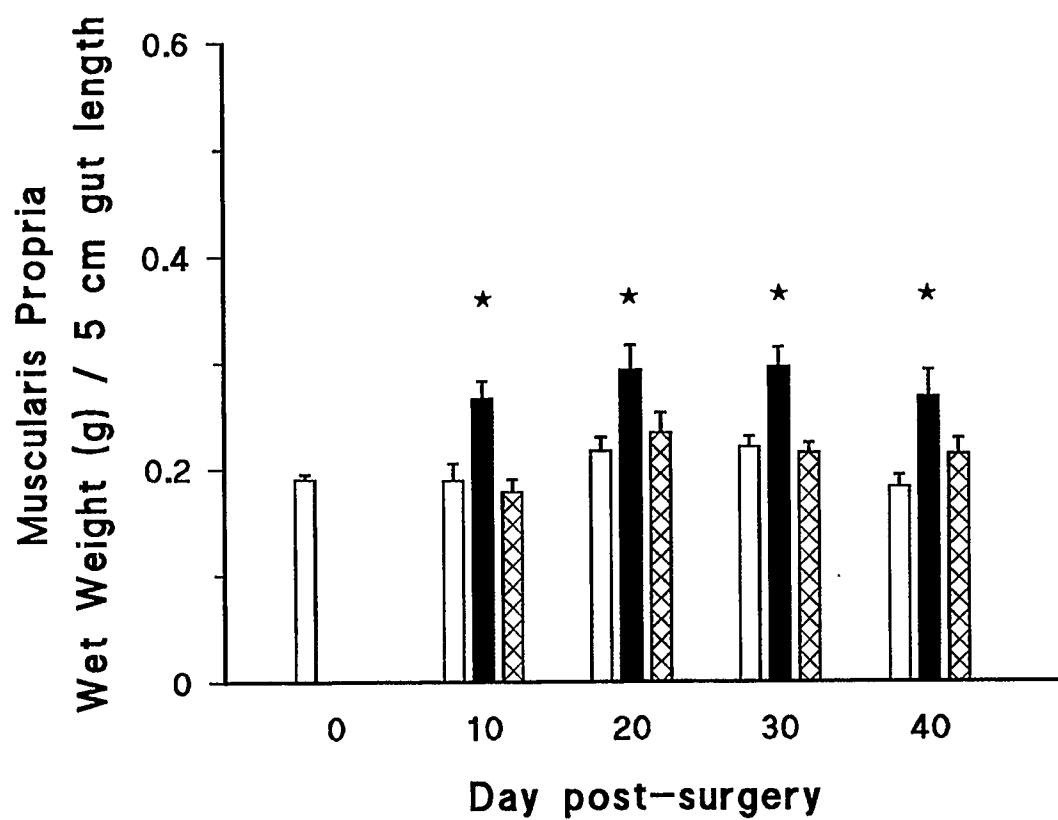
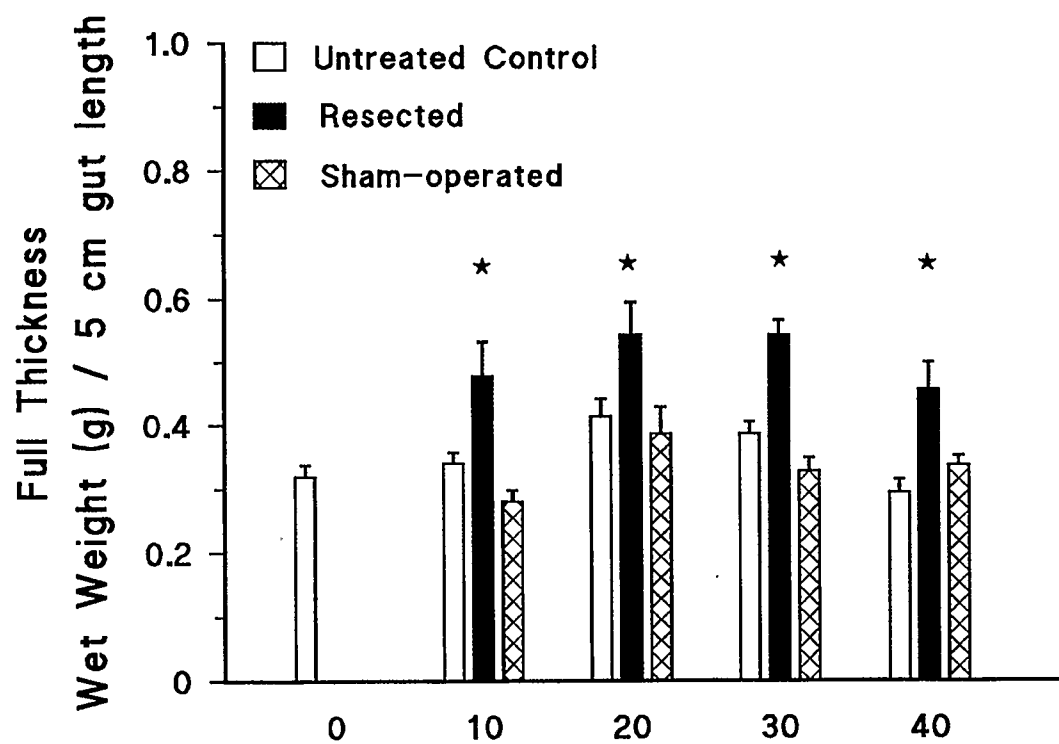


Figure 4.3. Jejunal circumference. The jejunal circumference (cm) of untreated, sham-operated and resected groups is shown. There were no significant temporal changes in intestinal circumference within either the untreated control or sham-operated groups. Compared to both other treatment groups, resection significantly increased jejunal circumference on post-operative days 30 and 40. ★ $p < 0.05$. $n = 14$ per treatment group.

Figure 4.4. Wet weight per unit length of full thickness jejunum and muscularis propria alone. Compared to both other treatment groups, resection produced a significant increase in the wet weight (g) per 5 cm length of both the full thickness jejunum (*upper panel*) and the muscularis propria (*lower panel*) alone. ★ $p < 0.05$. $n = 14$ per treatment group.



4.2.2. Histological assessment

To determine if, in addition to the increase in circumference, a concomitant increase in the thickness of the muscularis propria contributed to the greater wet weight post-resection, the tissue depth of the circular and the longitudinal muscle layers for each treatment group was assessed. As shown in Figure 4.5, there was no significant increase in the depth of either the circular (*upper panel*) or longitudinal (*lower panel*) muscle layers of resected rats at any time during the 40 day study period.

The adaptive increase in mass and circumference of the muscularis propria post-resection could be the result of an increased number (hyperplasia) or and increased size (hypertrophy) of the smooth muscle cells. Using histological cross-sections of the circular muscle layer (magnification 1000 x power) it was determined that cell density was not altered after massive resection. For untreated control, sham-operated and resected groups the number of smooth muscle cells per unit area was $78.7 \pm 13.7 \times 10^3 \text{ mm}^{-2}$, $58.8 \pm 8.7 \times 10^3 \text{ mm}^{-2}$, and $57.6 \pm 4.3 \times 10^3 \text{ mm}^{-2}$, respectively. This suggests that there was no change in the size of smooth muscle cells as part of the adaptive response to resection.

4.2.3. Biochemical assessment

Before the biochemical data (measurements of total protein and DNA per unit length of muscularis propria) could be assessed, preliminary histological evaluation of scraped tissue was performed to assess the effectiveness of the scraping technique for

removal of mucosa and submucosa from the muscularis propria. Duplicate samples from eight untreated control animals were assessed. Scraped tissues showed no residual mucosa, with some submucosal tissue remaining adherent to the muscularis propria in every sample. Scraping stretched and thinned the remaining tissue such that the total thickness of the residual submucosa, circular and longitudinal muscle layers was 43% of unscraped control tissue. The validity of the protein to DNA ratio depends upon whether the scraped preparation represents primarily muscle tissue and also upon the variability of that tissue content from sample to sample. To estimate these parameters, the number of cell nuclei in the residual submucosa, circular and longitudinal muscle layers were expressed as a percent of the total number of cell nuclei per linear mm of the tissue sections. $30 \pm 3\%$ of cells were found to lie in the residual submucosa, with $53 \pm 2\%$ and $17 \pm 1\%$ of cells belonging to the circular and longitudinal muscle layers, respectively. Thus, the preparation was very consistent in yielding tissue that on the basis of the numbers of cell nuclei was 70% muscularis propria.

The total protein and DNA content per cm length of jejunal muscularis propria are listed in Table 4.1. Protein and DNA content per cm were similar between untreated control and sham-operated animals. In contrast, compared to the sham-operation, resection produced a significantly greater protein (days 20, 30 and 40) and DNA (days 10, 20, 30 and 40) content per cm. However, as Figure 4.6 demonstrates, when the data are expressed as the ratio of protein : DNA, *i.e.*, mg protein per μg DNA per cm length of muscularis propria, there was no significant change in any treatment group over the 40

day post-operative period. This finding is consistent with the histological data, indicating that the adaptive increase in mass and circumference of the muscularis propria is hyperplasia, and not hypertrophy.

Figure 4.5. Depth of individual muscle layers. The figure shows the depth (μm) of jejunal circular and longitudinal muscle obtained from unoperated control, sham-operated and resected rats. Resection had no effect on the tissue depth of either muscle layer over the 40 day study period. $n=14$ per treatment group.

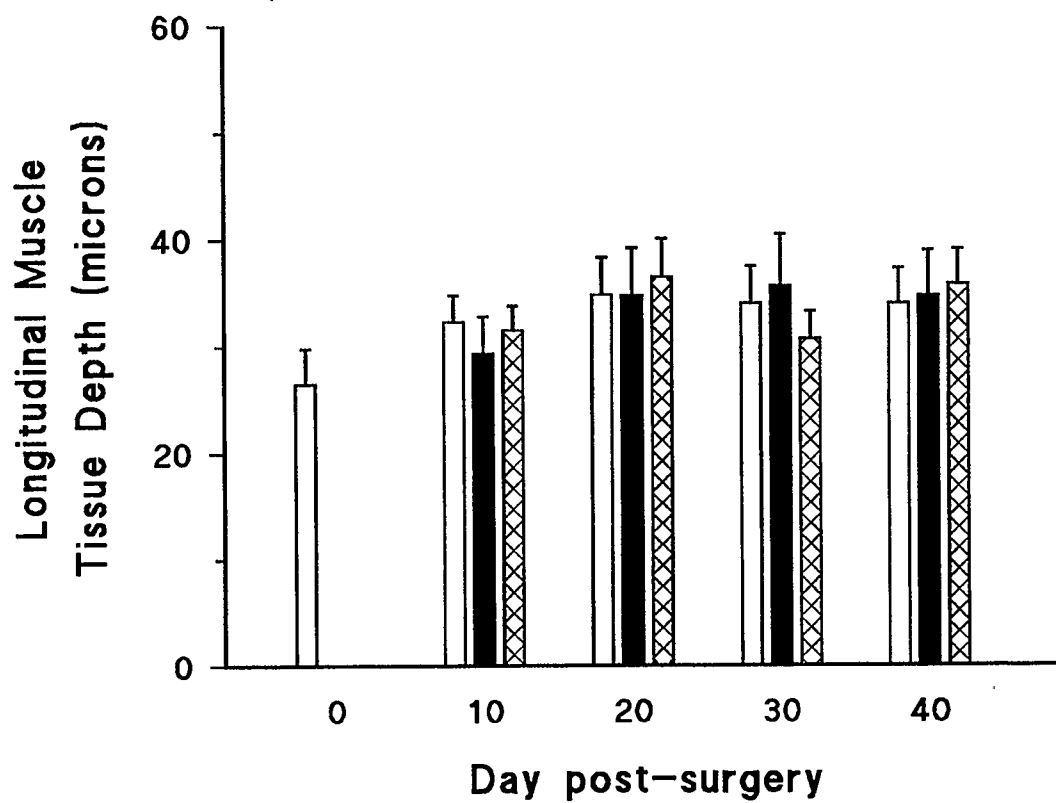
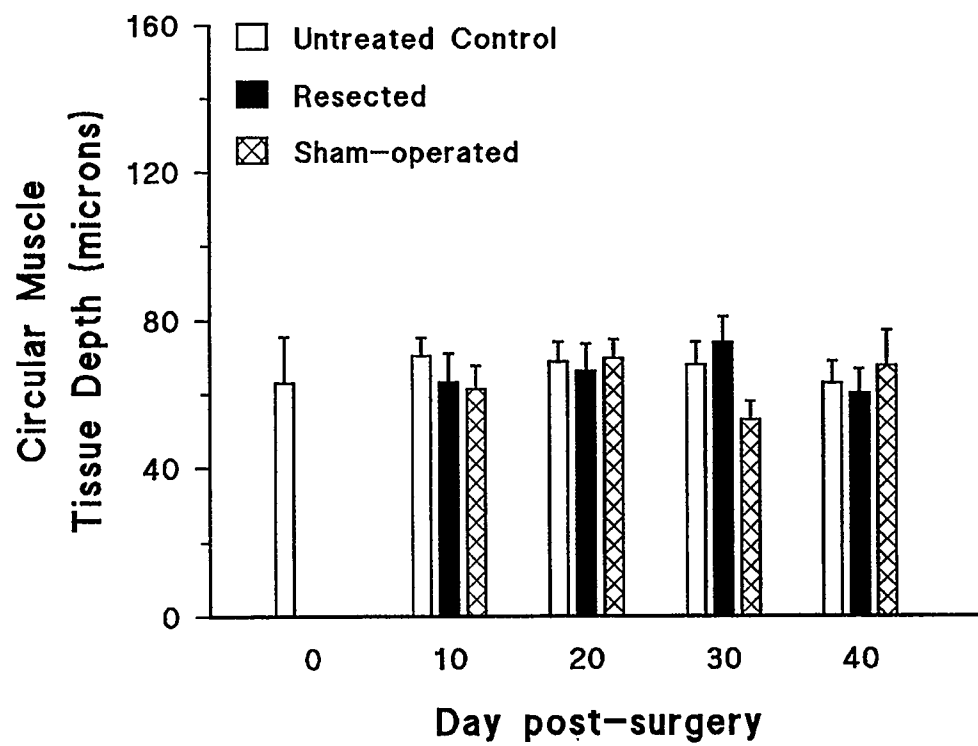


Table 4.1. Total protein and DNA content. The table shows the total protein (mg) and DNA content (μg) per cm length of muscularis propria obtained from untreated control, sham-operated and resected rats. The untreated control group was not significantly different from the sham-operated group at any given time point. For both groups, there was no temporal effect on either parameter. Compared to the sham-operated group, resection significantly increased both total protein and DNA content per unit gut length.

★ $p < 0.05$. $n = 14$ per treatment group.

Table 4.1. Total protein and DNA content.

Day	Group	mg protein/cm	μg DNA/cm
0	Control	7.19 ± 0.20	45.98 ± 2.74
10	Control	8.69 ± 0.48	46.53 ± 5.24
	Sham-operated	7.20 ± 0.96	37.07 ± 2.52
	Resected	11.69 ± 2.29	67.53 ± 14.10 *
20	Control	8.79 ± 0.48	46.07 ± 3.28
	Sham-operated	8.25 ± 1.02	43.79 ± 4.95
	Resected	14.76 ± 3.17 *	87.86 ± 21.37 *
30	Control	8.43 ± 0.39	39.92 ± 1.62
	Sham-operated	6.88 ± 0.87	41.02 ± 2.84
	Resected	10.13 ± 0.48 *	77.24 ± 11.79 *
40	Control	7.21 ± 0.41	38.82 ± 2.24
	Sham-operated	6.24 ± 0.58	33.66 ± 2.34
	Resected	9.15 ± 0.64 *	56.00 ± 5.14 *

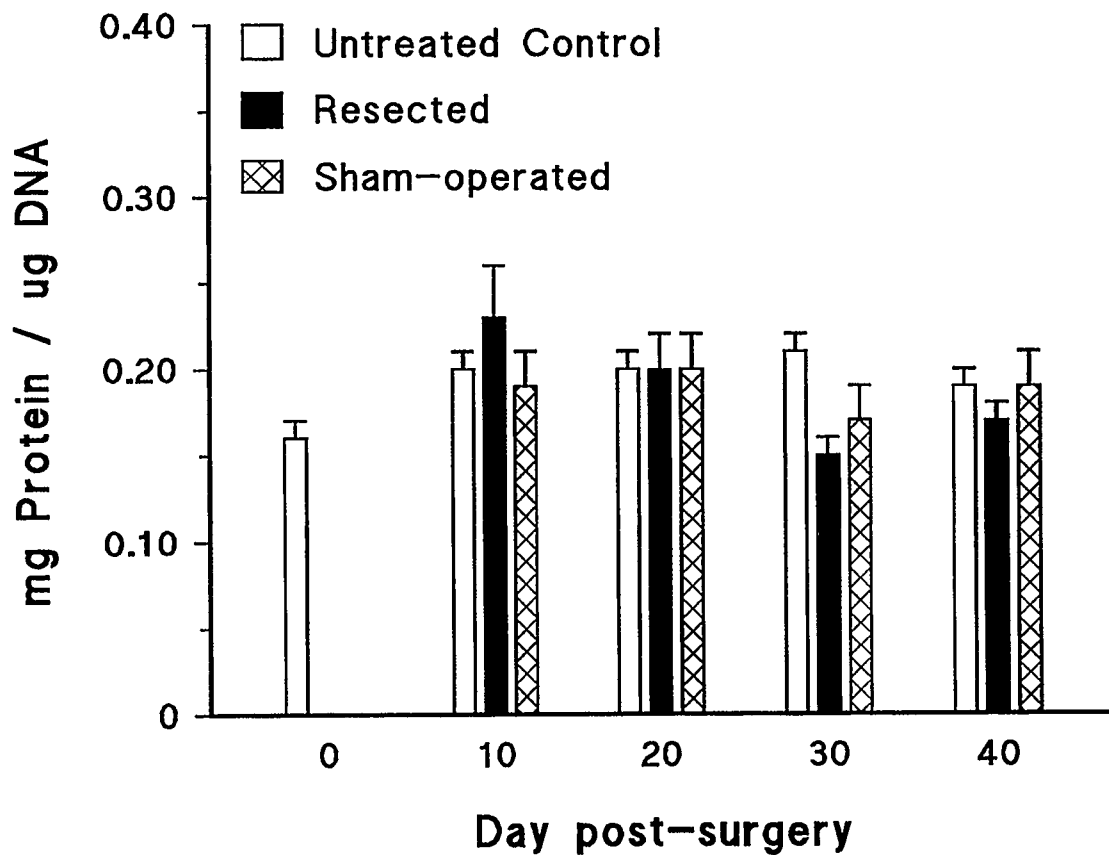


Figure 4.6. Ratio of total protein to DNA content. The figure shows the ratio of total protein to DNA content per cm length of muscularis propria (mg/ μ g/cm) obtained from untreated control, sham-operated and resected rats. Compared to untreated control and sham-operated groups, resection did not significantly alter this ratio at any time during the 40 day post-operative period, demonstrating that the post-resection adaptive response is characterized by hyperplasia, and not hypertrophy. $n=14$ per treatment group.

4.3. SUMMARY OF MORPHOLOGICAL STUDIES

Following massive intestinal resection, there was an initial period of significantly greater food intake. Resected animals were able to compensate for the impact of reduced absorptive surface area and maintain a normal growth velocity. Intestinal adaptation was characterized by a significant increase in the circumference, but not the length of the residual intestine. Jejunal wet weight per cm length of bowel, both the full thickness and the muscularis propria alone, was also significantly elevated, without an accompanying increase in the depth of the circular or longitudinal muscle layers. Concomitant with the increased circumference and mass of the muscularis propria per cm were increases in mg protein and μg DNA per cm. However, resection did not alter smooth muscle cell density or the ratio of mg protein/ μg DNA/cm length of bowel, indicating that the adaptive response of the muscularis propria represents smooth muscle hyperplasia and not hypertrophy.

CHAPTER FIVE

RESULTS II

LONGITUDINAL SMOOTH MUSCLE CONTRACTILITY

5.1. MORPHOLOGICAL ADAPTATION

Within the two treatment groups studied, sham-operated and resected, jejunal circumference did not differ significantly with respect to length of time post-surgery (days 10, 20, 30 and 40) and, therefore, for this parameter, data were pooled (n=28 per treatment group). Consistent with the findings of the characterization studies, jejunal circumference was significantly ($p < 0.05$) greater in resected (1.7 ± 0.1 cm) compared to sham-operated rats (1.3 ± 0.1 cm). Typical recordings of the spontaneous and bethanechol-stimulated contractile activity of jejunal longitudinal smooth muscle, taken on day 10 post-surgery, are shown in Figure 5.1.

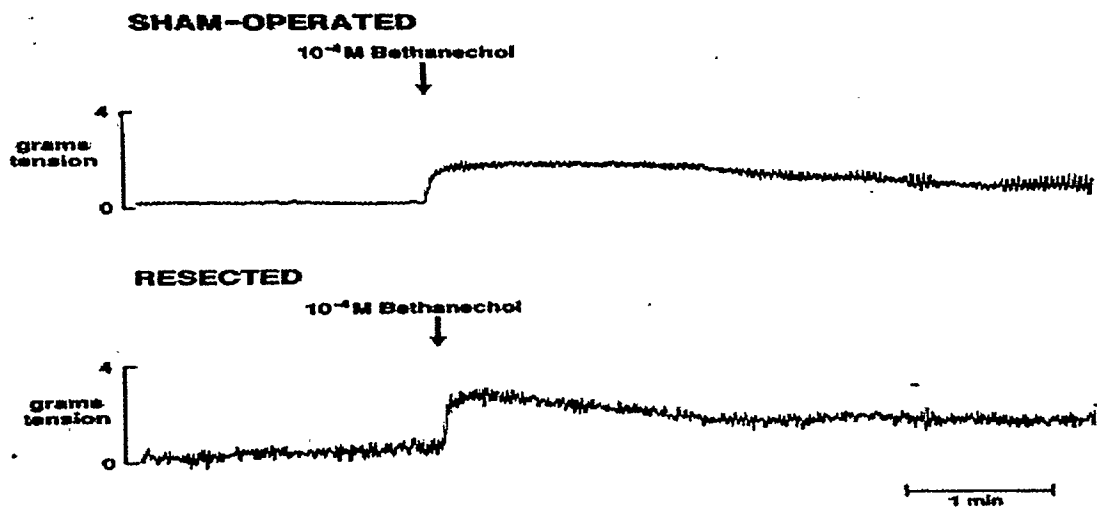


Figure 5.1. Representative tracings of jejunal longitudinal muscle contractile activity. A period of spontaneous phasic contractile activity precedes the ↓, which indicates the time of addition of the muscarinic agonist, bethanechol, to the tissue bath.

5.2. LENGTH-BASAL STRESS RESPONSE

Within both treatment groups at all times post-surgery, there was an exponential increase in basal stress in response to incremental stretch. The basal stress (S , in mNewtons/mm²) at any length (L , expressed as the percent increment of initial length (L_i)), is given by:

$$S = Ae^{(mL)} + C$$

where A , m and C are constants. For the purpose of these studies, $A = 1$, m defines the rate of exponential increase in tension per the percent increment in L_i , and C is the y axis intercept if tension is plotted against length on Cartesian co-ordinates. Since by definition tension equals zero when the tissue is at its initial resting length (percent increment of $L_i = 0$), then by substitution C must = -1. Using this formula, estimates were made of the curve parameter "m" for sham-operated and resected rats.

Table 5.1 shows that there were no significant differences in basal length-stress between treatment groups at any post-operative time, which indicates that factors such as tissue elasticity and alterations in the connective tissue matrix are unchanged post-resection. A representative length-basal stress response curve is presented in Figure 5.2.

Day	Sham-operated	Resected	p
10	0.068 ± 0.004	0.072 ± 0.003	ns
20	0.060 ± 0.002	0.050 ± 0.002	ns
30	0.054 ± 0.001	0.061 ± 0.003	ns
40	0.069 ± 0.064	0.058 ± 0.002	ns
combined 10 - 40	0.063 ± 0.002	0.064 ± 0.001	ns

Table 5.1. Basal stress "m" parameter values. Calculated from the length basal-stress data, the magnitude of the parameter "m" defines the rate of exponential increase in stress per percentage increment of initial unstretched tissue length (L_i) of longitudinal muscle. No differences were observed between the two treatment groups at any time during the study period, indicating that factors such as tissue elasticity and alterations in the connective tissue matrix are unchanged in longitudinal smooth muscle post-resection. ns, not significant. n=7 per treatment group.

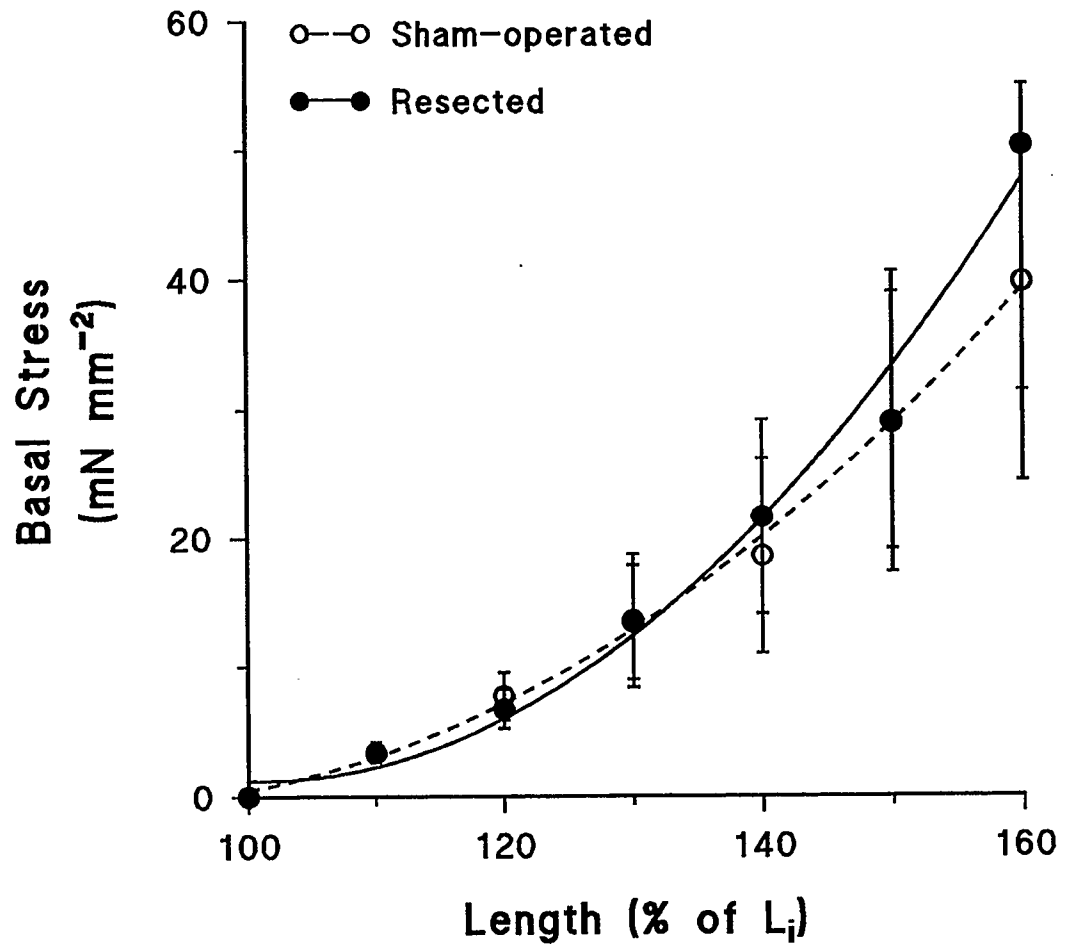


Figure 5.2. Length-basal stress response. A representative length-basal stress (% of L_i-mN mm⁻²) response curve is shown for jejunal longitudinal muscle obtained from sham-operated and resected rats on post-surgical day 10. Resection had no effect on the elastic properties of longitudinal smooth muscle. n=7 for both treatment groups.

5.3. ACTIVE TONIC CONTRACTILE RESPONSES

The following section deals with the tonic stress response of jejunal longitudinal muscle following stimulation. Figure 5.3 schematically illustrates this specific contractile parameter.

5.3.1. Length-active stress response and optimal length

For all muscular tissue there exists a muscle length at which peak active tension is developed in response to a contractile stimulus. This specific length is defined as the optimal length, L_o , for that muscle. In this model of massive resection, there was no effect of the length of time post-surgery on longitudinal muscle L_o for either the sham-operated or resected groups and, consequently, data were pooled within treatment groups. L_o (expressed as a percentage of L_i) for sham-operated and resected groups was $125.7 \pm 2.7\%$ and $131.8 \pm 3.1\%$, respectively, values which are not significantly different. For all subsequent experiments, tissues were studied at an L_o of 130% of L_i .

5.3.2. Concentration-tonic stress response to bethanechol

The active tonic stress generated by stimulation with the muscarinic receptor agonist bethanechol (10^{-9} to 10^{-4} M) was determined in longitudinally oriented jejunal tissues from sham-operated and resected animals on post-operative days 10, 20, 30 and 40. As Figure 5.4. shows, there were no significant differences in maximal stress (S_m), or in the EC_{50} (the concentration at which half-maximal stress is generated) values for the

two treatment groups 10 days post-surgery. Similarly, resection did not alter the bethanechol-stimulated concentration-stress responses of days 20, 30 and 40. Statistical analysis (ANOVA and Tukey's procedure) of the data did not permit pooling of the data with respect to length of time post-surgery within treatment groups, and as such only the data from post-surgical day 10 have been plotted (Figure 5.4). The data from days 20, 30 and 40 are presented in Table 5.2.

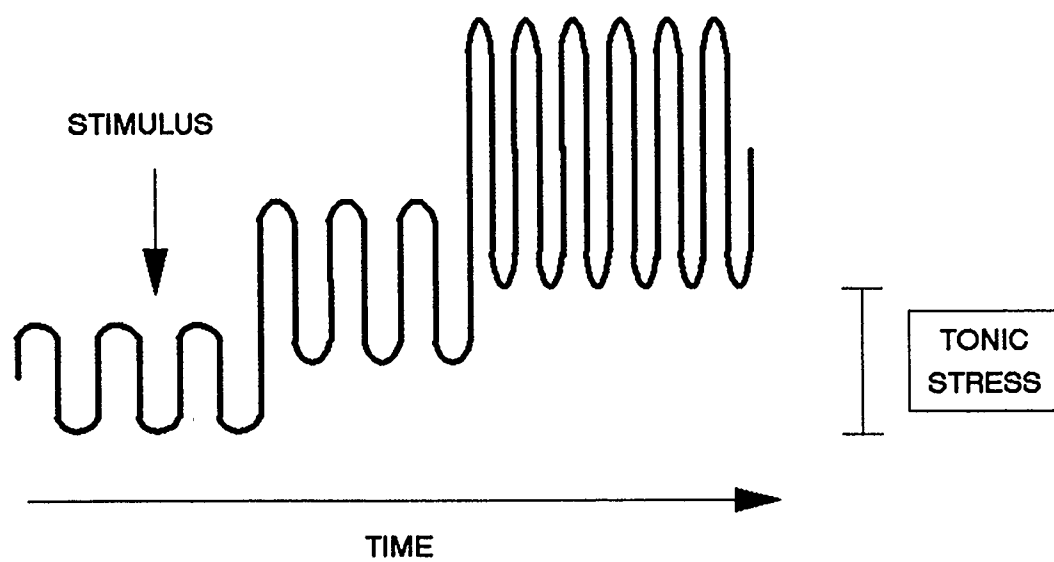


Figure 5.3. Schematic diagram of active tonic stress.

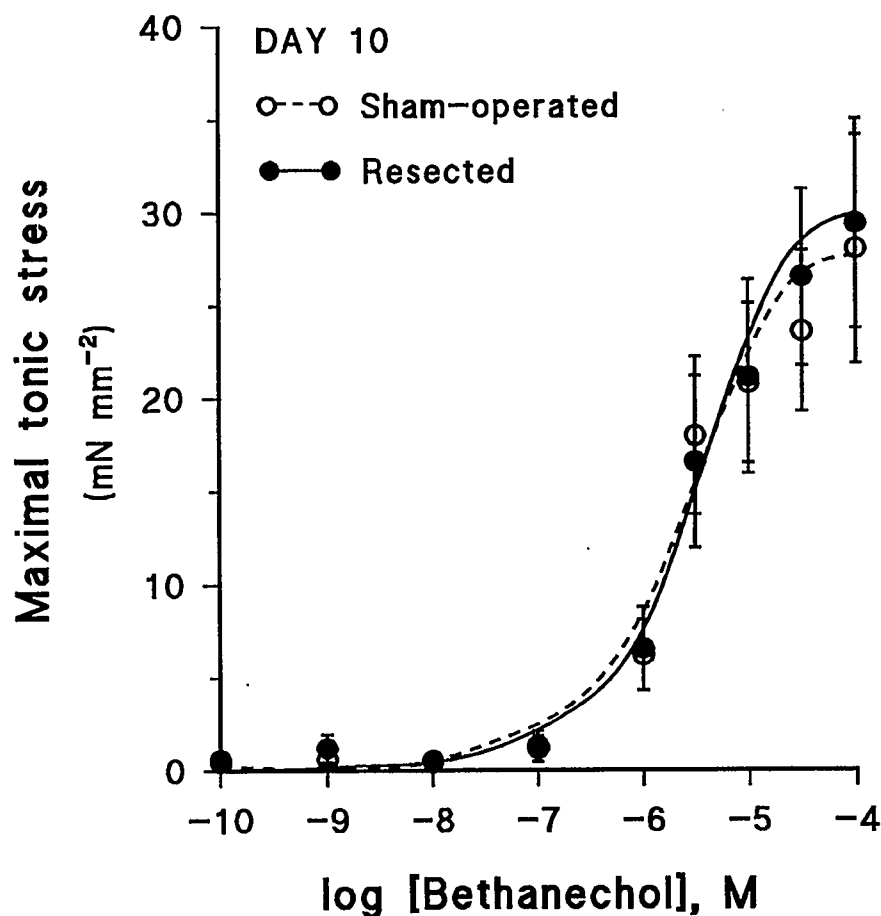


Figure 5.4. Day 10 concentration-ionic stress response to bethanechol. The maximal active tonic stress (mN mm⁻²) developed by jejunal longitudinal smooth muscle obtained from sham-operated and resected rats 10 days after surgery is shown. There were no significant differences in EC₅₀ (concentration at which half-maximal stress is generated) or S_m (maximal stress) between sham-operated and resected groups. n=7 per treatment group.

Table 5.2. Day 20, 30 and 40 concentration-tonic stress responses to bethanechol. The maximal active tonic stress (mN mm^{-2}) developed by jejunal longitudinal smooth muscle from sham-operated and resected rats in response to stimulation with bethanechol (Beth). Similar to the data from day 10, there were no significant differences in EC_{50} or S_m between groups on post-surgical days 20, 30 or 40. This information is presented in tabular format as statistical analysis would not permit pooling of the data over time within treatment groups. $n=7$ per group.

Table 5.2. Concentration-tonic stress responses to bethanechol.

log [Beth], M	Day 20		Day 30		Day 40	
	SHAM	RES	SHAM	RES	SHAM	RES
-10	0.74 ± 0.52	0.16 ± 0.11	0.48 ± 0.29	0.17 ± 0.17	0.12 ± 0.09	0.23 ± 0.12
-9	0.46 ± 0.17	0.25 ± 0.18	0.42 ± 0.16	0.85 ± 0.50	0.30 ± 0.11	0.36 ± 0.21
-8	0.45 ± 0.21	0.31 ± 0.11	0.24 ± 0.16	0.46 ± 0.22	0.12 ± 0.09	0.42 ± 0.20
-7	1.03 ± 0.22	1.74 ± 0.87	0.84 ± 0.31	0.71 ± 0.40	0.69 ± 0.32	0.89 ± 0.21
-6	7.93 ± 2.59	8.44 ± 3.10	4.35 ± 0.95	3.57 ± 0.58	3.42 ± 0.93	6.23 ± 2.30
-5.5	15.32 ± 4.77	14.76 ± 4.55	9.93 ± 1.67	8.01 ± 1.19	9.29 ± 1.67	14.31 ± 4.02
-5	20.95 ± 5.98	19.52 ± 4.76	13.30 ± 1.47	10.75 ± 1.26	12.25 ± 2.13	15.92 ± 4.00
-4.5	24.11 ± 5.65	24.53 ± 3.77	16.71 ± 1.44	18.12 ± 1.36	18.55 ± 3.88	17.92 ± 1.51
-4	25.56 ± 5.74	24.54 ± 2.48	19.51 ± 3.02	18.52 ± 1.18	17.79 ± 4.52	21.26 ± 3.45

5.3.3. Concentration-tonic stress response to KCl

Similar to the findings with bethanechol stimulation, tissues from sham-operated and resected rats did not differ in the amount of active tonic stress generated following graded depolarization with KCl. These data are presented in Table 5.3.

Table 5.3. Concentration-tonic stress responses to KCl. The maximal tonic stress (mN mm⁻²) developed by jejunal longitudinal smooth muscle taken from sham-operated (SHAM) and resected (RES) rats is shown. ★ p<0.05 SHAM vs. RES. n=7 per treatment group for each time point studied.

Table 5.3. Concentration-tonic stress responses to KCl.

[KCl] (mM)	Day 10		Day 20		Day 30		Day 40	
	SHAM	RES	SHAM	RES	SHAM	RES	SHAM	RES
5.9	16 ± 4	15 ± 3	13 ± 4	19 ± 2	10 ± 2	15 ± 2	11 ± 2	15 ± 2
10	21 ± 4	9 ± 2*	26 ± 5	27 ± 2	22 ± 3	16 ± 3	19 ± 4	17 ± 3
20	33 ± 6	18 ± 4	31 ± 6	26 ± 4	26 ± 5	18 ± 2	13 ± 5	20 ± 3
30	35 ± 7	23 ± 5	34 ± 6	25 ± 3	28 ± 5	20 ± 2	17 ± 5	22 ± 3
40	37 ± 7	25 ± 4	37 ± 4	34 ± 3	30 ± 4	24 ± 2	28 ± 5	26 ± 4
60	37 ± 8	28 ± 3	36 ± 5	35 ± 4	31 ± 5	22 ± 2	30 ± 6	24 ± 3
80	27 ± 2	28 ± 3	39 ± 5	36 ± 4	29 ± 4	22 ± 2	29 ± 6	25 ± 4

5.4. ACTIVE PHASIC CONTRACTILE ACTIVITY

The phasic contractile activity of intestinal smooth muscle consists of two components, frequency and amplitude, which are superimposed on the distinct tonic contractile activity of the tissue. These parameters are illustrated in Figure 5.5.

5.4.1. Basal and bethanechol-stimulated phasic frequency

Within treatment groups, the frequencies of spontaneous and bethanechol-stimulated phasic contractile activity were not different with respect to length of time post-surgery and, therefore, data were pooled (Appendices I, II). Comparison between treatment groups revealed that tissues from resected rats demonstrated a significant ($p < 0.05$) increase in phasic contractile frequency in both the basal state and after bethanechol stimulation. These results are presented in Figure 5.6. The concentration of 10^{-6} M was chosen to approximate the EC_{50} , while 10^{-4} M was used to provoke a maximal response.

5.4.2. Basal and bethanechol-stimulated phasic amplitude

Within each treatment group, the amplitude of phasic contractile activity before and after stimulation with bethanechol was not significantly different with length of time post-surgery and, therefore, data were pooled (Appendices III, IV). As shown in Figure 5.7, tissues from resected rats exhibited a significantly greater amplitude of phasic contractile activity both in the basal state and following stimulation with bethanechol.

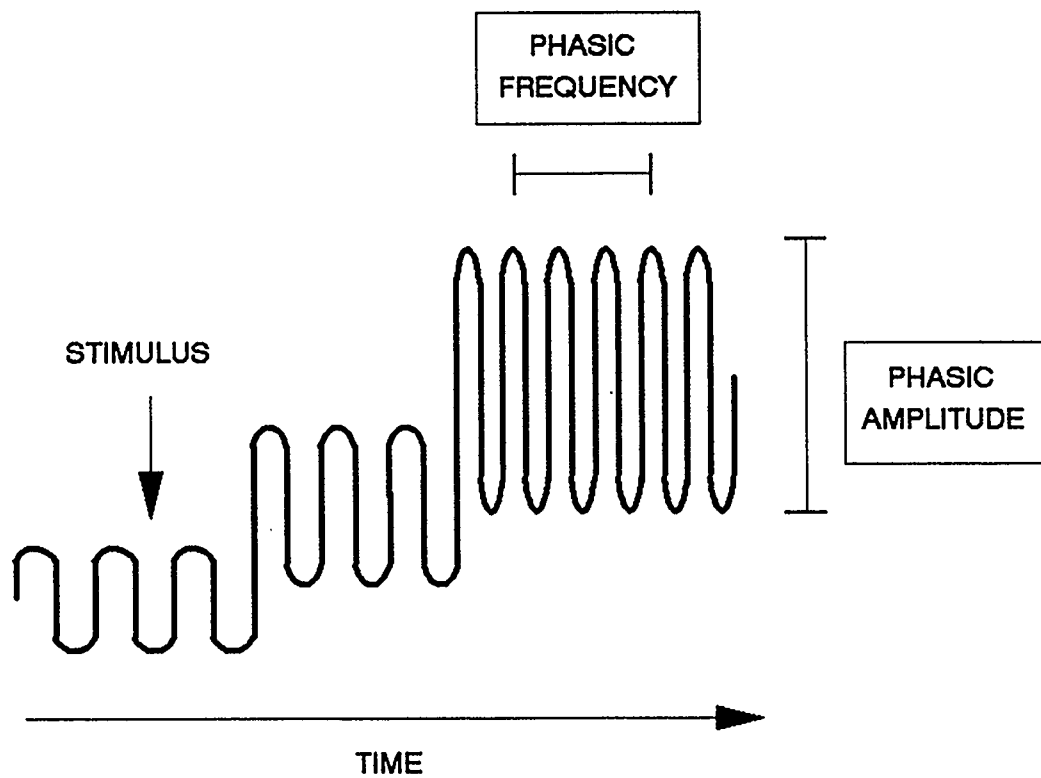


Figure 5.5. Schematic diagram of phasic frequency and amplitude.

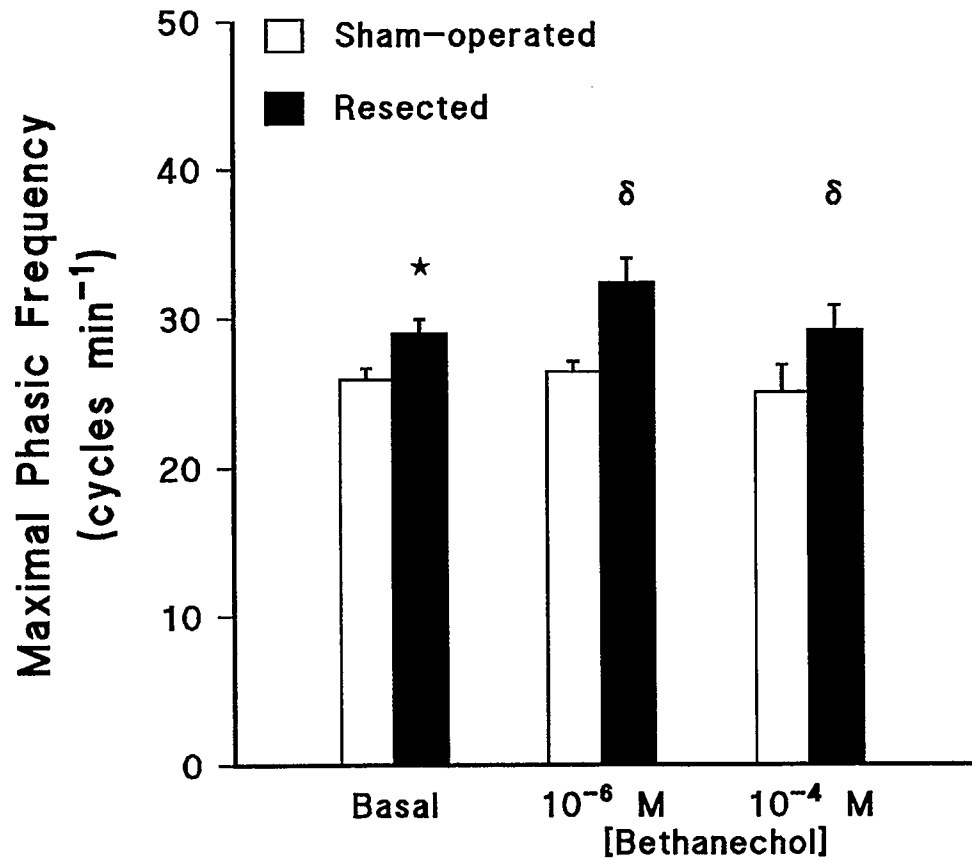


Figure 5.6. Frequency of phasic contractile activity. Basal and bethanechol-stimulated phasic contractile frequencies (cycles min⁻¹) of jejunal longitudinal muscle from sham-operated and resected rats. ★ indicates $p < 0.05$, under basal conditions. δ indicates a significant increase in the response of resected tissues post-bethanechol stimulation ($p < 0.05$, pooled data, ANOVA). $n = 7$ per treatment group.

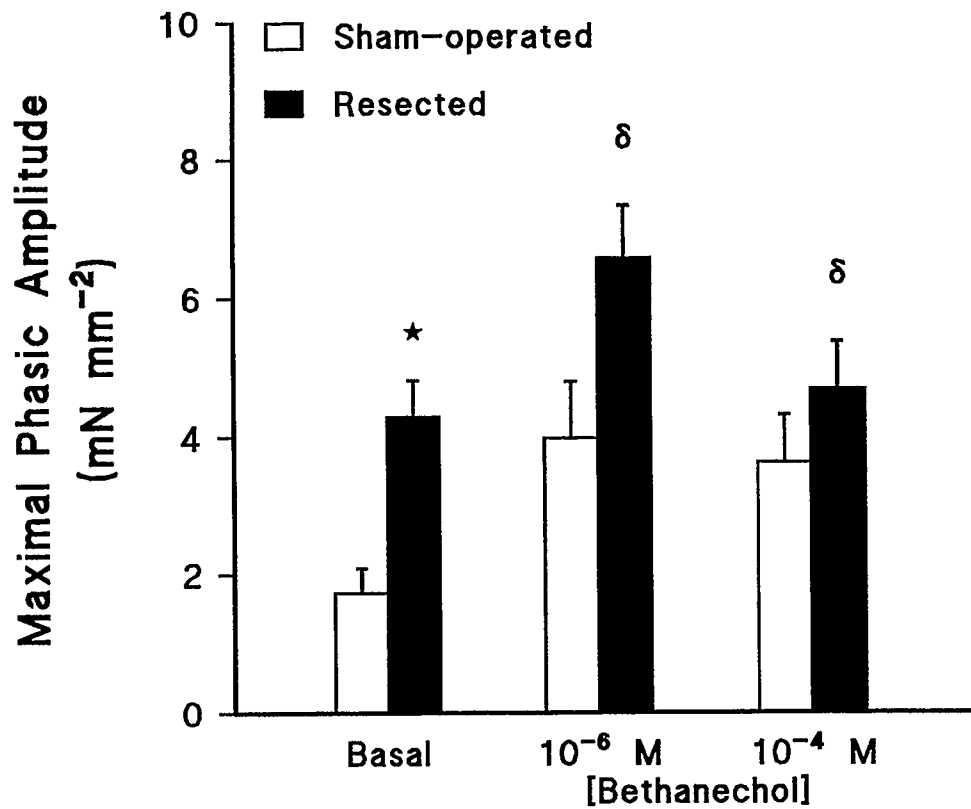


Figure 5.7. Amplitude of phasic contractile activity. Basal and bethanechol-stimulated maximal amplitude (mN mm⁻²) of phasic contractile activity for jejunal longitudinal muscle from sham-operated and resected groups. ★ indicates $p < 0.05$, under basal conditions. δ indicates a significant increase in the response of resected tissues post-bethanechol stimulation ($p < 0.05$, pooled data, ANOVA). $n = 7$ per treatment group.

5.4.3. Tetrodotoxin and phasic contractility

To assess whether the altered phasic contractile response of jejunal tissues from resected rats was the result of changes in neurogenic function, contractile experiments were performed with and without 10^{-6} M TTX. For both phasic frequency and amplitude, the only two parameters which demonstrated a significant change post-resection, the presence of TTX had no effect on either the basal or bethanechol-stimulated responses. These results are presented in Figures 5.8 and 5.9.

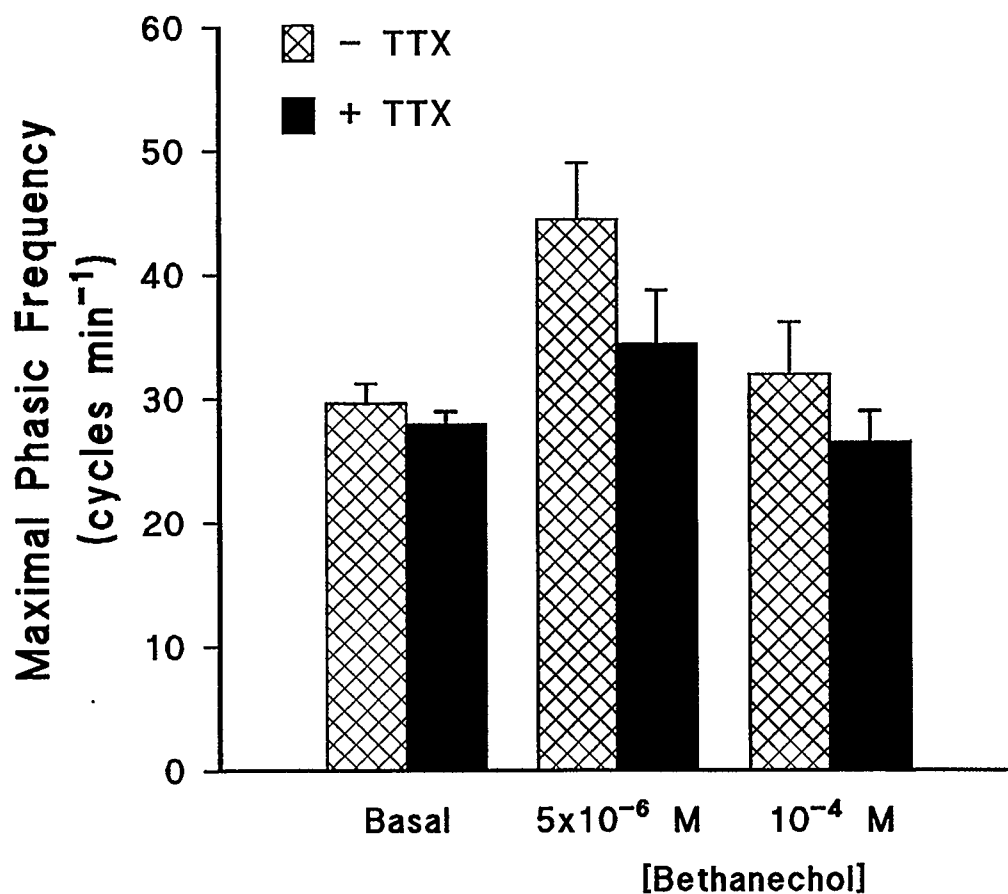


Figure 5.8. The effect of tetrodotoxin on phasic contractile frequency. The frequency (cycles min⁻¹) of phasic contractile activity of jejunal longitudinal muscle from resected rats only in the absence and presence of 10⁻⁶ M TTX. Blockade of neurogenic function had no effect on the basal or bethanechol-stimulated contractile responses. n=7 per treatment group.

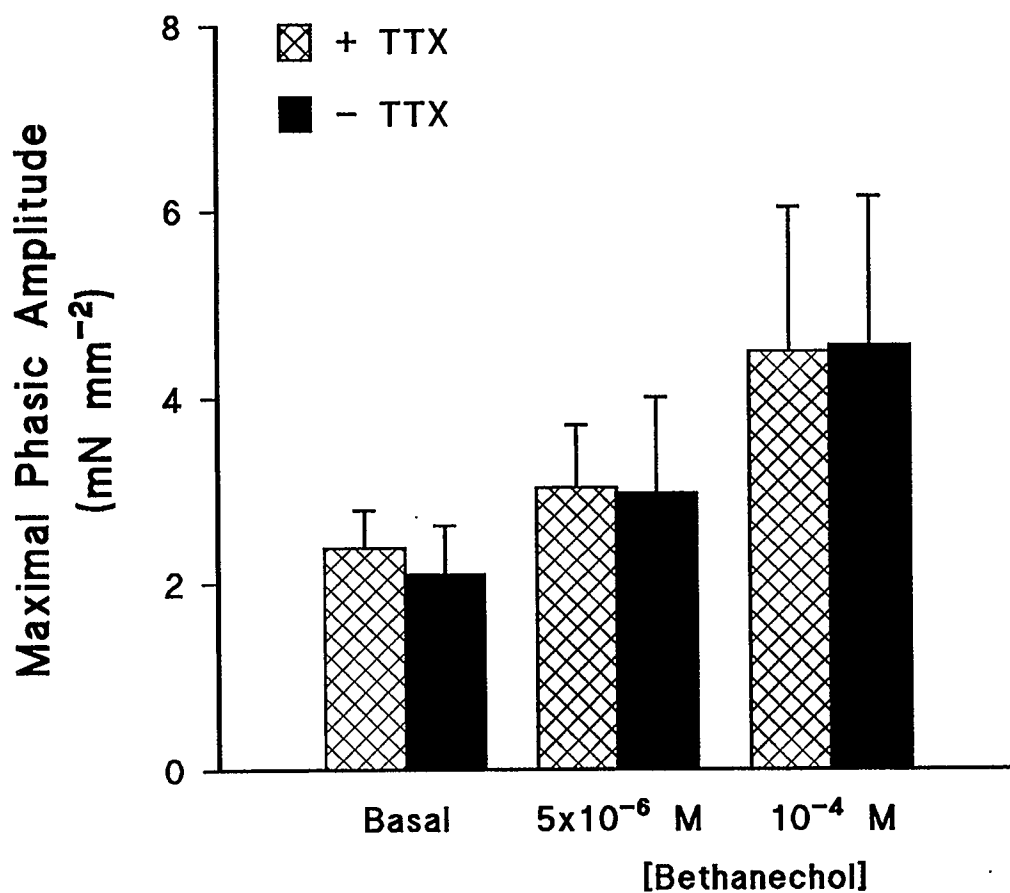


Figure 5.9. The effect of tetrodotoxin on phasic contractile amplitude. The maximal amplitude (mN mm⁻²) of phasic contractile activity of jejunal longitudinal muscle from resected rats only in the absence and presence of 10⁻⁶ M TTX. Blockade of neurogenic function had no effect on the basal or bethanechol-stimulated contractile responses. n=7 per treatment group.

5.5. SUMMARY OF LONGITUDINAL MUSCLE CONTRACTILITY

Subsequent to massive small intestinal resection, the longitudinal smooth muscle of the residual jejunum exhibited no adaptive change in basal stress, optimal length for development of active tension, or active stress response following stimulation with bethanechol or KCl. However, significant increases in both the frequency and amplitude of phasic contractile activity were observed in the basal state and after bethanechol stimulation. These alterations were myogenic in origin.

CHAPTER SIX

RESULTS III

CIRCULAR SMOOTH MUSCLE CONTRACTILITY

6.1. MORPHOLOGICAL ADAPTATION

Jejunal circumference, measured with tissues at their initial unstretched length, did not differ over time (days 10, 20, 30 and 40) and thus data were pooled. Consistent with the previous studies of massive resection (model characterization, longitudinal muscle contractility) jejunal circumference was significantly increased post-resection. The mean circumference of the sham-operated group was 1.44 ± 0.04 cm compared to 1.63 ± 0.05 cm for the resected group ($p < 0.05$).

Typical recordings of the spontaneous and bethanechol-stimulated contractile activity of circular jejunal muscle are depicted in Figure 6.1. The recordings are of tissues from sham-operated and resected rats taken on day 10 post-surgery.

6.2. LENGTH-BASAL STRESS RESPONSE

Within both treatment groups at all times post-surgery, there was an exponential increase in basal stress in response to incremental stretch of the circular smooth muscle. As previously stated in section 5.2, the curve parameter "m" describes the rate of exponential increase in stress per percentage increment in the initial unstretched tissue length, L_i . For jejunal circular muscle, estimates of this parameter were similar for sham-operated and resected groups at all times studied, indicating that factors such as tissue elasticity and alterations in the connective tissue matrix are unchanged post-resection. The results are listed in Table 6.1. A representative length-basal stress response curve is presented in Figure 6.2.

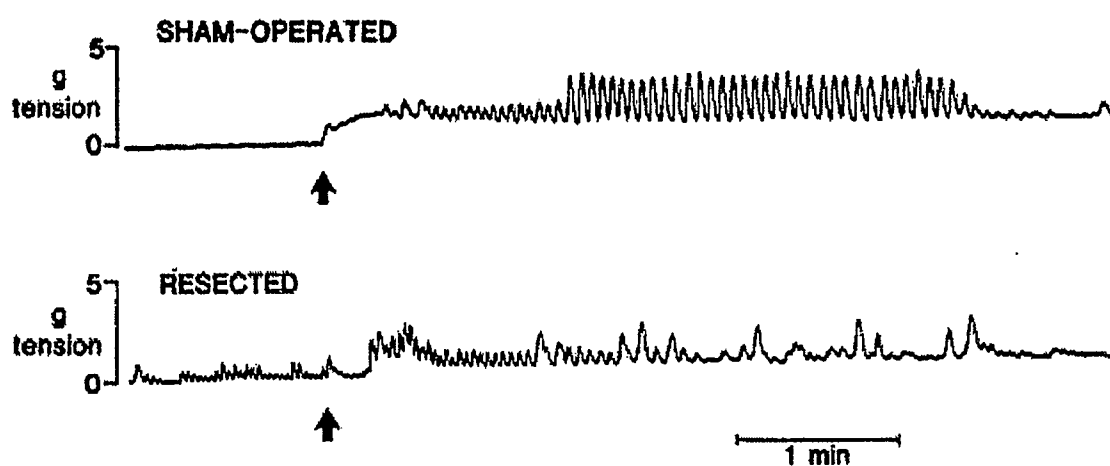


Figure 6.1. Representative tracings of jejunal circular muscle contractile activity. A period of spontaneous phasic contractile activity precedes the \uparrow , which indicates the time of addition of 10^{-4} M bethanechol to the tissue bath. Note the increases in tonic tension, frequency and amplitude of phasic contractile activity following stimulation with the muscarinic agonist.

Table 6.1. Basal stress "m" parameter values. Incremental stretch of a muscular tissue generates basal stress as an exponential (hyperbolic) function of the stretch. The basal stress (S, in mNewtons mm⁻²) at any length (L, expressed as the percent increment of initial length (L_i)) is given by

$$S = Ae^{mL} + C$$

where A, m and C are constants. For these studies, A = 1, m defines the rate of exponential increase in stress per the percent increment in L_i, and C is the y axis intercept if stress is plotted against length on Cartesian co-ordinates. Since by definition stress equals zero when the tissue is at its initial resting length (percent increment of L_i=0) then by substitution C must equal -1. The data demonstrate that estimates of the "m" parameter were not different between the two treatment groups at any time during the study. Thus, similar to longitudinal muscle, factors such as tissue elasticity and alterations in the connective tissue matrix are unchanged in circular smooth muscle post-resection. ns, not significant. n=6 per treatment group per day.

Table 6.1. Basal stress “m” parameter values.

Day	Sham-operated	Resected	p value
10	0.058 ± 0.002	0.058 ± 0.002	ns
20	0.057 ± 0.002	0.049 ± 0.001	ns
30	0.049 ± 0.001	0.048 ± 0.002	ns
40	0.052 ± 0.001	0.060 ± 0.003	ns

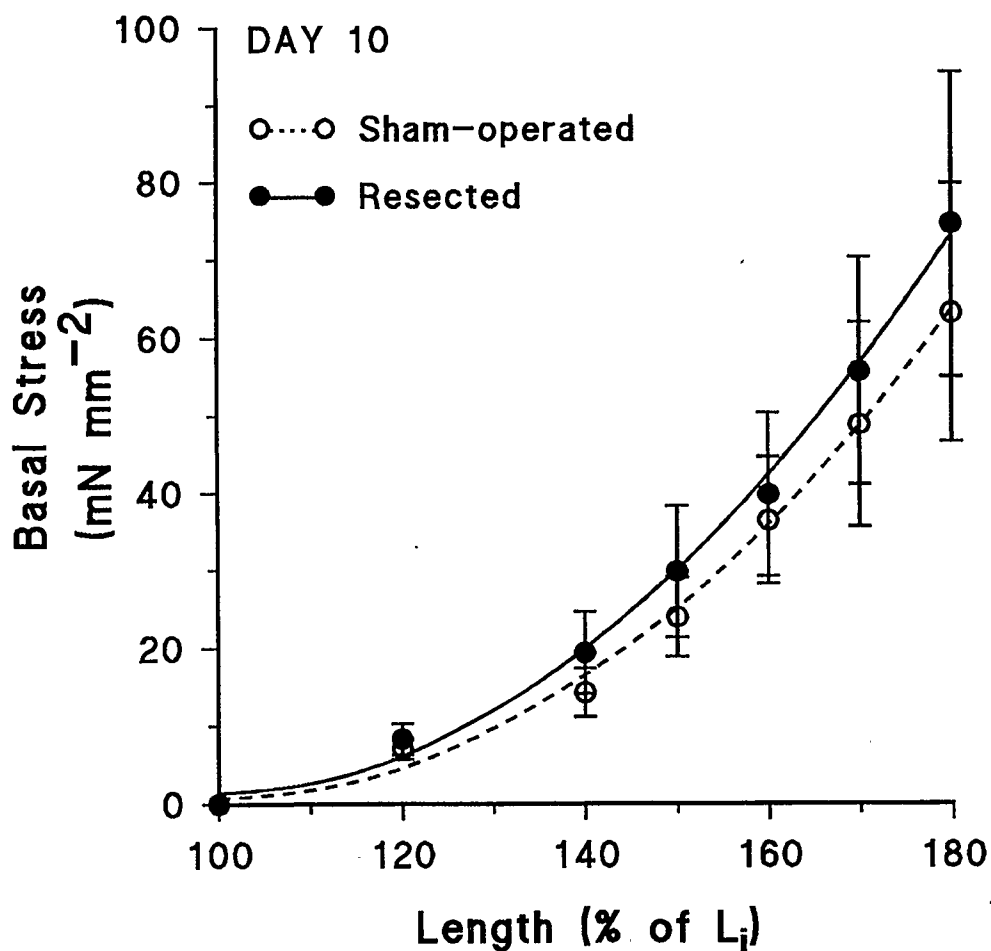


Figure 6.2. Length-basal stress response. A representative length-basal stress (% of L_i-mN mm⁻²) response curve is shown for jejunal circular muscle obtained from sham-operated and resected rats on post-surgical day 10. Consistent with the findings of longitudinal muscle contractility, resection had no effect on the elastic properties of circular smooth muscle. n=6 for both treatment groups.

6.3. ACTIVE TONIC CONTRACTILE RESPONSE

The following section deals with the tonic stress response of jejunal circular muscle after stimulation. Figure 6.3 schematically illustrates this specific contractile parameter.

6.3.1. Length-active stress response and optimal length

The muscle length at which peak active tension (L_o) developed in response to 10^{-4} M bethanechol was not different with length of time after surgery within treatment groups, or between sham-operated and resected groups. All subsequent concentration-response experiments were conducted with circular muscle stretched to L_o . For both treatment groups L_o was 160% of the initial unstretched tissue length.

There was no statistically significant change in any contractile parameter with time after surgery in the sham-operated or resected group (Appendices V-X). Hence, in all subsequent analyses the data within the sham-operated and resected groups were pooled for all parameters studied, giving an $n=24$ for both treatment groups.

6.3.2. Concentration-tonic stress response to bethanechol

The maximal active tonic stress developed by jejunal circular muscle in response to increasing concentrations of bethanechol is shown in Figure 6.4. Both the EC_{50} and S_m were significantly reduced post-resection.

The length of time taken to reach maximal tonic stress was measured at the two highest bethanechol concentrations tested. In both cases, tissues from resected rats took significantly less time to reach maximal stress. At 5×10^{-5} M bethanechol, sham-operated rats took 1.29 ± 0.18 min compared to 0.58 ± 0.07 min for resected animals ($p < 0.05$).

Similarly, at 10^{-4} M bethanechol, the time taken to develop maximal stress for the sham-operated and resected groups was 1.44 ± 0.19 min and 0.75 ± 0.10 min, respectively ($p < 0.05$).

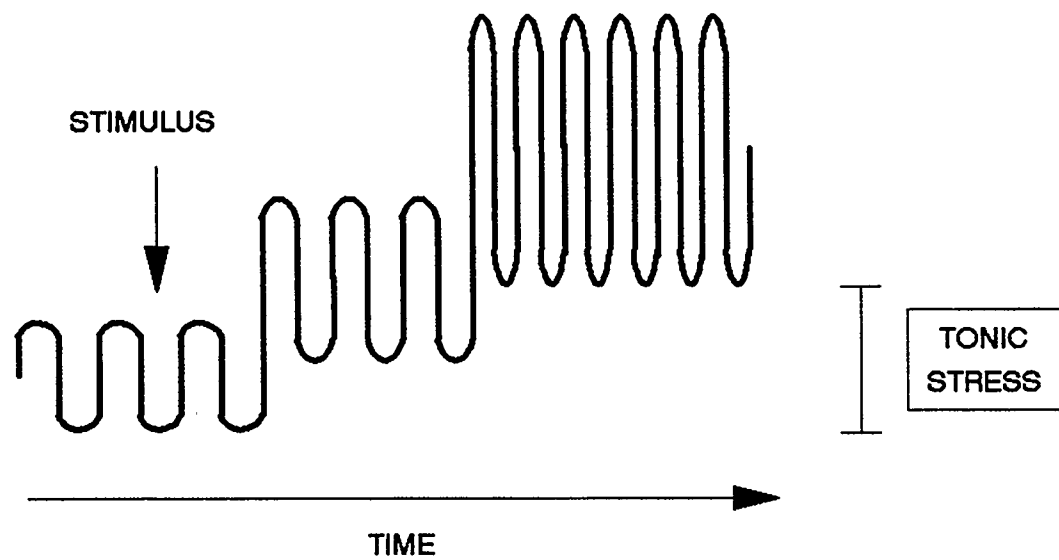


Figure 6.3. Schematic diagram of active tonic stress.

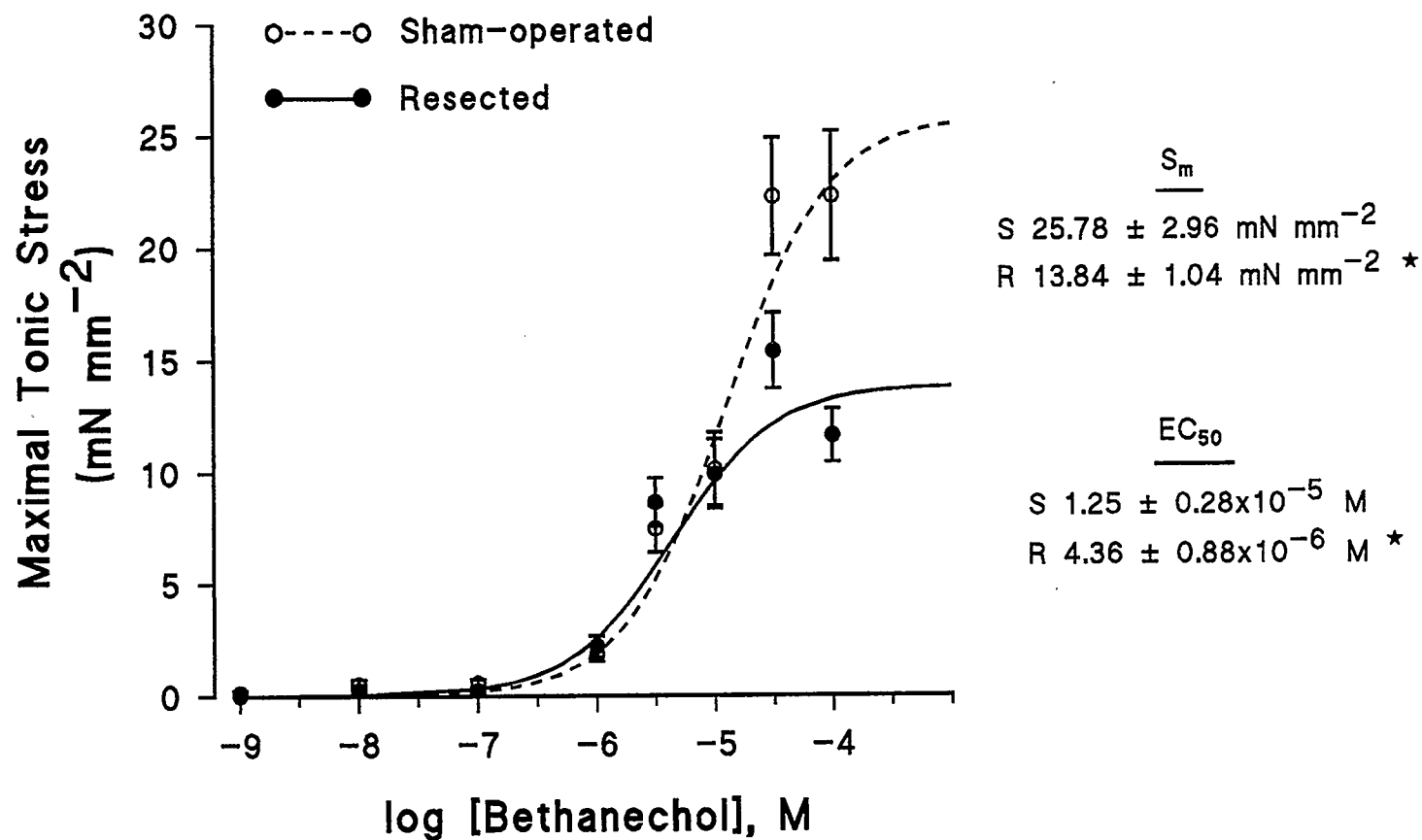


Figure 6.4. Concentration-tonic stress response to bethanechol. The maximal active tonic stress (mN mm⁻²) developed by jejunal circular muscle from sham-operated and resected rats is shown. Resection significantly reduced both the EC₅₀ and maximal stress, S_m . ★ $p < 0.05$. $n = 24$ per treatment group.

6.3.3. Concentration-tonic stress response to serotonin

The results of these experiments are presented in Figure 6.5. In contrast to stimulation with bethanechol, the maximal active tonic stress developed by jejunal circular muscle in response to increasing concentrations of 5-HT was significantly increased in tissues from resected rats. Resection had no effect on the EC_{50} .

6.3.4. Concentration-tonic stress response to KCl

The results of these experiments are presented in Table 6.2. Maximal active tonic stress induced by KCl-depolarization did not differ between sham-operated and resected groups at five of the six concentrations tested. These data suggest that the function of the contractile apparatus in circular smooth muscle remains intact following massive resection.

6.3.5. Electrical field stimulation and tonic stress

The results of these experiments are presented in Figure 6.6. Compared to the control condition of 10^{-4} M bethanechol, the EFS conditions used in these experiments (80 volts, 10 pulses sec^{-1} , 10 msec pulse $^{-1}$) resulted in a 38% decrease in the tonic stress response of the sham-operated group, with no change in the response of the resected group. Between treatment groups, maximal tonic stress was not different during EFS. Together with the KCl data, these findings support the interpretation that contractile function initiated beyond the point of receptor-stimulation is unaffected by resection.

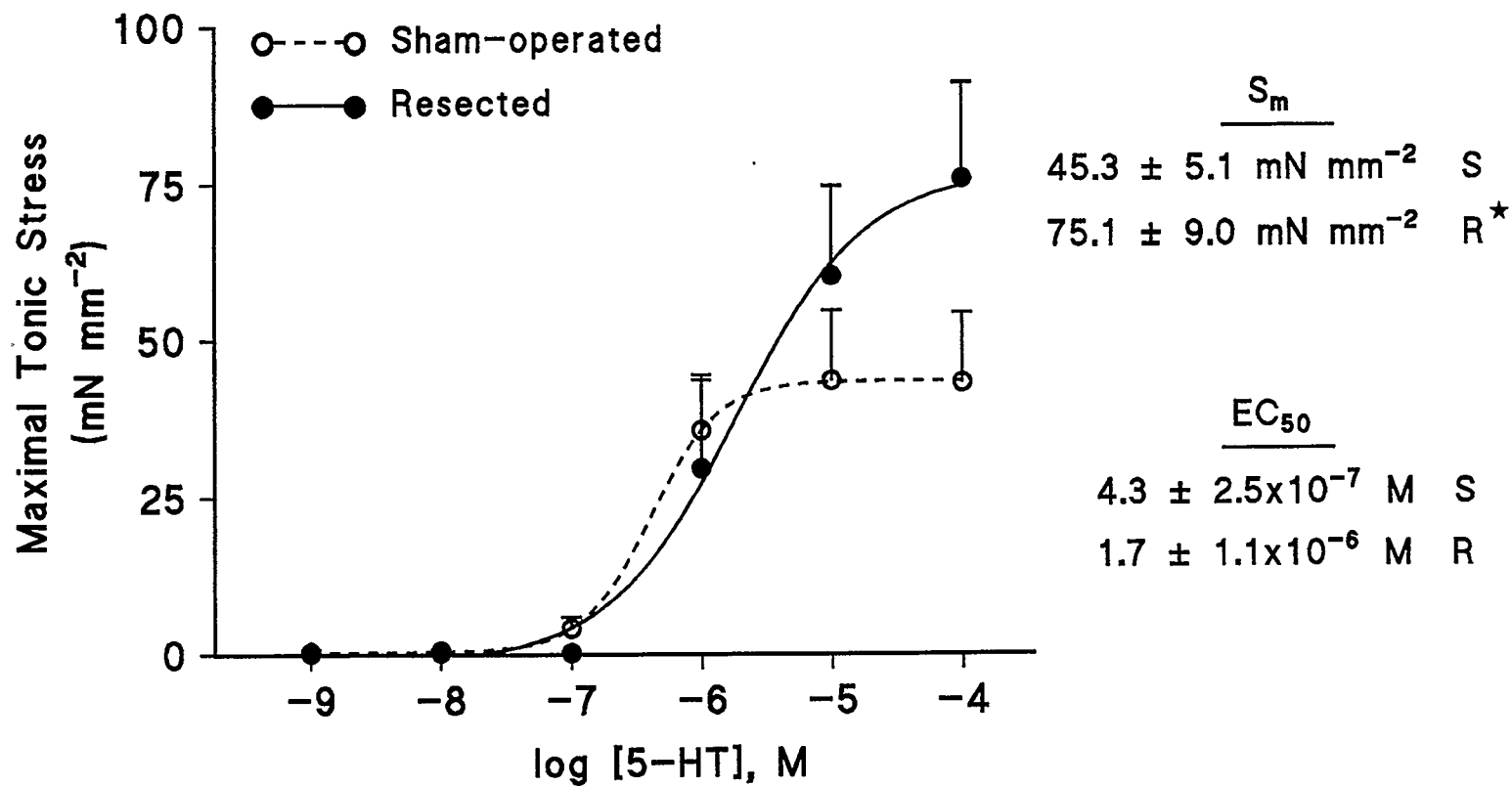


Figure 6.5. Concentration-tonic stress response to serotonin. The figure shows the maximal tonic stress (mN mm⁻²) developed by jejunal circular muscle from sham-operated and resected rats in response to serotonin (5-HT) stimulation. In contrast to bethanechol, stimulation of resected tissues with 5-HT produced a significant increase in maximal stress, S_m , while the EC_{50} was unaffected. ★ $p < 0.05$. $n = 7$ or 8 for sham-operated, and 5 or 6 for resected groups.

[KCl], mM	Sham-operated	Resected
10	-0.28 ± 0.47	0.14 ± 0.20
20	0.59 ± 0.58	$4.62 \pm 1.44^{\star}$
30	6.24 ± 2.77	12.62 ± 2.54
40	24.92 ± 5.00	14.02 ± 2.53
60	29.73 ± 5.11	21.13 ± 5.03
80	31.48 ± 4.89	21.23 ± 4.40

Table 6.2. Concentration-tonic stress response to KCl. The table shows the active maximal tonic stress (mN mm^{-2}) developed by jejunal circular muscle from sham-operated and resected groups in response to membrane depolarization 10 days after surgery. The similar responses of the two groups at five of the six concentrations tested suggest that the contractile apparatus of circular smooth muscle is not affected by resection. $\star p < 0.05$. $n=6$ per treatment group.

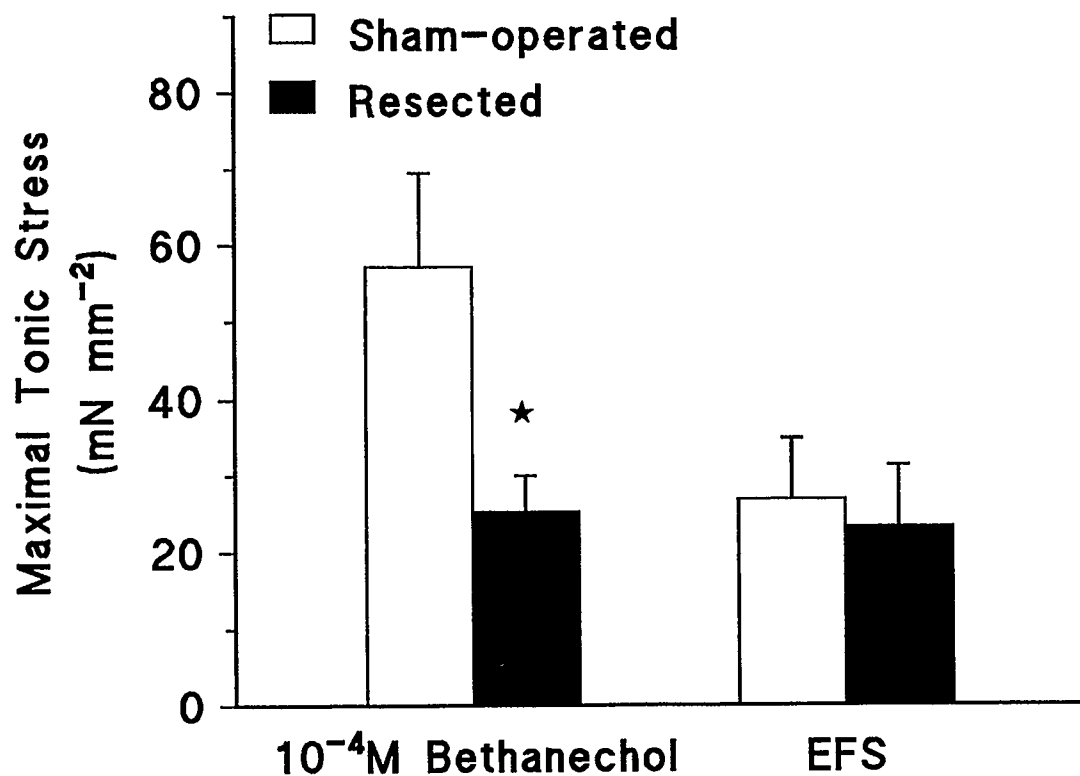


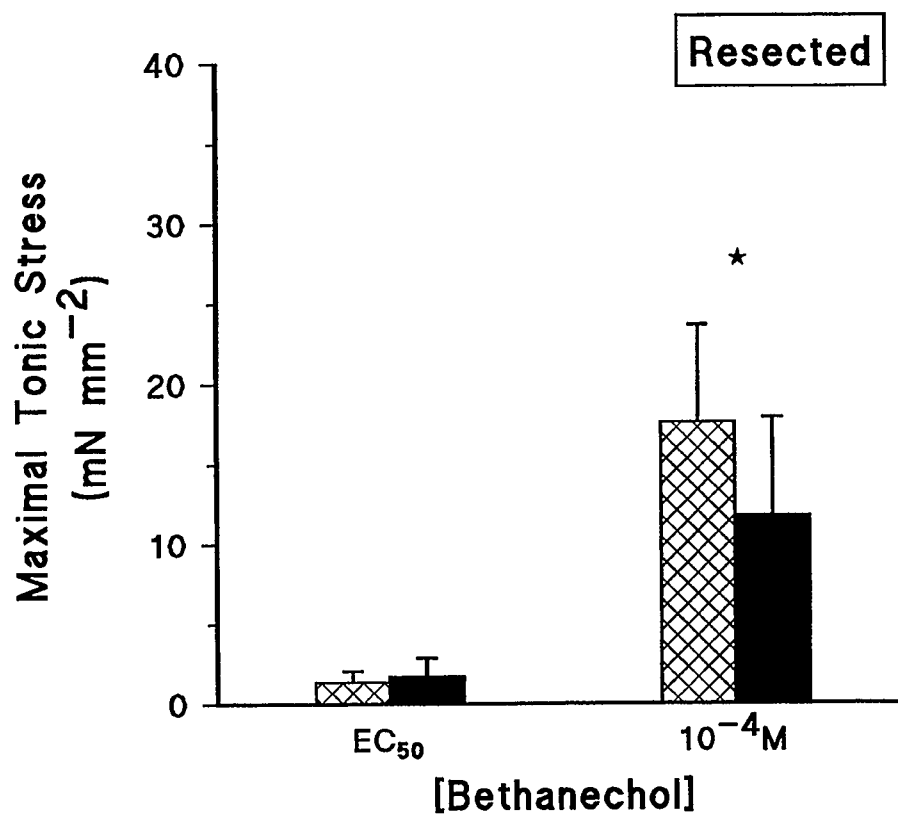
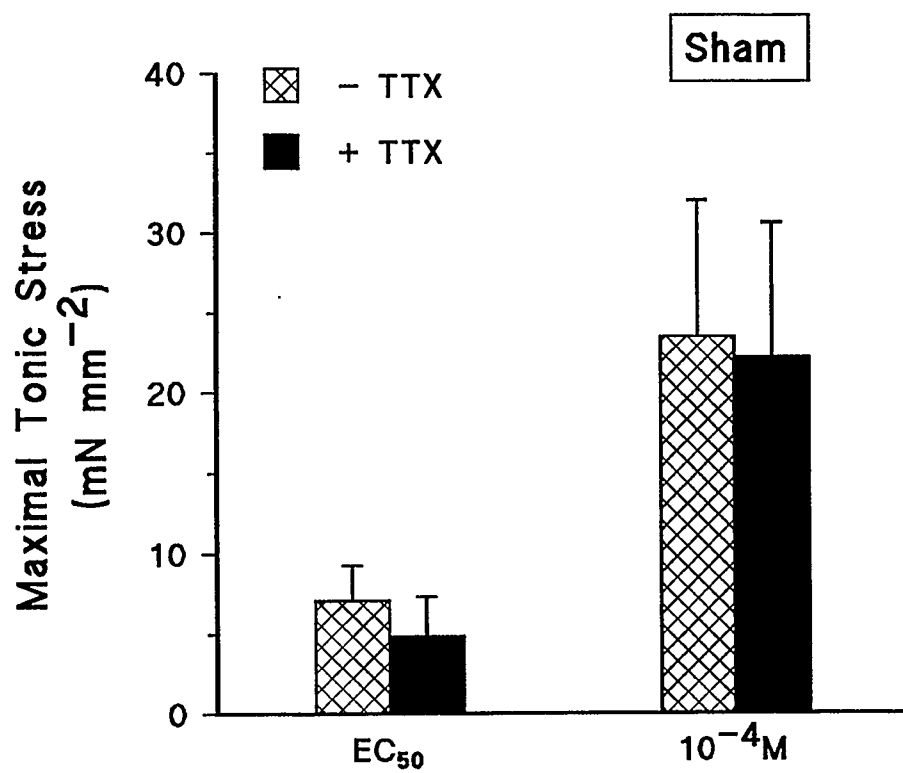
Figure 6.6. Electrical field stimulation and tonic stress. The tonic stress (mN mm⁻²) developed by jejunal circular muscle from sham-operated and resected rats developed in response to 10⁻⁴ M bethanechol, and electrical field stimulation is shown. EFS consisted of an 80 volt charge delivered at a rate of 10 pulses sec⁻¹, 10 msec pulse⁻¹ with no delay over a 10 sec period. Consistent with previous findings, resection significantly reduced the bethanechol-stimulated tonic stress response. In contrast, EFS evoked similar tonic stress responses in both groups. Taken together with the KCl data, the evidence indicates that contractile function beyond the point of receptor stimulation is not altered by resection. n=4 and 6 for sham-operated and resected groups, respectively.

6.3.6. Tetrodotoxin, bethanechol and tonic stress

To determine whether neurogenic influences contributed to the alterations in bethanechol-stimulated tonic stress, contractility experiments were conducted in the presence of 10^{-6} M TTX. As shown in Figure 6.7, the presence of TTX did not alter the active stress response of jejunal circular muscle from sham-operated rats. In contrast, at the higher bethanechol concentration tested, TTX significantly decreased the stress developed by resected tissues.

Figure 6.7. The effect of tetrodotoxin on the tonic stress response of bethanechol-stimulated circular muscle. The figure shows active stress (mN mm^{-2}) development in the absence and then presence of 10^{-6} M TTX for tissues from sham-operated and resected rats. No effect of TTX was found in sham-operated tissues. At the higher bethanechol concentration, TTX significantly decreased the tonic stress response of resected tissues.

★ $p < 0.05$. $n = 7$ per treatment group.



6.4. ACTIVE PHASIC CONTRACTILE ACTIVITY

The following section deals with the two components of phasic contractile activity, *i.e.*, frequency and amplitude. These parameters are illustrated in Figure 6.8.

6.4.1. Basal and bethanechol-stimulated phasic frequency

The results of these experiments are shown in Figure 6.9. Resection significantly reduced both the basal and active phasic contractile frequencies of jejunal circular muscle. Indeed, a significant reduction in the phasic frequency of resected tissues was observed at all concentrations of bethanechol tested.

6.4.2. Basal and bethanechol-stimulated phasic amplitude

As shown in Figure 6.10, under basal conditions, resection significantly elevated the phasic amplitude of jejunal circular muscle. In the stimulated state, this relationship was maintained at lower bethanechol concentrations. However, at the three highest concentrations, resection significantly decreased maximal phasic amplitude.

6.4.3. Serotonin-stimulated phasic amplitude

The results of these experiments are presented in Figure 6.11. The maximal amplitude of phasic activity in response to increasing concentrations of 5-HT did not demonstrate a clear concentration-dependency for either treatment group. In contrast to

stimulation with bethanechol, the responses of circular muscle from sham-operated and resected rats were not different at any concentration of 5-HT.

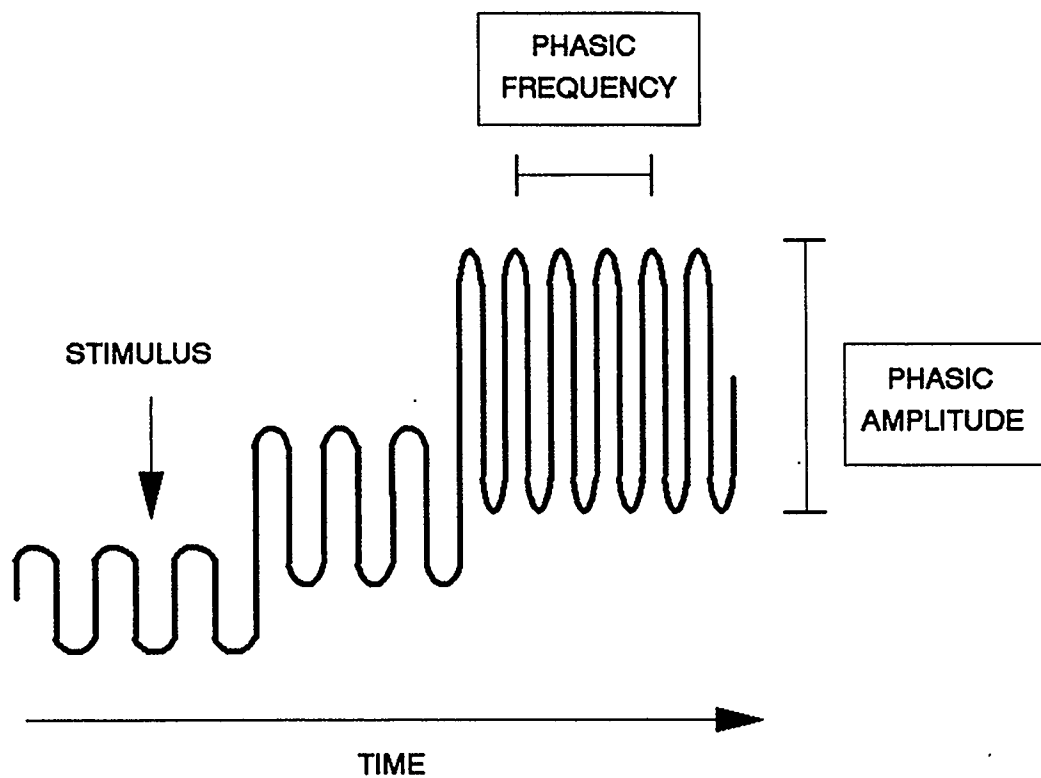


Figure 6.8. Schematic diagram of phasic frequency and amplitude.

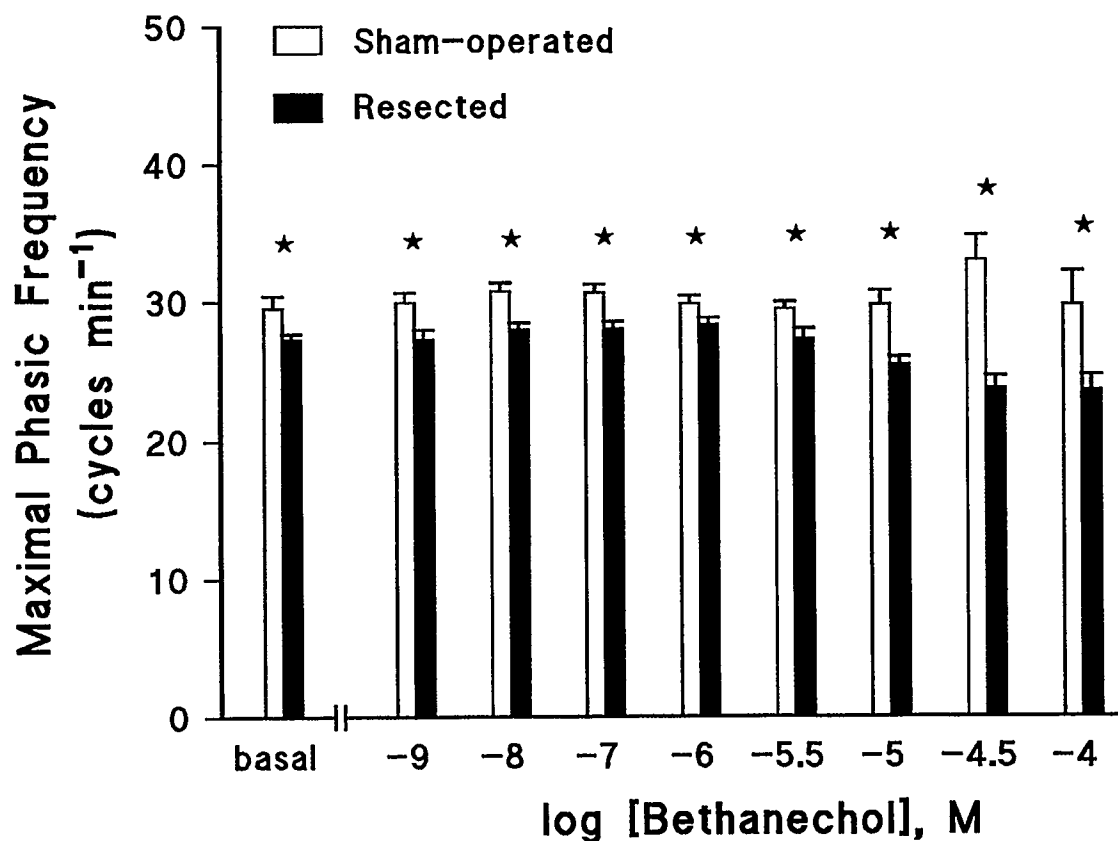


Figure 6.9. Frequency of phasic contractile activity. The figure shows the basal and active phasic contractile frequencies (cycles min⁻¹) of jejunal circular muscle from sham-operated and resected rats. Resection significantly reduced this parameter at all conditions tested. ★ $p < 0.05$. For basal responses, $n = 12$ per treatment group, with 7 repeated measures. For active (stimulated) responses, $n = 24$ per treatment group.

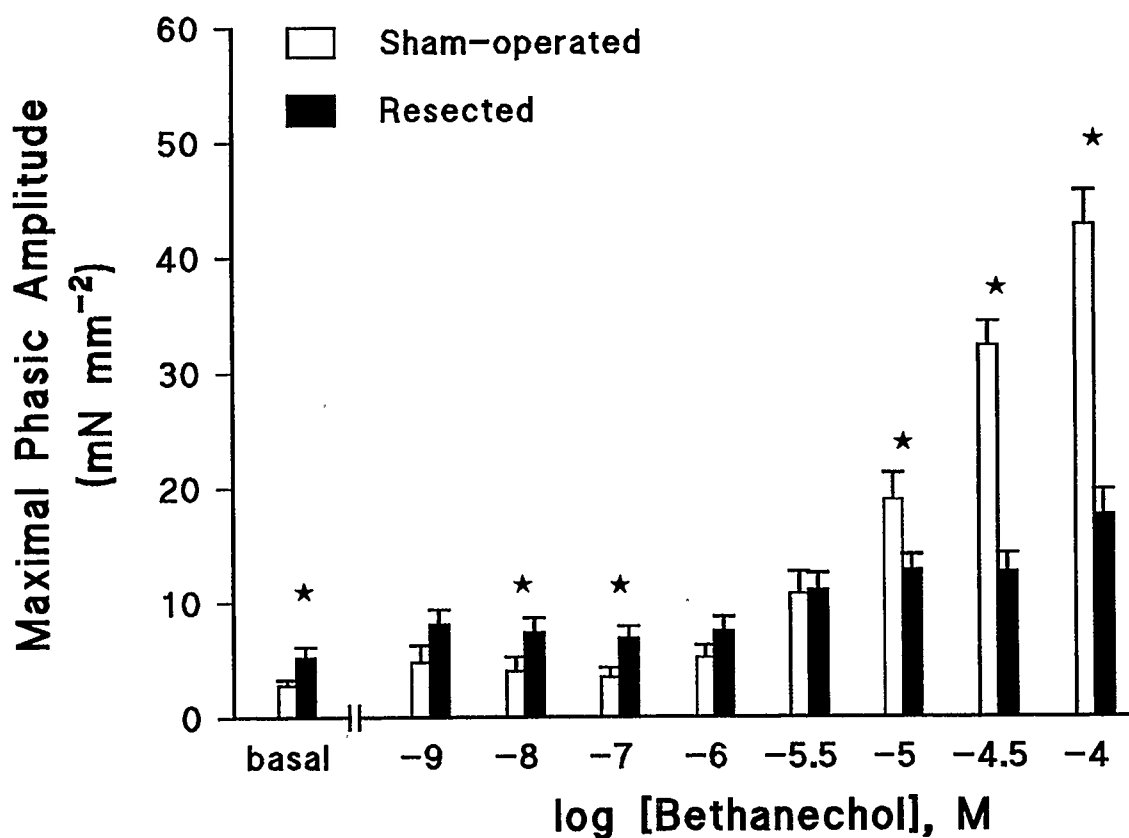


Figure 6.10. Amplitude of phasic contractile activity. The figure shows the basal and active maximal amplitude (mN mm⁻²) of jejunal circular muscle from sham-operated and resected rats. Resection produced an increase in maximal amplitude under basal conditions and at lower concentrations of bethanechol. This effect was reversed at higher agonist concentrations. ★ $p < 0.05$. For basal responses, $n=24$ per treatment group with 5 repeated measures. For active (stimulated) responses, $n=24$ per treatment group.

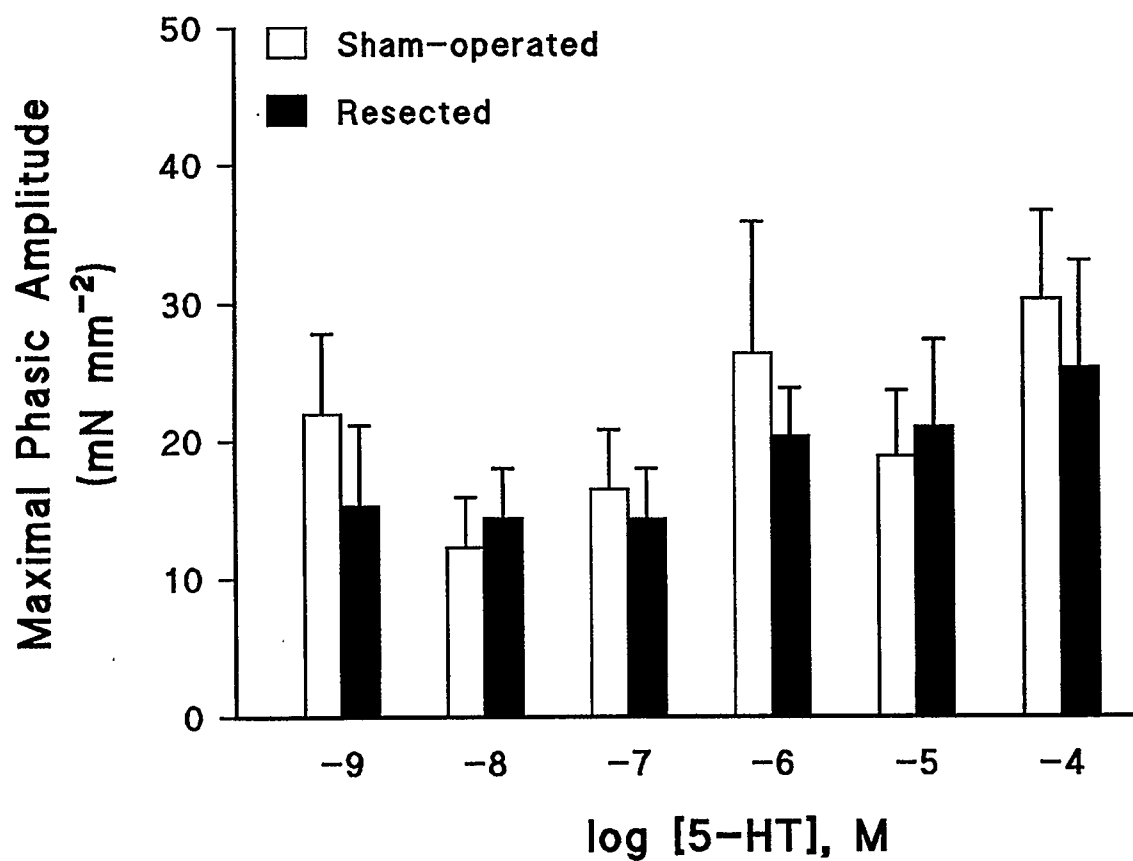


Figure 6.11. Serotonin-stimulated contractile amplitude. The maximal amplitude (mN mm⁻²) of phasic activity of jejunal circular muscle from sham-operated and resected rats in response to stimulation with 5-HT is shown. This parameter was unaffected by resection. $n=7$ or 8 for sham-operated, and 5 or 6 for resected groups.

6.4.4. Electrical stimulation and phasic amplitude

The results of these experiments are shown in Figure 6.12. In response to EFS, sham-operated and resected tissues were able to generate phasic contractions with a maximal amplitude of 16% and 34%, respectively, of that observed in response to 10^{-4} M bethanechol. However, the absolute magnitude of the phasic response to EFS was not different between treatment groups. These findings are similar to the results of the serotonin experiments, both of which contrast with the significantly reduced phasic amplitude observed in the bethanechol studies.

6.4.5. Tetrodotoxin, bethanechol and phasic contractility

The results involving phasic frequency are presented in Figures 6.13 and 6.14. Exposure to 10^{-6} M TTX significantly reduced, but did not abolish, the basal and bethanechol-stimulated phasic contractile frequencies within both the sham-operated and resected groups (Figure 6.13.). Comparison between treatment groups revealed that in the presence of TTX, resection still resulted in a significant reduction in phasic contractile frequency (Figure 6.14.). Compared to the sham-operated group, the magnitude of this reduction was $11.7 \pm 3.1\%$ ($p < 0.05$) under basal conditions and $11.2 \pm 2.7\%$ ($p < 0.05$) in response to the EC_{50} concentration of bethanechol.

As shown in Figure 6.15., 10^{-6} M TTX did not alter the basal or bethanechol-stimulated maximal amplitude of phasic contractions in either group.

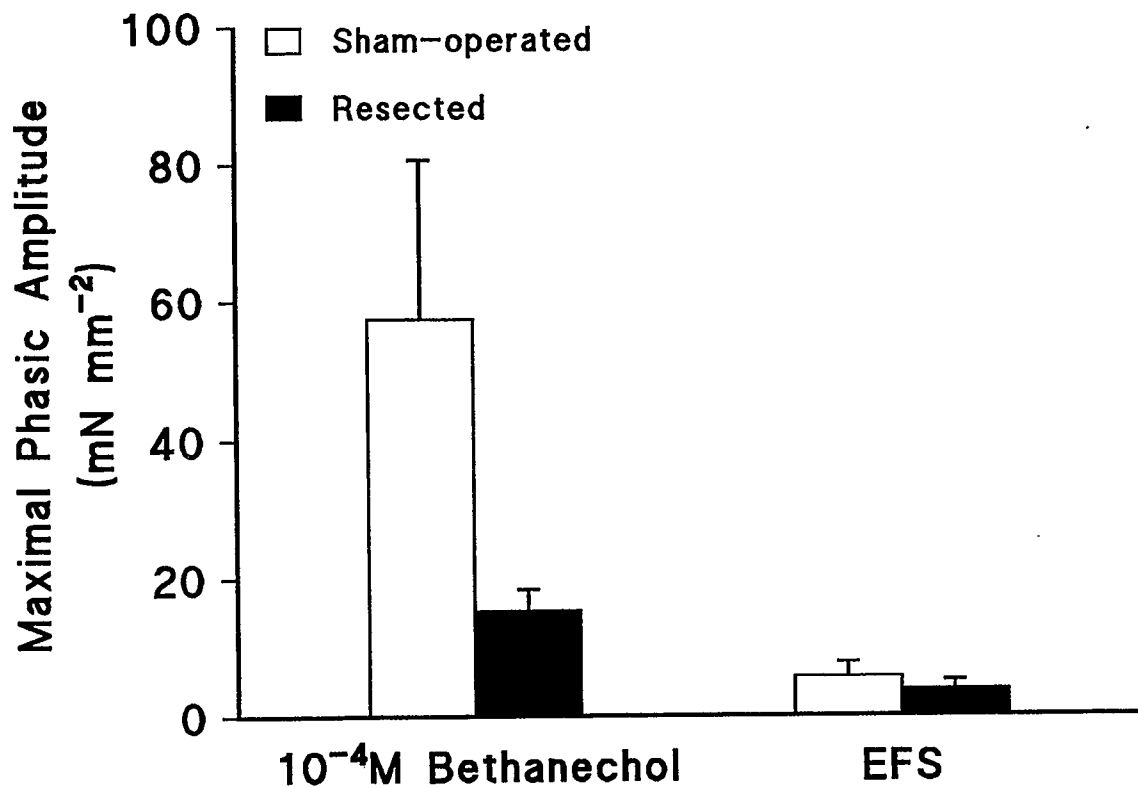
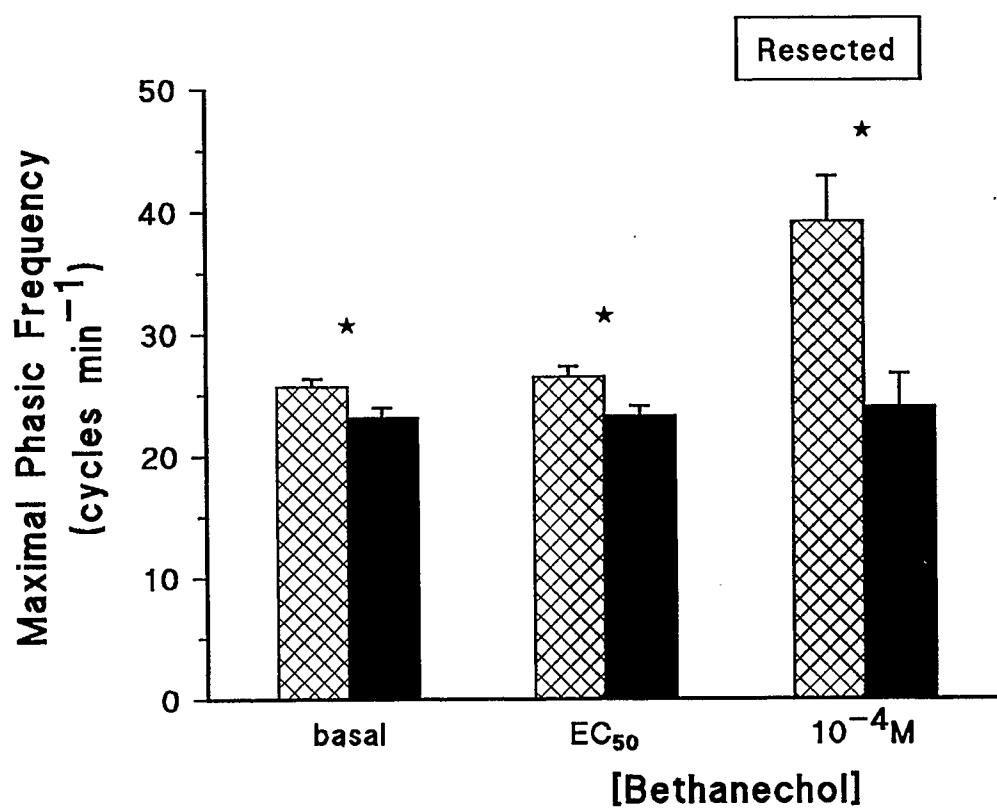
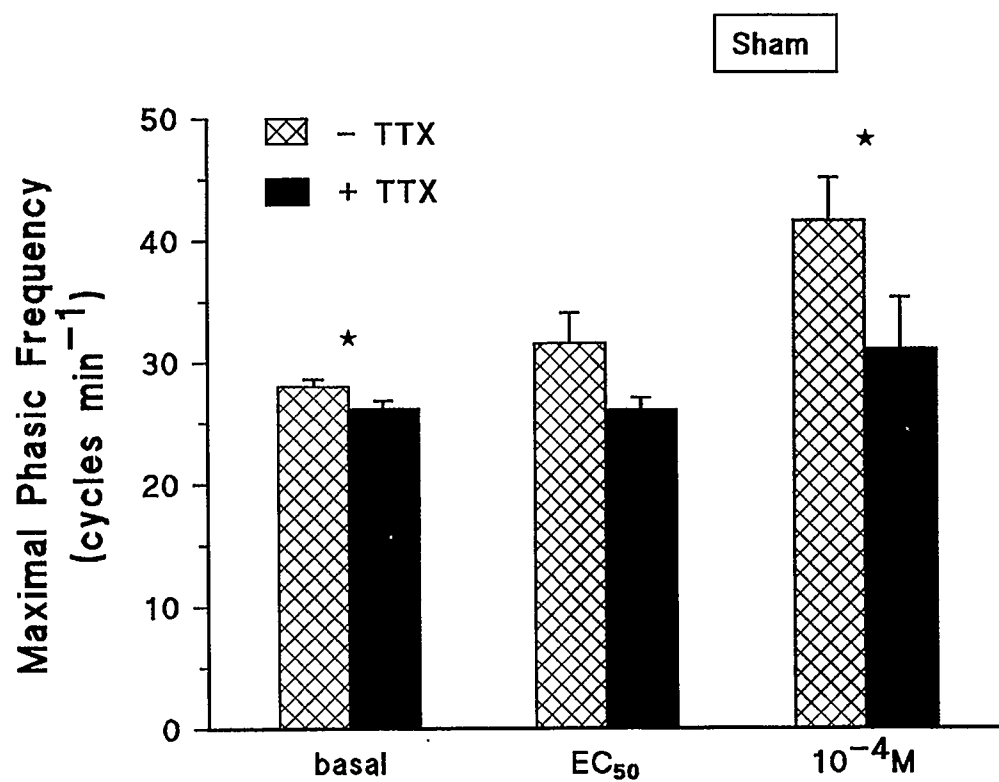


Figure 6.12. Electrical field stimulation and phasic amplitude. The maximal amplitude (mN mm⁻²) of jejunal circular muscle from sham-operated and resected rats in response to 10⁻⁴ M bethanechol and electrical field stimulation is shown. EFS consisted of an 80 volt charge delivered at a rate of 10 pulses sec⁻¹, 10 msec pulse⁻¹ with no delay for a period of 10 sec. While the magnitude of the phasic response to EFS was reduced within each treatment group, there was no significant difference in maximal amplitude between the sham-operated and resected groups. n=8 and 9 for sham-operated and resected groups, respectively.

Figure 6.13. The effect of tetrodotoxin on phasic contractile frequency within treatment groups. The frequency (cycles min^{-1}) of phasic contractile activity of jejunal circular muscle from sham-operated and resected rats in the absence and presence of 10^{-6} M TTX. Blockade of neurogenic function significantly reduced, but did not abolish, the phasic contractile frequency for both treatment groups. ★ $p < 0.05$. $n = 7$ per treatment group.



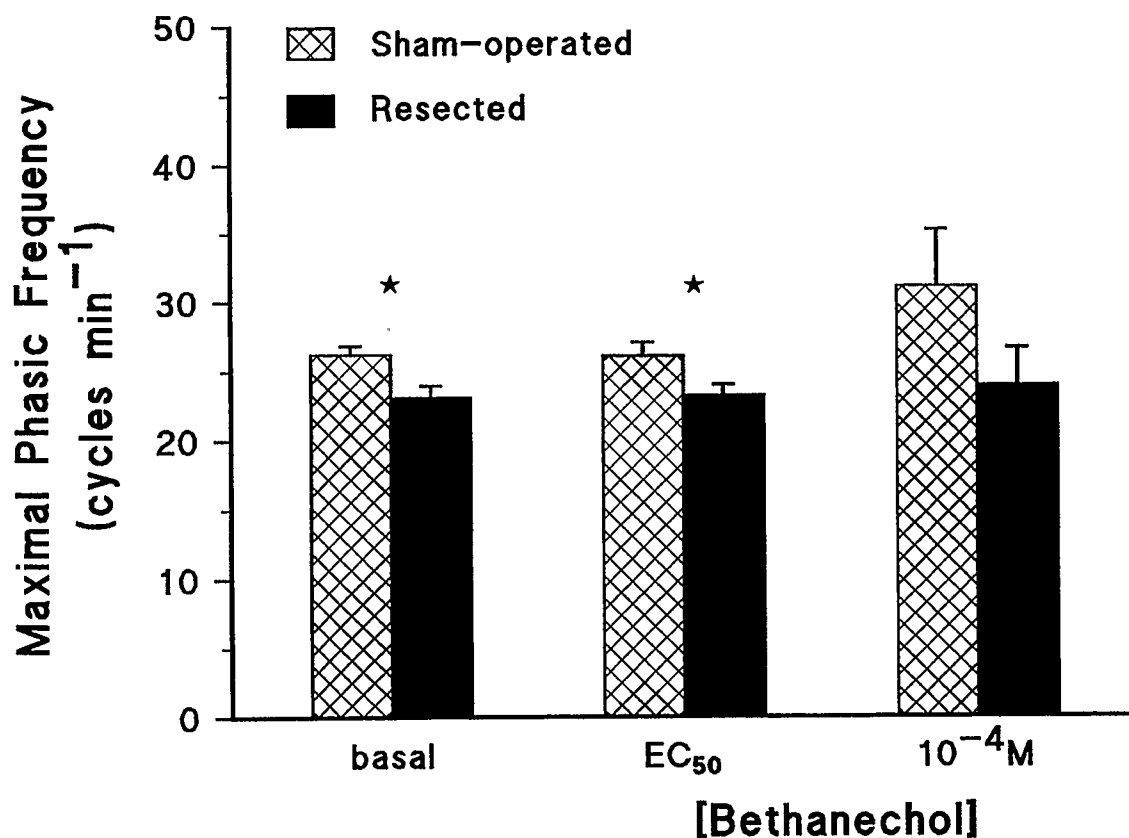
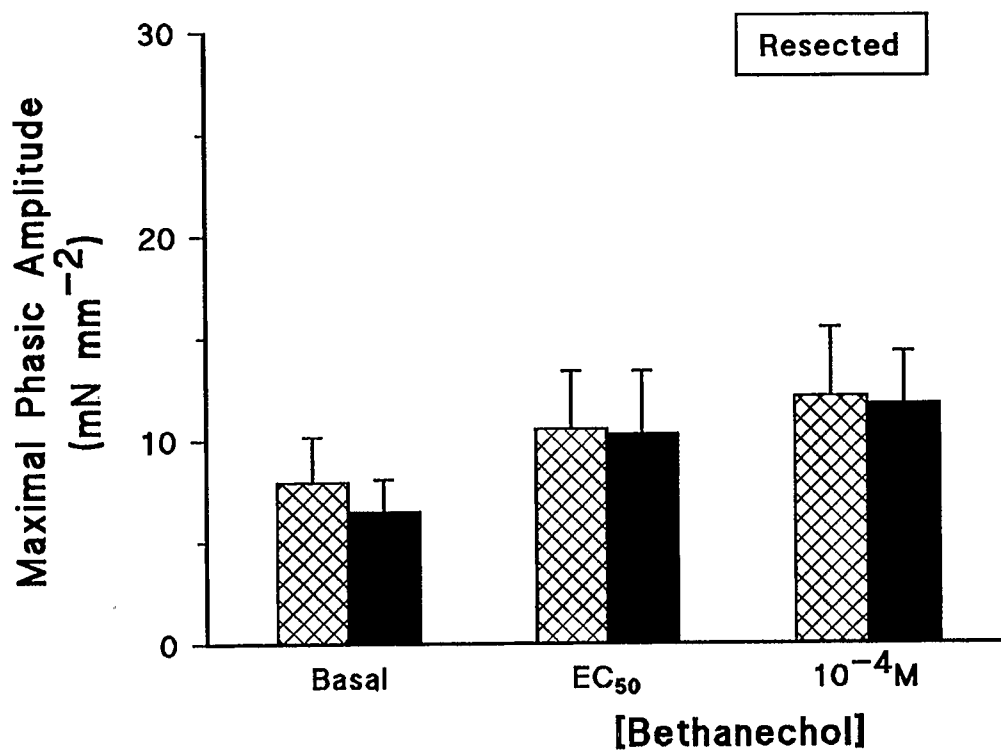
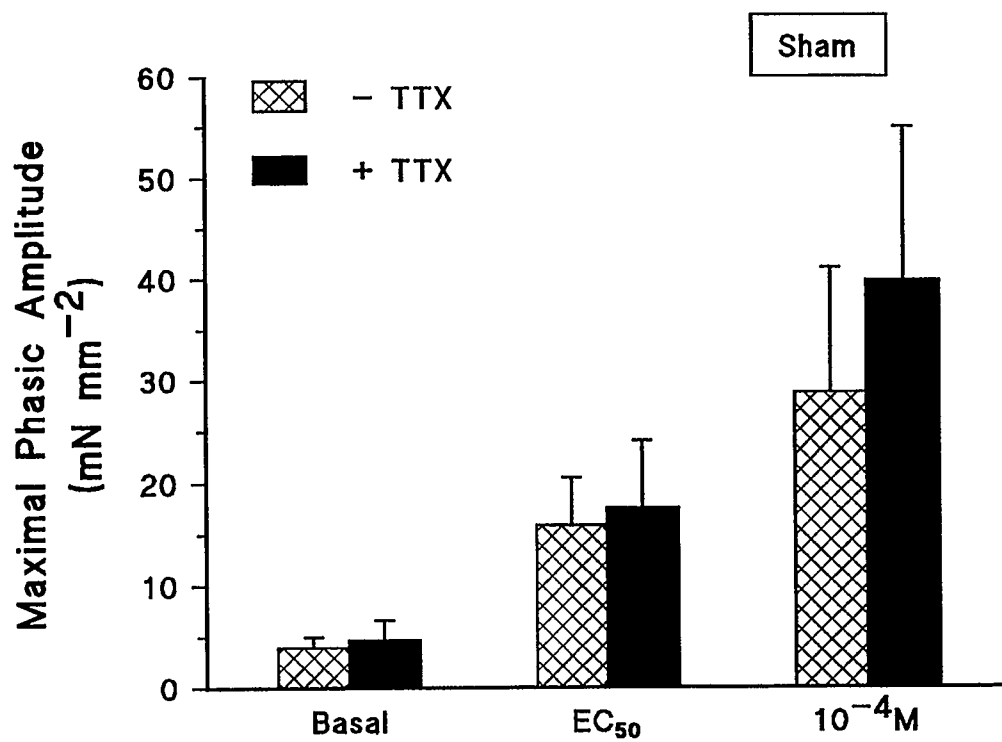


Figure 6.14. The effect of tetrodotoxin on phasic contractile frequency between treatment groups. The frequency (cycles min⁻¹) of phasic contractile activity of jejunal circular muscle from sham-operated and resected rats in the presence of 10⁻⁶ M TTX. Comparison of sham-operated and resected tissue responses while in the presence of TTX reproduced the original finding of a significant reduction in phasic frequency post-resection (see Section 6.4.5.). ★ $p < 0.05$. $n = 7$ per treatment group.

Figure 6.15. The effect of tetrodotoxin on phasic contractile amplitude. The maximal amplitude (mN mm^{-2}) of phasic contractile activity of jejunal circular muscle from sham-operated and resected rats in the absence and presence of 10^{-6} M TTX. The presence of TTX had no effect on this contractile parameter for either treatment group. $n=7$ per treatment group.



6.5. SUMMARY OF CIRCULAR MUSCLE CONTRACTILITY

Subsequent to massive small intestinal resection, the circular smooth muscle of the residual jejunum displays altered contractile function. Although the generation of basal stress in response to stretch and the optimal length for the development of active tension were unchanged after surgical resection, the development of active stress and the frequency of phasic contractions were significantly decreased following bethanechol stimulation. While the amplitude of spontaneous phasic activity was significantly increased after resection, the increase in amplitude in response to cholinergic stimulation was significantly reduced. These adaptations were present by the tenth post-surgical day. The depressed contractile activity of bethanechol-stimulated jejunal circular muscle is not characteristic of all excitatory stimuli since the tonic contractile response of resected tissues was not different from sham-operated rats in response to electrical field stimulation, and was significantly greater in response to serotonin.

CHAPTER SEVEN

RESULTS IV

GASTROINTESTINAL TRANSIT

7.1. FASTED TRANSIT

The distribution of ^{51}Cr along the length of the gastrointestinal tract 30 min after instillation into fasted rats is presented in Figure 7.1. The percentage of total counts of ^{51}Cr remaining in the stomach after 30 min, an indication of gastric emptying time, did not differ between sham-operated ($43 \pm 11\%$) and resected ($43 \pm 7\%$) rats. The geometric centre of isotope distribution, which identifies a segment number and has no units, was determined to be 8.0 ± 0.6 for the sham-operated group, and 5.0 ± 0.4 for the resected group. Using these data, the velocity of aboral propagation of luminal contents was calculated. As shown in Figure 7.2, resection significantly reduced the velocity of intestinal transit ($p < 0.05$).

7.2. FED TRANSIT

Although the distribution of ^{51}Cr in fasted animals was unaffected by resection, it remained entirely possible that such would not be the case after feeding. To better approximate the fed state, the transit experiments were repeated in rats instilled with 6 ml of a liquid, elemental diet (Sustacal) containing the radioactive marker. Under these conditions the distribution of ^{51}Cr represents the emptying of the liquid phase of a meal. These results, shown in Figure 7.3, resemble the data from the fasted transit studies, with the percentage of isotope remaining in the stomach 30 min after instillation similar in both treatment groups. The geometric centres for sham-operated and resected groups were

8.74 ± 0.26 and 5.20 ± 0.54 , respectively. As shown in Figure 7.4, resection also significantly reduced the velocity of intestinal transit after feeding ($p < 0.01$).

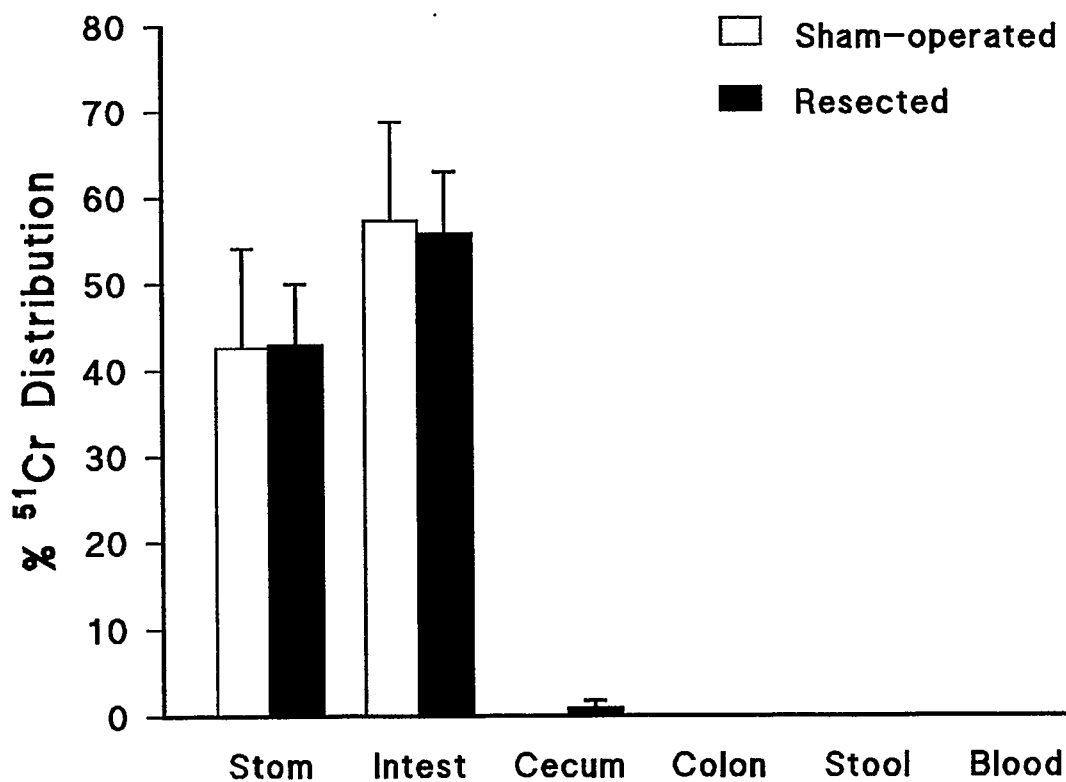


Figure 7.1. Distribution of ^{51}Cr in fasted rats. The figure shows the distribution (percentage of total counts) of $\text{Na}_2^{51}\text{CrO}_4$ + saline along the gastrointestinal tract of sham-operated and resected rats 30 min after instillation. The pattern of isotope distribution was similar between treatment groups. $n=7$ and 8 for sham-operated and resected groups, respectively.

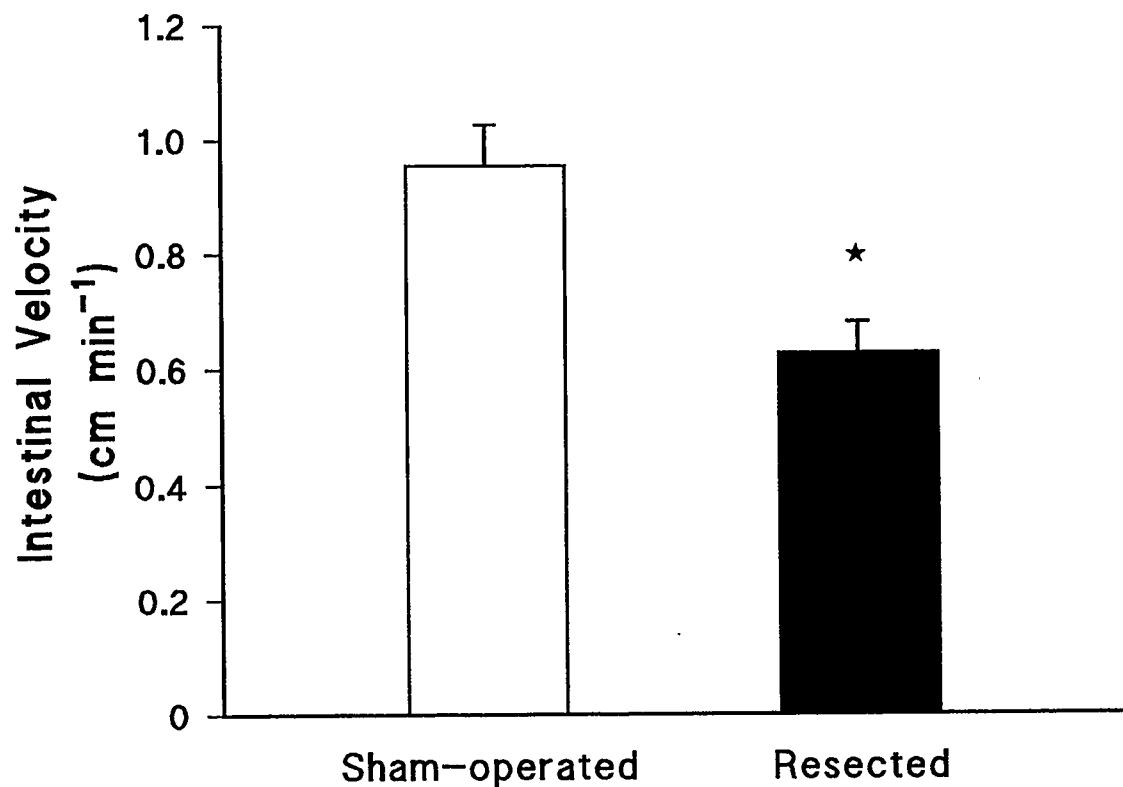


Figure 7.2. Velocity of intestinal transit in fasted rats. For both sham-operated and resected groups, the portion of radioactivity associated with the small intestine was subjected to further analysis (^{51}Cr distribution data from Figure 7.1). Partitioning of the small intestine permitted calculation of the geometric centre of ^{51}Cr distribution. However, since the absolute lengths of the small intestine of the two groups were inherently dissimilar, geometric centre was normalized to the common measure of velocity (cm min^{-1}). The figure shows that the velocity of intestinal transit was significantly reduced in resected rats. $\star p < 0.05$. $n=7$ and 8 for sham-operated and resected groups, respectively.

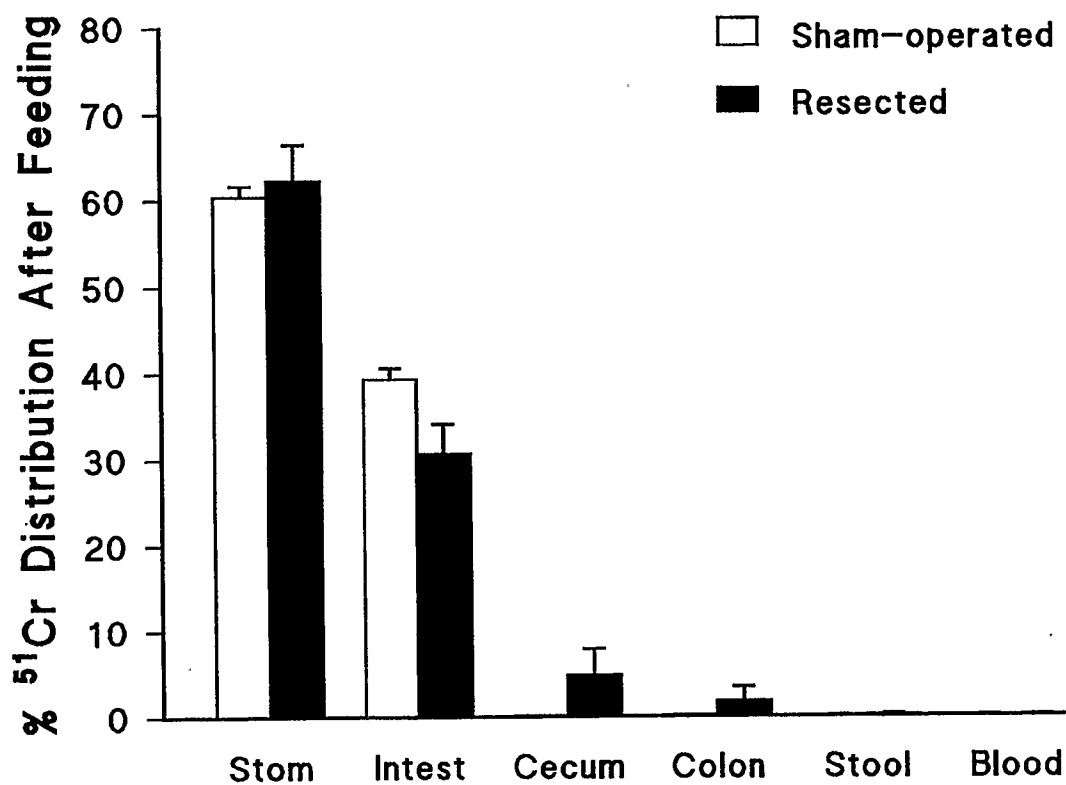


Figure 7.3. Distribution of ^{51}Cr in fed rats. The figure shows the distribution (percentage of total counts) of $\text{Na}_2^{51}\text{CrO}_4$ + 6 ml of a liquid elemental diet (Sustacal) along the gastrointestinal tract of sham-operated and resected rats 30 min after instillation. As observed in the fasted state, the pattern of isotope distribution after feeding was similar between treatment groups. $n=8$ and 6 for sham-operated and resected groups, respectively.

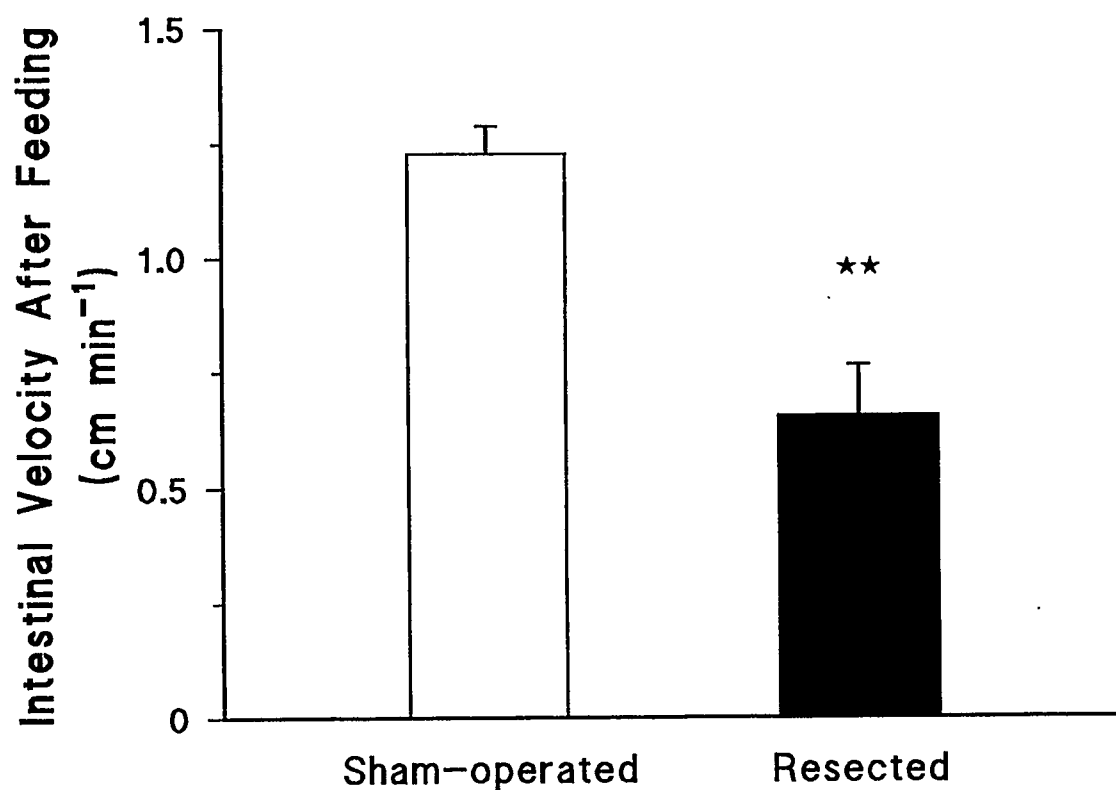


Figure 7.4. Velocity of intestinal transit in fed rats. For both sham-operated and resected groups, the portion of radioactivity associated with the small intestine was subjected to further analysis (^{51}Cr distribution data from Figure 7.3). Partitioning of the small intestine permitted calculation of the geometric centre of ^{51}Cr distribution. However, since the absolute lengths of the small intestine of the two groups were inherently dissimilar, geometric centre was normalized to the common measure of velocity (cm min^{-1}). Similar to the findings of the fasted transit studies, the velocity of intestinal transit after feeding was significantly reduced in resected rats. $\star\star p < 0.01$. $n=8$ and 6 for sham-operated and resected groups, respectively.

7.3. SUMMARY OF THE EFFECT OF RESECTION ON GASTROINTESTINAL TRANSIT

Resection had no effect on the rate of gastric emptying or the distribution of ^{51}Cr under fasting (instilled with saline) or “fed” conditions (instilled with a liquid elemental diet). However, the velocity of aborad propulsion of luminal contents through the length of the small intestine was significantly reduced post-resection in both the fasted and fed states.

CHAPTER EIGHT**RESULTS V****STRATEGIES TO EXPLORE MECHANISM**

8.1. RELEVANCE OF CONTRACTILE PROTEIN FUNCTION

Although several pieces of information (contractile activity following stimulation with KCl and EFS; ratios of S_m : time taken to reach S_m) have been presented which indicate that massive resection does not alter contractile protein function, these data were not available when assays to measure contractile protein content from intestinal smooth muscle were being developed as a potentially useful investigative tool. Ultimately, the data did not support the hypothesis that a significant change in contractile protein content or isoform distribution was responsible for the decreased contractile response of jejunal circular muscle in the rat model of massive resection. While the contractile protein immunoassays were not utilized in the model of resection, it was, however, applicable to another model system.

The use of the immunoassay technique to measure relative protein levels is of distinct benefit when compared to the more complex method of gel electrophoresis and analysis. The ease, rapidity and more direct nature of an immunoassay far outweigh the more labour-intensive, time-consuming approach of gel electrophoresis, Western blotting and quantification of individual bands by scanning densitometry. For this reason, a brief summary of the immunoassay experiments is presented. As previously elaborated in section 3.7, the model used for assay development was one of *Yersinia enterocolitica* infection in rabbits. In those separate studies, the above-mentioned immunoassays were utilized to demonstrate that the enhanced stress response of ileal longitudinal smooth

muscle from undernourished rabbits was not due to alterations in contractile protein content or isoform distribution.

8.1.1. Contractile protein immunoassay

For all immunoassays, the protein concentration of the sample or standard was proportional to optical density. This linear relationship was reproducible and r values were consistently above 0.94.

Due to the highly conserved nature of the amino acid sequences of the contractile proteins, the isoactin and myosin antibodies are reactive in several species, including the rabbit (Lessard, J.L., personal communication; specifications from Sigma, ICN). The ability of each antibody to preferentially recognize specific isoactins (Lessard, 1988; Sawtell, et al., 1989; Skalli, et al., 1986) or myosin heavy chain (Longtine, et al., 1985; Benzonana, et al., 1988) has been documented in the literature. Experiments were performed to confirm the reported specificity of antibody reactivity. As shown in Figure 8.1, the antibody to γ -enteric isoactin (B4) was unable (appropriately) to recognize actin from rat abdominal aorta but did elicit a positive, proportional response to commercially prepared chicken gizzard actin. The antibody to α -vascular isoactin (1A4) gave positive, proportional responses to rat aorta, and also to chicken gizzard actin, although its sensitivity for the latter was ~8-fold less than the γ -enteric antibody. These results are presented in Figure 8.2.

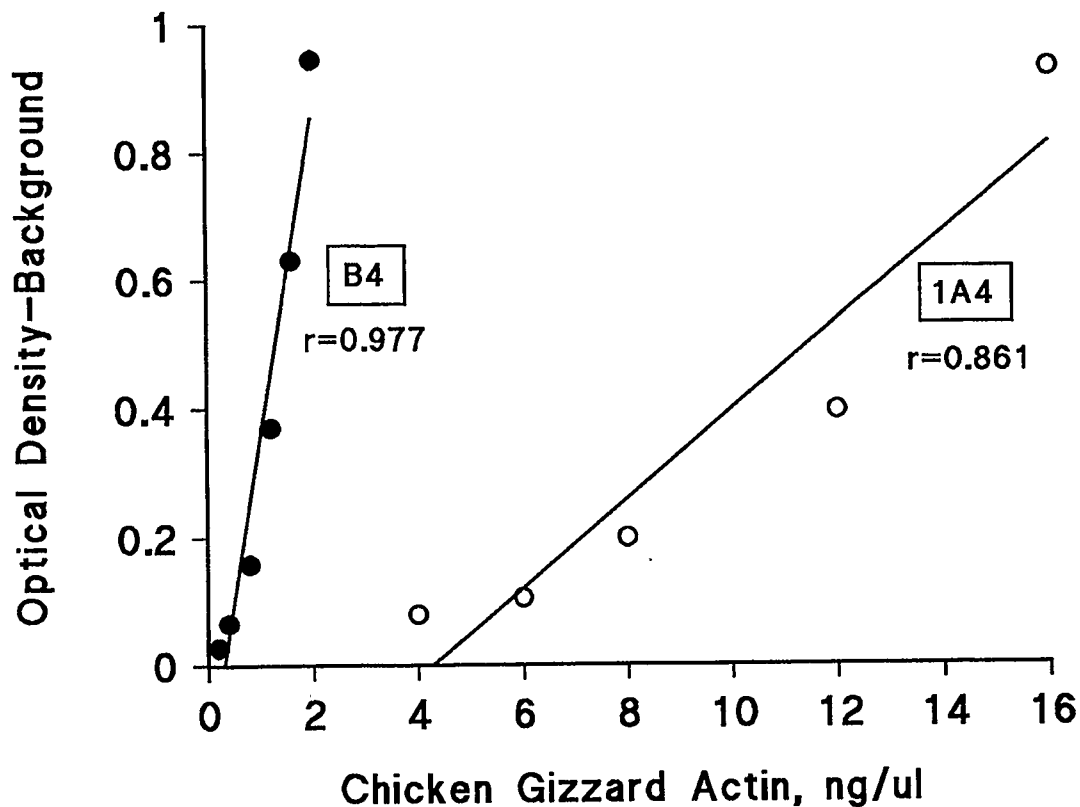


Figure 8.1. Representative standard curve of chicken gizzard actin. Commercially available chicken gizzard actin was serially diluted and assayed using a monoclonal antibody (B4) directed against γ -enteric isoactin (solid circles). Regression analysis indicates a linear relationship with an r value of 0.977. A standard curve could also be generated using a monoclonal antibody directed against α -vascular isoactin (1A4), although its sensitivity for gizzard actin was much less than that of the γ -enteric antibody, B4.

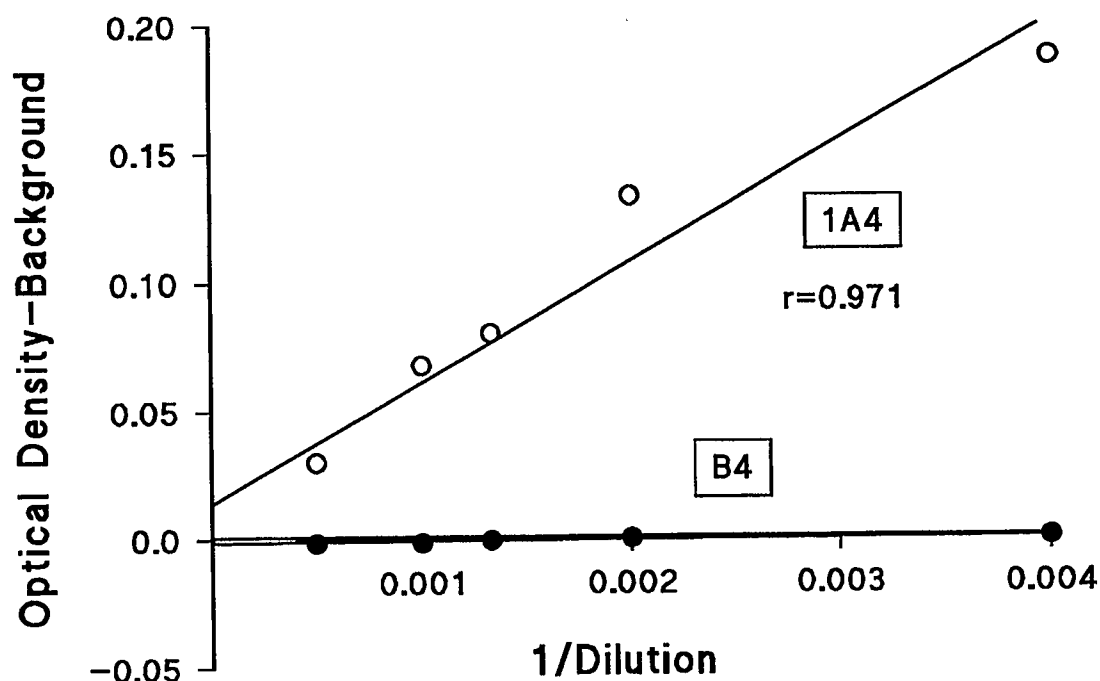


Figure 8.2. Representative standard curve of rat abdominal aorta. A sample of rat abdominal aorta was serially diluted and assayed using a monoclonal antibody directed against α -vascular isoactin (1A4). Regression analysis indicates a linear relationship with an r value of 0.971 (open circles). For comparison, the serially diluted sample was also assayed using antibody B4. For this monoclonal antibody directed against γ -enteric isoactin, optical density never exceeded the level of background at any concentration tested (solid circles).

8.2. INFLUENCE OF EXTRACELLULAR CALCIUM

The following section deals with both active tonic stress and active amplitude of phasic activity. These two contractile parameters are illustrated in Figure 8.3.

8.2.1. Extracellular calcium and bethanechol-stimulated tonic stress

Prior to alteration of extracellular calcium flux, the circular smooth muscle from the proximal jejunum of sham-operated and resected rats was stimulated with 10^{-4} M bethanechol in normal Krebs buffer. As shown in Figure 8.4. (upper and lower panels), bethanechol-stimulated tissues from resected rats generated significantly less tonic stress. This finding reproduces the results of previous experiments. The upper panel of Figure 8.4 shows the results of switching the external bathing buffer to one of modified Krebs containing $0 \text{ Ca}^{2+} + 2 \text{ mM EGTA}$ and then re-exposing the tissues to 10^{-4} M bethanechol. The magnitude of the tonic stress response was dramatically reduced in both treatment groups such that sham-operated tissues developed only 17%, and resected tissues only 44%, of the stress previously generated in normal Krebs buffer. The lower panel of Figure 8.4 shows that similar results were observed when tissues were pre-treated with the L-type calcium channel blocker, verapamil (10^{-6} M). Compared to control levels, the amount of stress generated by sham-operated and resected was only 8% and 28%, respectively. However, between sham-operated and resected groups, the bethanechol-stimulated tonic stress response was not different during blockade of extracellular calcium flux by either method.

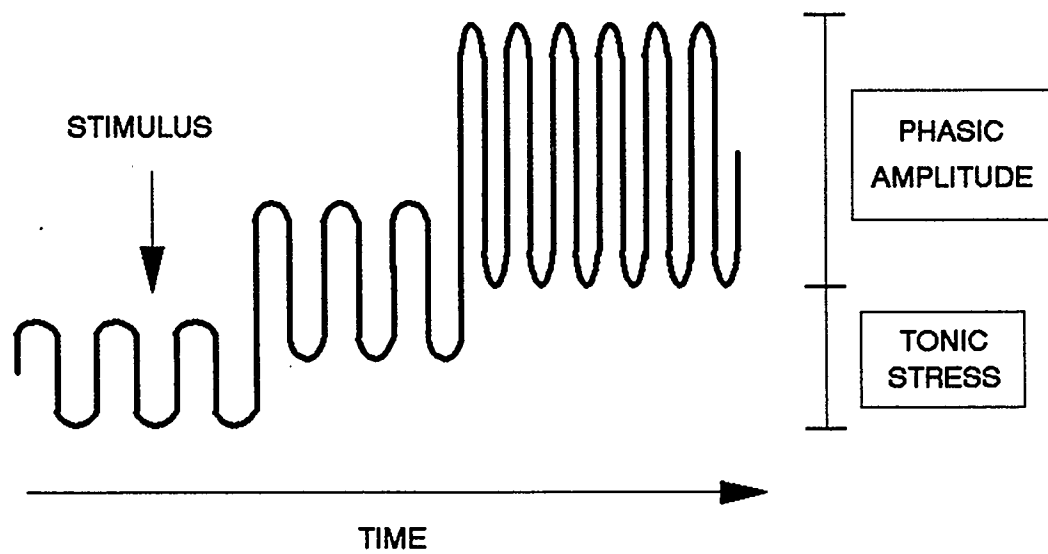
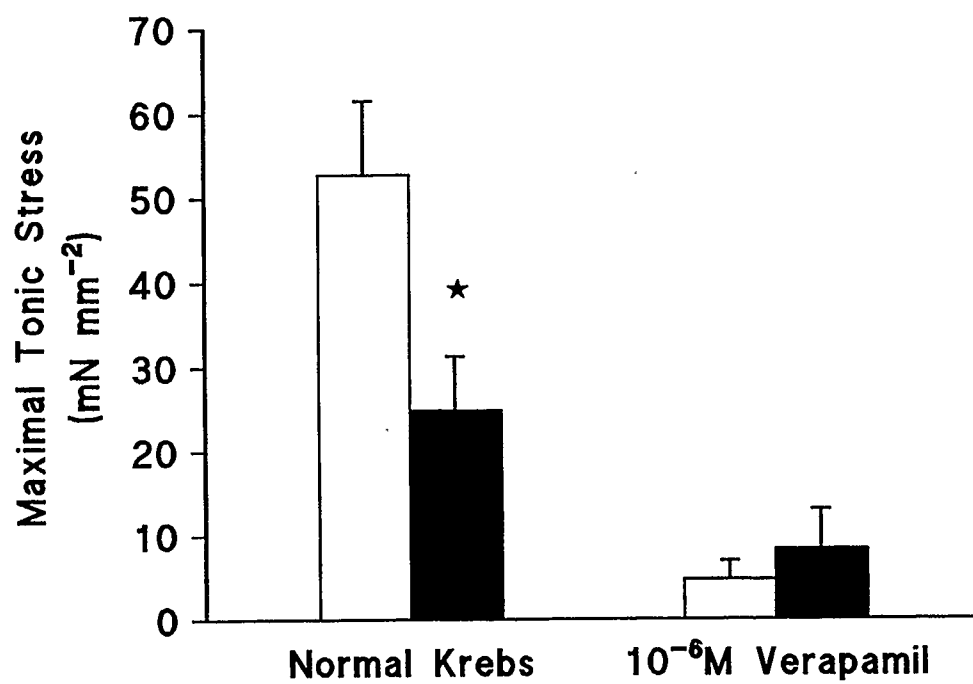
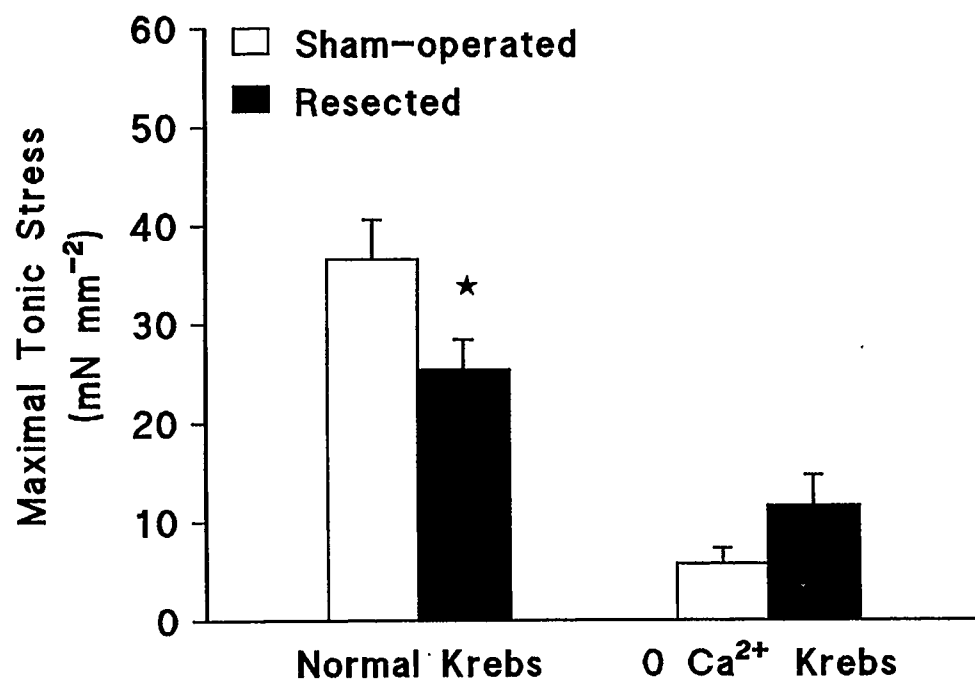


Figure 8.3. Schematic diagram of active tonic stress and phasic amplitude.

Figure 8.4. Extracellular calcium and bethanechol-stimulated tonic stress. The figure shows the maximal tonic stress (mN mm^{-2}) developed by jejunal circular muscle from sham-operated and resected rats following stimulation with 10^{-4} M bethanechol. *upper panel:* in normal Krebs buffer, and in modified Krebs buffer containing $0 \text{ Ca}^{2+} + 2 \text{ mM EGTA}$ (0 Ca^{2+} Krebs). *lower panel:* a separate experiment with normal Krebs buffer, and following pre-treatment with 10^{-6} M verapamil. Blockade of extracellular calcium flux by either method produced similar stress responses for sham-operated and resected groups. ★ $p < 0.05$. $n=4$ and 7 for sham-operated and resected groups, respectively.



8.2.2. Extracellular calcium and EF-stimulated tonic stress

In a subset of tissues used for the electrical field stimulation experiments, the tonic stress response to EFS was measured after exposure to 10^{-6} M nifedipine. As shown in Figure 8.5, this contractile parameter was reduced in both treatment groups and showed no significant difference between sham-operated and resected tissues.

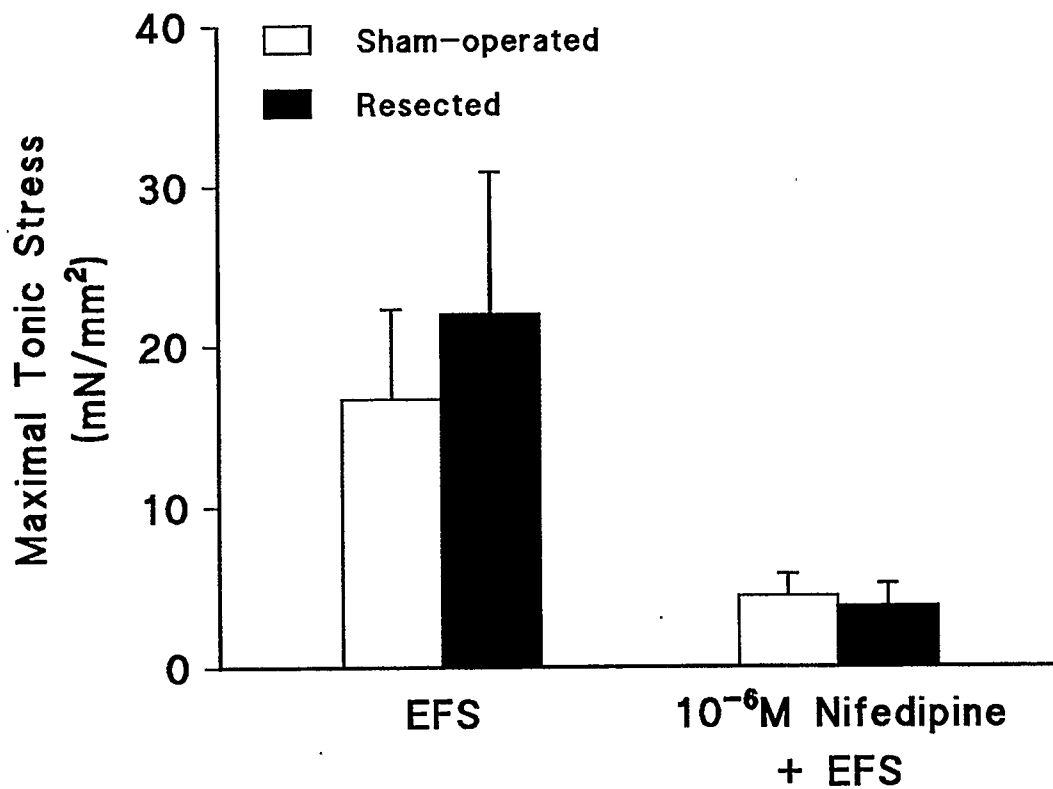


Figure 8.5. Extracellular calcium and EF-stimulated tonic stress. The figure shows the maximal tonic stress (mN mm^{-2}) developed by jejunal circular muscle from sham-operated and resected rats in response to electrical field stimulation both in the absence and presence of 10^{-6} M nifedipine. EFS consisted of an 80 volt charge delivered as 10 pulses sec^{-1} , 10 msec pulse $^{-1}$ with no delay for a period of 10 sec. In the presence of calcium channel blockade, non-receptor-mediated stimulation, like muscarinic-receptor activation, evoked similar responses in both treatment groups. $n=4$ and 6 for sham-operated and resected groups, respectively.

8.2.3. Extracellular calcium and bethanechol-stimulated phasic amplitude

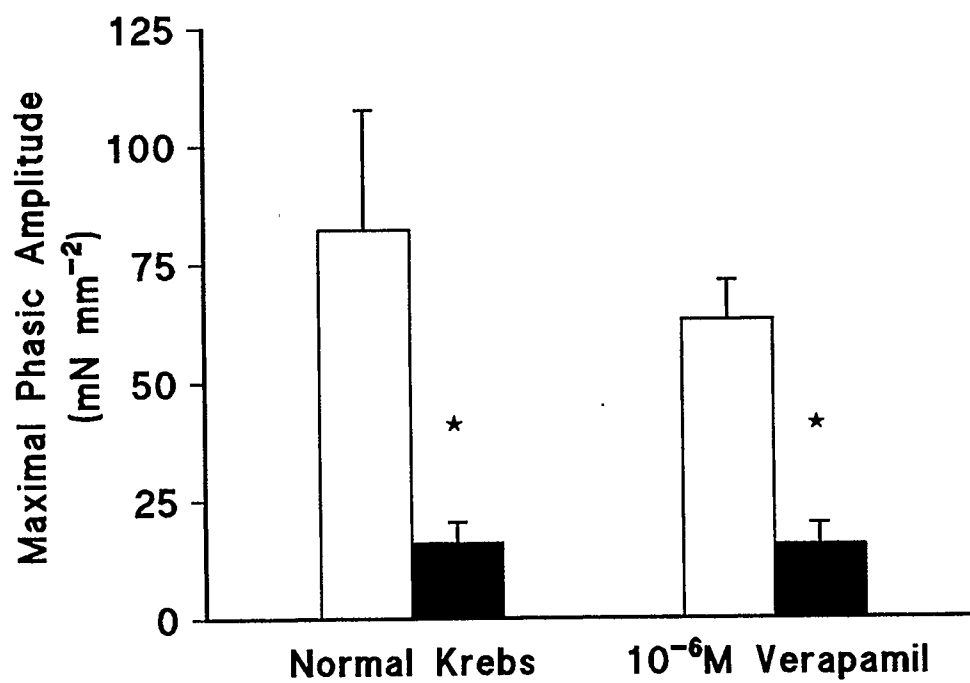
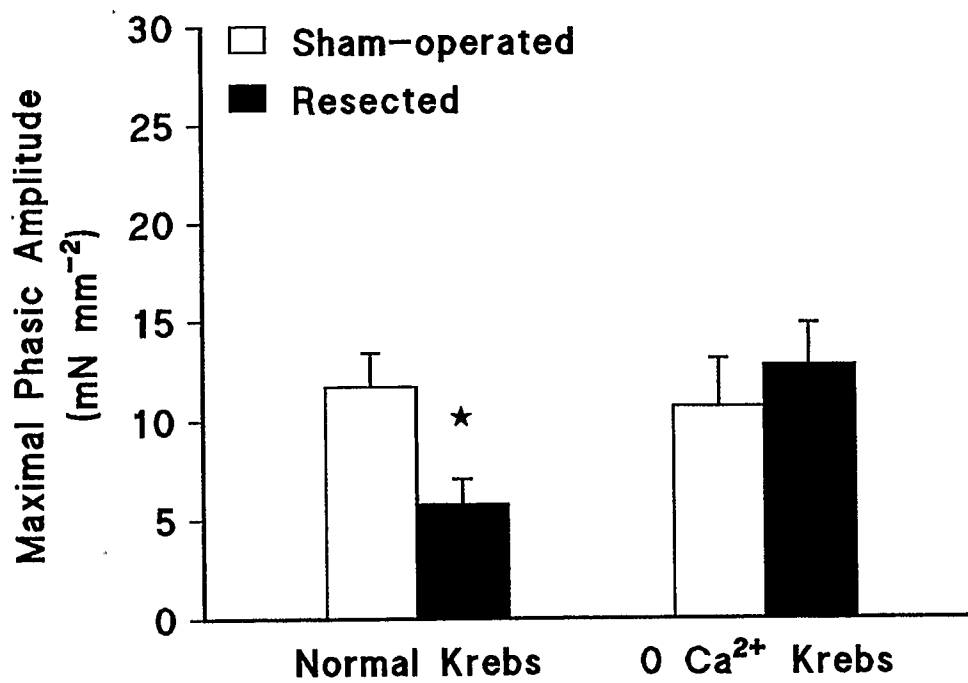
The results of these experiments are shown in Figure 8.6. Again, consistent with previous findings, bethanechol-stimulated tissues from resected rats developed significantly less phasic amplitude than sham-operated controls in normal Krebs buffer. The upper panel of Figure 8.6 shows the phasic amplitude response to 10^{-4} M bethanechol in modified Krebs buffer containing $0 \text{ Ca}^{2+} + 2 \text{ mM EGTA}$. Under these conditions, and in contrast to the tonic stress response (Figure 8.4), phasic amplitude was not diminished for either treatment group. In fact, resected tissues were able to generate 2.2 times more stress than under control conditions, thereby eradicating the significant difference observed between treatment groups. As shown in the lower panel of Figure 8.6, unlike the results with 0 Ca^{2+} buffer, pre-treatment of tissues with 10^{-6} M verapamil had no effect on the bethanechol-stimulated phasic amplitude of either sham-operated or resected tissues.

8.2.4. Extracellular calcium and EF-stimulated phasic amplitude

In a subset of tissues used for the electrical field stimulation experiments, the maximal phasic amplitude in response to EFS was measured in the presence of 10^{-6} M nifedipine. As shown in Figure 8.7, under these conditions phasic amplitude was further diminished and very nearly abolished in both treatment groups.

Figure 8.6. Extracellular calcium and bethanechol-stimulated phasic amplitude. The figure shows the maximal phasic amplitude (mN mm^{-2}) of jejunal circular tissue from sham-operated and resected rats following stimulation with 10^{-4} M bethanechol. *upper panel:* in normal Krebs buffer, and in modified Krebs buffer containing $0 \text{ Ca}^{2+} + 2 \text{ mM EGTA}$ (0 Ca^{2+} Krebs). *lower panel:* a separate experiment with normal Krebs buffer, and following pre-treatment with 10^{-6} M verapamil. The two conditions of extracellular calcium exclusion gave disparate results. In the case of 0 Ca^{2+} buffer, sham-operated and resected groups responded similarly. In contrast, the significantly reduced phasic amplitude of resected tissues was maintained in the presence of 10^{-6} M verapamil.

★ $p < 0.05$. $n=4$ and 7 for sham-operated and resected groups, respectively.



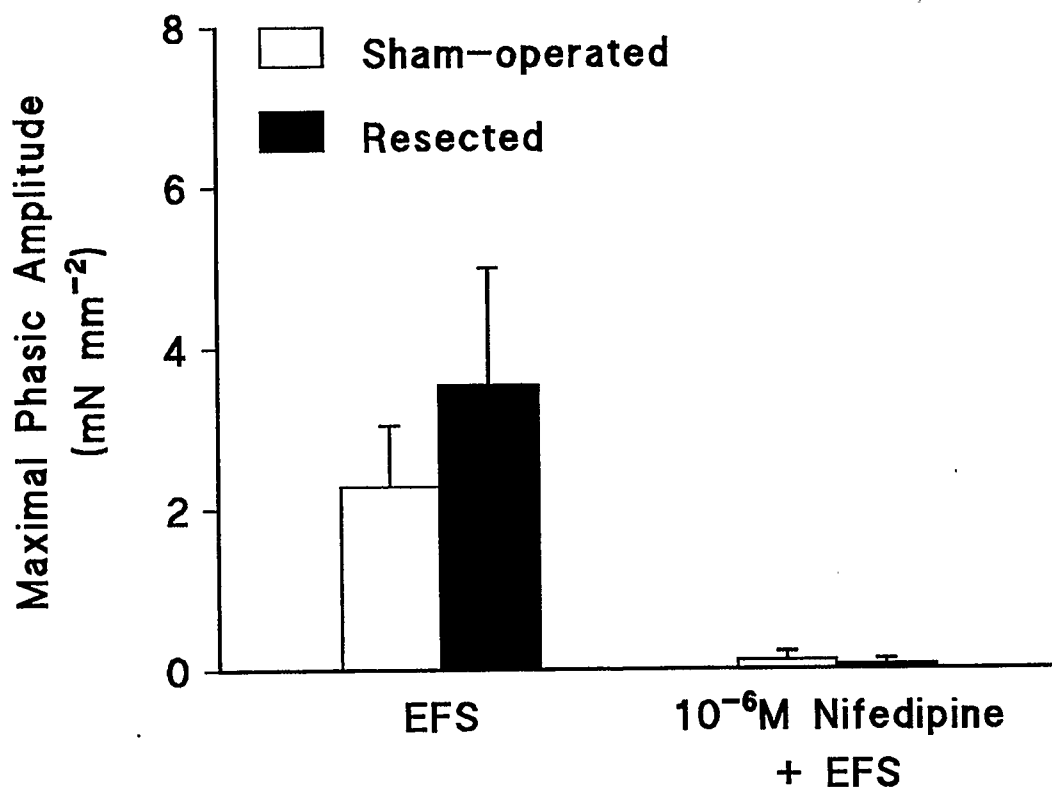
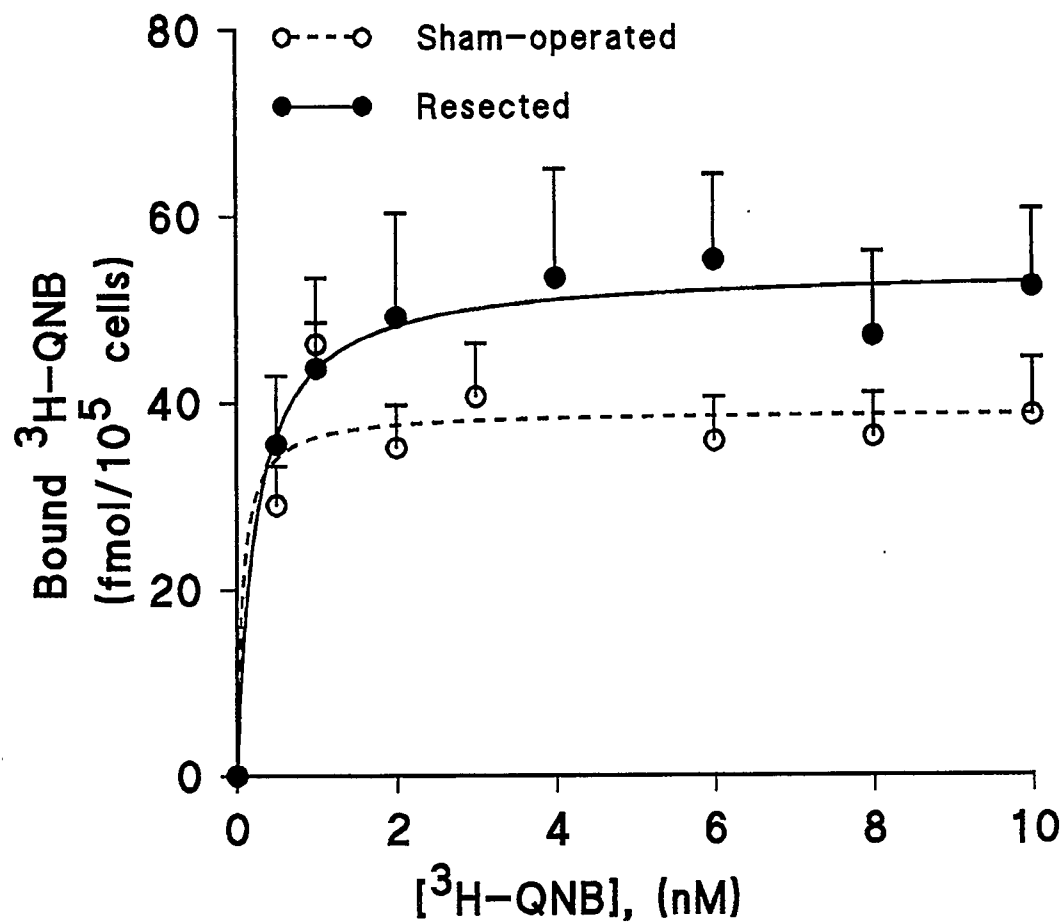


Figure 8.7. Extracellular calcium and EF-stimulated phasic amplitude. The figure shows the maximal phasic amplitude (mN mm⁻²) of jejunal circular muscle from sham-operated and resected rats in response to EFS in the absence and presence of 10⁻⁶ M nifedipine. EFS consisted of an 80 volt charge delivered as 10 pulses sec⁻¹, 10 msec pulse⁻¹ with no delay for a period of 10 sec. In the presence of calcium channel blockade, phasic amplitude was very nearly abolished for both treatment groups. n=4 and 6 for sham-operated and resected groups, respectively.

8.3. MUSCARINIC CHOLINERGIC RECEPTORS

The specific binding of ^3H -QNB to smooth muscle cells isolated from the proximal jejunum of sham-operated and resected rats is shown in Figure 8.8. Resected tissues demonstrated a significant increase in muscarinic receptor density, B_{max} , with no change in K_d .

Figure 8.8. Specific binding of ^3H -QNB. The specific binding of ^3H -QNB (fmol) to 10^5 smooth muscle cells isolated from the proximal jejunum of sham-operated and resected rats is shown. The data represent the difference between total and non-specific binding, the latter being determined in the presence of 10 μM atropine. Resection produced a significant increase in muscarinic receptor density, B_{max} , without altering K_d . ★ $p < 0.05$. $n=5$ for both groups.



<u>B_{max}</u>		
40.53 ± 2.66	S	
53.75 ± 5.03	R	*
<u>K_d</u>		
0.019 ± 0.066 nM	S	
0.243 ± 0.160 nM	R	

8.4. SUMMARY OF EXCLUDED POTENTIAL MECHANISMS

The depressed contractile response of jejunal circular muscle post-resection is not due to a change in the source (extracellular or intracellular) or the availability of intracellular calcium required for excitation-contraction coupling, nor is it due to a reduction in the number or the affinity of muscarinic receptors. On the contrary, the number of muscarinic receptors is significantly elevated on jejunal smooth muscle cells isolated from the muscularis propria of resected rats.

CHAPTER NINE**DISCUSSION**

9.1. MORPHOLOGICAL ALTERATIONS OF THE RESIDUAL BOWEL FOLLOWING MASSIVE INTESTINAL RESECTION

9.1.1. Intestinal length, circumference and wet weight

An increase in the length of the residual intestine did not constitute part of the adaptive response in the present model of resection. It appears from the literature that this particular aspect of adaptation is equivocal. In his extensive study, Nygaard (1967a) documented significant increases in both ileal and jejunal length post-resection, while others have reported no statistically significant changes in the intestinal length of the rat (Loran and Althausen, 1958) or in dogs with resections of up to 80% (Clatworthy et al., 1952; Flint, 1921). Studies in the human suggest that the potential for adaptive increases in intestinal length after resection may be greater in the pre-term versus full-term newborn infants (Touloukian and Walker-Smith, 1983), and other authors have suggested that an increase in intestinal length is not part of the adaptive response in the adult human (Bristol and Williamson, 1985; Dowling, 1982). If there is a tendency to increased length of residual intestine after resection, its magnitude and physiological relevance in other than pre-term infants would certainly appear to be of less importance than the adaptive changes in intestinal diameter or circumference.

As demonstrated by the present study, and those of others (Nygaard, 1967a; Dowling and Booth, 1967; Wilmore et al., 1971; Thompson et al., 1994), a consistent feature following extensive resection is a significant increase in the luminal diameter or external circumference of the residual bowel. It is the increment in this parameter, in

combination with mucosal hyperplasia, that permits dramatic increases in mucosal surface area and contributes to enhanced segmental absorption (Williamson, 1978).

The fact that significant increases in wet weight per unit length of full thickness gut or muscularis propria (Figure 4.4.) were accompanied by increases in total protein and DNA content per unit length of muscularis propria (Table 4.1) indicates that the greater wet weight of resected tissues cannot be explained by changes in water content. This finding of increased tissue mass post-resection has also been reported by others (Nygaard, 1967c; Hanson et al., 1977a; Wittman et al., 1986).

9.1.2. Hypertrophy versus hyperplasia

Although the increase in mucosal mass cm^{-1} observed after resection is very clearly due to mucosal hyperplasia (Williamson, 1978; Johnson, 1988), the significant increase in the circumference and weight cm^{-1} of muscularis propria has only been loosely described as "hypertrophic", based on macroscopic observations (Nygaard, 1967a; Wittman et al., 1986). Although quantification of the number of cells in the muscle layer was lacking, it has been reported that resection causes an increase in number, rather than size, of muscle cells (Nygaard, 1967a; Hanson et al., 1977a). This is the first study to objectively evaluate the adaptive response of the muscularis propria to resection using both morphometric and biochemical techniques. A hypertrophic tissue response would be expected to decrease the number of cross-sectioned circular smooth muscle cells per unit area and thereby increase the ratio of mg protein: μg DNA per cm length of muscularis

propria. In the case of a hyperplastic response, no change would be expected in either the number of cross-sectioned circular smooth muscle cells per unit area, or the ratio of mg protein:μg DNA per unit length of muscularis propria. A third possibility exists, exemplified by uterine smooth muscle during pregnancy (Van Der Heijden and James, 1975), and by vascular smooth muscle in response to hypertension (Owens and Schwartz, 1983), in which the number of cross-sectioned cells per unit area decreases (hypertrophy), but because polyploidy occurs in association, the ratio of protein:DNA is not elevated as would be expected with a hypertrophic response. In the present model of intestinal resection in the rat, there were no significant changes in cell density or the ratio of protein:DNA per unit length of muscularis propria. Taken together, these findings are consistent with a hyperplastic, rather than hypertrophic, adaptation.

9.1.3. Model design for subsequent studies

Analysis of the data generated in the studies characterizing the rat model of massive intestinal resection demonstrated no significant differences between the responses of unoperated control and sham-operated rats. For this reason, all subsequent experiments were designed including only two treatments, resection, and its proper surgical control, sham-operation.

9.2. LONGITUDINAL MUSCLE CONTRACTILITY

9.2.1. Basal stress in response to stretch

Since the development of basal stress in response to stretch was similar between treatment groups (Table 5.1), factors such as tissue elasticity and changes in the connective tissue matrix are unlikely to contribute to the alterations in phasic contractile activity observed in resected rats following stimulation with bethanechol.

9.2.2. Changes in contractility are distinct from circular muscle

The findings of the present studies involving longitudinal smooth muscle are in marked contrast to the striking alterations in contractile function of residual *circular* smooth muscle subsequent to massive small intestinal resection. In the latter tissue, the development of tonic stress (Figure 6.4), the frequency of phasic contractions (Figure 6.9) and the amplitude of phasic activity (Figure 6.10) were all significantly decreased following stimulation with bethanechol. In the case of bethanechol stimulation of longitudinal muscle, resection had no effect on tonic stress (Figure 5.4; Table 5.2), while increasing phasic frequency (Figure 5.6) and amplitude (Figure 5.7). Thus, the contractile parameter(s) affected by resection and the direction of their change (increase or decrease) differs between the two muscle layers.

In the small intestine the circular and longitudinal muscle layers are oriented in such a fashion that they develop tension in planes positioned at 90° relative to each other; contraction of circular muscle is associated with reduction in luminal diameter while

contraction of longitudinal muscle results in relative shortening of the intestinal segment. Functional motility requires co-ordination of these complementary capabilities, and not surprisingly the two muscle layers manifest differences in structure and innervation, presumably reflecting their reciprocal roles. For example, while neuronal projections from the myenteric plexus extend to the circular muscle layer (Brookes et al., 1991), such is not the case with the longitudinal muscle layer of the rodent. The comparatively thinner longitudinal muscle layer is innervated only at its interface with the myenteric plexus. Neurotransmitters are released from axonal varicosities (regions of the nerve fibres devoid of the glial sheath), reaching their effector organ, the longitudinal muscle, by diffusion (Gershon et al., 1994). The complementary nature of circular and longitudinal muscle function has been classically demonstrated as the law of the intestine by Bayliss and Starling (1899, 1900a, 1900b), and was later shown to be an intrinsic reflex of isolated guinea pig intestine by Trendelenberg (1917). The reflex, initiated by balloon distention of the lumen, co-ordinates a proximal propulsive and a more distal receiving segment. The receiving segment is configured by contraction of the longitudinal muscle and inhibition of the circular muscle in that segment, while in the propulsive segment the longitudinal muscle is relaxed and the circular muscle contracts. The situation *in vivo* is more complex. In the post-prandial state, small intestinal motility is characterized by rhythmic segmenting contractions which promote mixing, while over a long segment of bowel there is co-ordination of numerous short, overlapping propulsive and receiving segments. The co-ordination of reciprocal motor activity *in vivo* was

demonstrated very clearly in the canine small intestine (Sarna, 1993) and is thought to be mediated by neural modulation of smooth muscle contractility.

9.2.3. Functional relevance

While it is necessary that co-ordination of the complementary activity of intestinal circular and longitudinal muscle exists, there are also examples of differential development of active stress in circular and longitudinal muscle in response to a variety of agonists or treatments, including the model of massive intestinal resection described herein. As has been demonstrated by Minocha and Galligan (1991), pre-treatment of tissues with erythromycin inhibited the contractile response of longitudinal muscle to bethanechol and substance P, but had no effect on the responses of circular muscle in the same guinea-pig model. In response to stimulation with carbachol, longitudinal muscle from patients with Crohn's disease generated significantly greater maximal stress without an alteration in the EC_{50} , whereas circular muscle similarly stimulated showed no change in maximal stress and significant decrease in EC_{50} (Vermillion et al., 1993).

While in the present studies the longitudinal and circular muscle layer may show an intrinsic difference in phasic contractile frequency when stimulated independently *in vitro* (increased in longitudinal muscle; decreased in circular muscle), it is unlikely that a difference in the frequency of phasic activity between the two muscle layers exists *in vivo*. In the intact animal co-ordinated activity of the circular and longitudinal muscle layers is required for functional motility and effective propulsion, and myogenic, neural and

hormonal factors interact to establish a uniform slow wave frequency. While it is assumed that discordant contractile frequencies do not exist between the two muscle layers *in vivo*, previous studies of intestinal resection in rats in which *in vivo* myoelectric activity has been examined have not assessed the slow wave frequencies of circular and longitudinal muscle (Wittman et al., 1986, 1988).

With regard to the increase in amplitude of phasic activity observed in longitudinal muscle *in vitro* after resection, this may well occur *in vivo* and may represent an adaptation to enhance mixing of chyme in the context of significant increases in luminal diameter. The preservation of normal tonic contractile function of longitudinal muscle *in vitro*, in contrast to the significant decrease in tonic contractile ability of circular muscle, would not predict any change in the role of this muscle layer in tonic contractile activity *in vivo*. Overall, the combination of the adaptive changes in both circular and longitudinal muscle contractility observed *in vitro* in this model of resection are associated with a significant reduction in the velocity of transit of luminal contents (Figures 7.2, 7.4).

9.3. CIRCULAR MUSCLE CONTRACTILITY

9.3.1. Basal stress in response to stretch

Similar to the findings with longitudinal muscle, the observation that basal stress development was similar between sham-operated and resected rats (Table 6.1) indicates that factors such as tissue elasticity and alterations in the connective tissue matrix are

unlikely to contribute to the reduced contractile function observed in resected rats following stimulation with bethanechol.

9.3.2. Functional relevance of depressed contractility in response to bethanechol

The functional importance of acetylcholine, *in vivo*, to stimulate intestinal smooth muscle contraction cannot be under-estimated. Of all the neurotransmitters and neuromodulators studied to date, acetylcholine mediates the final common pathway for muscle excitation and hence is of primary importance in the regulation of gastrointestinal motility (Burks, 1994). The present studies have shown that in response to stimulation with the cholinergic analogue, bethanechol, several parameters of jejunal circular muscle contractile function (active tonic stress, basal and active phasic frequency and active phasic amplitude) are significantly depressed following massive intestinal resection. Given the major importance of acetylcholine in the contraction of intestinal muscle, the physiological relevance of this adaptation must be considered. After massive resection, the primary adaptive response of the residual intestine must be to compensate for the reduced absorptive surface. The mucosa proliferates to meet this demand (Dowling and Booth, 1967; Porus, 1965; Weser and Hernandez, 1971), with similar hyperplasia being observed in the muscularis propria (present study) in association with an increase in the circumference of the residual intestine (Nygaard, 1967c; Hanson et al., 1977a). The reduced ability of circular muscle from resected rats to generate tonic stress in response to bethanechol stimulation will not compensate for the increase in luminal diameter but will,

in fact, render the residual gut less capable of generating intraluminal pressure and, presumably, normal propulsion. This is substantiated by the significant decrease in the aboral velocity of transit of intestinal luminal contents in resected compared to sham-operated rats (Figures 7.2, 7.4). The obvious benefit is to increase mucosal contact time and segmental rates of absorption, especially if the increased amplitude of basal phasic contractile activity (Figure 6.10) continued to stir the chyme.

9.3.3. Source of the altered stress response

In the past, it has been generally accepted that bethanechol is a non-selective muscarinic agonist and, as such, these data would indicate that the origin of the depressed function is the circular smooth muscle itself. However, functional effects due to the activation of muscarinic receptors located in the submucous and myenteric plexuses have been reported (Kimura et al., 1994; Barocelli et al., 1994; Xu and Gintzler, 1992). Therefore, it must be considered that the alterations in contractility may be the result of neurogenic modulation. If, in the present studies, it is assumed that bethanechol acted via neural pathways to elicit a reduction in active stress development, then blockade of inhibitory nerve function with the Na^+ channel conductance blocker TTX should have produced an increase in the stress response. However, no change in response was observed at the lower bethanechol concentration and, in fact, a significant decrease was seen at the higher concentration (Figure 6.7). This latter observation could possibly be explained by the loss of an excitatory neural transmitter in response to bethanechol-

stimulation, but if this were the case, resected tissues should have generated significantly greater stress in the absence of TTX. This was not observed (Figure 6.4). Given that the magnitude of the stress developed in response to bethanechol did not change in the presence of TTX, the data are most consistent with a change in myogenic function after massive resection.

9.3.4. Source of the alterations in phasic contractility

Neural inputs clearly contribute to the generation of an increased frequency of phasic contractions in both the sham-operated and resected groups, since significant reductions were observed after pre-treatment of tissues with TTX (Figure 6.13). Compared to the sham-operated group, the reduced phasic contractile frequency in the basal state, and at lower concentrations of bethanechol post-resection while in the presence of TTX (Figure 6.14), demonstrates that a myogenic factor influencing phasic frequency is also altered in resected tissues.

A similar argument can be made for phasic amplitude. The fact that exposure to TTX did not alter the amplitude of phasic activity in tissues from either treatment group (Figure 6.15) indicates that the elevated basal and depressed active amplitude responses to bethanechol stimulation (Figure 6.10) were also myogenic in origin.

9.3.5. Relevance of the stress response to serotonin

It is interesting that, in contrast to the findings with bethanechol, resected tissues were able to generate more tonic stress than sham-operated tissues when stimulated with 5-HT. Since these experiments were conducted in the presence of the Na⁺ channel blocker tetrodotoxin (10^{-6} M), the contractile effects of 5-HT which occur via activation of neural pathways can be discounted. Thus, the increased tonic stress of resected tissues in response to 5-HT indicates an alteration at the level of the smooth muscle itself. As there exist both 5-HT₁ and 5-HT₂ receptors on gastrointestinal smooth muscle (Farthing, 1991), this finding may indicate changes in receptor number and/or affinity, as well as subtype. While the alteration in 5-HT-stimulated contraction occurs *in vitro*, its relative importance *in vivo* remains to be determined since it is acetylcholine which is the primary neurotransmitter responsible for the initiation of intestinal smooth muscle contraction.

It is not clear why 5-HT stimulation induces significant increases in maximal stress post-resection. It has long been speculated that 5-HT in the intestine is responsible for the initiation of the peristaltic reflex (Bülbring, 1958). There is evidence to suggest that 5-HT, released from enterochromaffin cells in response to activation of pressure-sensitive receptors (due to the presence of a luminal bolus), diffuses through the lamina propria to stimulate enteric neurons of the submucosal and myenteric plexuses. The resultant release of acetylcholine from neurons of the myenteric plexus causes contraction of the smooth muscle (Gershon, 1994). In the present studies of 5-HT and resection, the presence of 10^{-6} M TTX excludes the possibility of activation of neuronal pathways to

elicit muscle contraction. While 5-HT receptors are also present on smooth muscle, it appears that, at least in the longitudinal muscle of the guinea pig, much higher concentrations of neurotransmitter are required for muscle stimulation than for neuronal activation (Buchheit et al., 1985), calling into question the physiological relevance of the former.

9.4. POTENTIAL MECHANISMS OF ADAPTATION

9.4.1. Contractile machinery of smooth muscle

Given the extensive literature on the adaptive changes in cardiac muscle after pressure-overload induced hypertrophy, it was originally hypothesized that, if altered contractility of intestinal smooth muscle was observed after massive resection, then alterations in contractile protein function (interactions between actin and myosin) could be responsible. However, in the present model, such was not the case. This conclusion, that the function of the contractile apparatus remains intact post-resection, is based on the following evidence. Firstly, resection did not alter the maximal stress response of jejunal circular smooth muscle to KCl (Table 6.2). Secondly, the ratios of maximal stress:response time (*i.e.*, rate of stress development) for sham-operated and resected rats were not different (section 6.3.2). Thirdly, it was observed that contraction of jejunal circular muscle using a non-receptor-mediated stimulus, namely electrical field stimulation, was not affected by resection (Figures 8.5, 8.7). Thus, the site of the

alteration responsible for the diminished bethanechol-stimulated stress response is most likely proximal to activation of the contractile apparatus.

9.4.2. Extracellular calcium and stress

Another potential mechanism to explain the depressed contractility of circular muscle of the remnant bowel may be an alteration in the source (extracellular or intracellular) of calcium utilized during excitation-contraction coupling. This phenomenon has been observed in jejunal longitudinal muscle from rats parasitized with the nematode, *Nippostrongylus brasiliensis*. In that model, infected tissues exhibited a much greater dependence on extracellular Ca^{2+} for carbachol-stimulated muscle contraction, concomitant with changes in tonic muscle contractility (Fox-Robichaud and Collins, 1986). In the present studies, when extracellular calcium entry was prevented, whether by its absence from the external bathing medium or by calcium channel blockade, the magnitude of the tonic stress generated in response to bethanechol stimulation, albeit reduced in both groups from control levels, was unaffected by resection (Figure 8.4). This indicates that the release of Ca^{2+} from intracellular stores in response to muscarinic receptor activation is unchanged following resection, but that intracellular Ca^{2+} stores account for only a minor portion of the total stress response of both the sham-operated and resected groups. This implies that under normal conditions, muscarinic receptor activation leads to mobilization of calcium from both intracellular and extracellular stores, a finding that has also been observed in intestinal smooth muscle from the guinea pig

(Isenberg, 1993; Prestwich and Bolton, 1995). It is also interesting that in response to non-receptor mediated stimulation, specifically EFS, in the presence of the L-type calcium channel blocker nifedipine, there remains a small, measurable tonic stress response in both groups (Figure 8.5), which is similar in magnitude to that generated by bethanechol-stimulation in the presence of verapamil (Figure 8.4). Whether contraction is mediated through receptor activation or membrane depolarization, the observation that similar levels of stress were generated under these two conditions indicates that the availability of calcium from the intracellular store is not somehow compromised during bethanechol stimulation. Taken together, these data demonstrate that the normal tonic stress response of circular smooth muscle utilizes both extracellular and intracellular sources of calcium. Massive intestinal resection did not alter this Ca^{2+} distribution, nor did it affect the availability of Ca^{2+} from the intracellular store alone.

9.4.3. Extracellular calcium and phasic amplitude

The present studies suggest that the pool of calcium utilized in excitation-contraction coupling is different for the generation of phasic amplitude versus tonic stress. In the sham-operated group, the magnitude of phasic amplitude was not affected by either means of excluded calcium entry, suggesting that the entire phasic contractile response can be achieved by the release of calcium from the intracellular compartment alone (Figure 8.6). There is some inconsistency of the data with regard to the effects of the two modes of calcium exclusion on phasic contractility within the resected group. The

magnitude of the phasic contractile response of resected tissues is the same as sham-operated animals in 0 Ca^{2+} Krebs, but significantly reduced compared to sham-operated controls in verapamil (Figure 8.6). However, since the phasic contractile response of resected tissues with extracellular Ca^{2+} excluded was not decreased compared to the magnitude of the response when it was available (Figure 8.6), it is concluded that the phasic contractile response of resected tissues is also derived from intracellular calcium stores alone. Taken together, the independent nature of the tonic stress and phasic amplitude responses suggests that the tonic and phasic components of muscle contraction in response to bethanechol are mediated via separate mechanisms. To date, the mechanisms within smooth muscle which mediate the tonic versus the phasic aspects of intestinal contractile function are not well understood. Similar knowledge is lacking at the level of neuronal control, but it is speculated that subpopulations of excitatory motor neurons must exist that separately control muscle tone and phasic activity in order to achieve the precision necessary for the moment-to-moment regulation of muscle contractile function (Wood, 1994).

9.4.4. Interpretation of binding studies

The specific nature of the depressed contractility of circular muscle in response to bethanechol, and not 5-HT, KCl, or electrical field stimulation, leads to the question "Does resection alter muscarinic receptor number and/or affinity?". To answer this question, receptor binding assays were performed using ^3H -QNB, a muscarinic

cholinergic antagonist. This radioligand has been extensively used to quantify muscarinic receptors using a variety of tissues (Yamamura and Snyder, 1974; Kloog and Sokolovsky, 1977; Fields et al., 1978; Rimele et al., 1979). Ideally, the source of tissue for these assays should have been limited to the circular muscle alone. However, in the rat, separation of the circular from the longitudinal muscle layer is technically very difficult and severely limits the amount of tissue from which smooth muscle cells can be isolated. From the studies involving characterization of the resection model, it was determined that the longitudinal muscle represents the minor portion of the total thickness of the muscularis propria, only ~35% (Figure 4.5). In addition, functional assay of the tonic stress developed by jejunal longitudinal muscle in response to bethanechol stimulation was shown to be unchanged following resection (Figure 5.4; Table 5.2). Thus, for technical reasons the ^3H -QNB binding experiments were conducted on smooth muscle cells isolated from the intact muscularis propria, *i.e.*, both circular and longitudinal muscle, although the contribution of the latter is assumed to be minimal.

The data from the binding experiments showed, unexpectedly, that the previously demonstrated depressed contractile response of circular smooth muscle from the jejunum of resected rats (Figure 6.4) was associated, not with a decrease, but rather a significant increase in the total number of muscarinic receptors (^3H -QNB does not distinguish among muscarinic receptor types) (Figure 8.8). The present data did not demonstrate any significant alteration in K_d following resection, although the inclusion of additional data points in the range of 0 to 1 nM ^3H -QNB might have indicated otherwise. In any event,

despite an increase in the number of muscarinic receptors, the bethanechol-stimulated contractile response of resected circular muscle remains significantly reduced. Although intact muscularis propria was used to isolate smooth muscle cells for the ^3H -QNB binding studies, for the reasons previously stated, it is assumed that the increased number of muscarinic binding sites must be attributed in large part to alteration in the quantitatively much larger circular smooth muscle layer.

It is interesting to speculate as to the reason for an adaptive increase in muscarinic receptor density following resection. At the level of smooth muscle function, the up-regulation of muscarinic receptors may have arisen to offset whatever mechanism(s) served to significantly reduce the contractile response to cholinergic stimulation. Presumably, without this increase, contractile activity would be even further reduced. While a certain degree of depressed contractile activity might confer alterations in motor patterns concomitant with a decreased rate of transit, there may exist a point at which severely depressed contractility leads to dysfunctional motility and impaired nutritional status. The present studies may represent a balance between these two states.

9.5. ALTERATIONS *IN VIVO* - GASTROINTESTINAL TRANSIT

The importance of any adaptive changes in muscle contractile function following resection must be to increase transit time and, by extension, increase the contact time of chyme with the digestive and absorptive surfaces of the mucosa. Indeed, the changes in *in vitro* smooth muscle contractility in the present model are associated with a reduction

in the velocity of intestinal transit (Figures 7.2, 7.4), without a change in the rate of gastric emptying (Figures 7.1, 7.3). This suggests that a functional ileal brake is not operating to slow gastric emptying. It may be that the adaptive responses in the residual jejunal segment, mucosal and muscular, are sufficient to achieve maximal absorption, thereby preventing significant levels of lipid reaching the distal ileum and initiating the reflex. The normal growth rate of resected rats over the study period (Figure 4.1) would support this contention. Alternatively, the ileal brake may be intact and functioning to reduce the rate of emptying of solids from the stomach, without affecting the gastric emptying of liquids. The former aspect of gastrointestinal transit could not be measured in the present studies, as ^{51}Cr remains associated with the liquid phase of the test meal. There remains a third possibility, namely that fat malabsorption and a dysfunctional ileal brake ensue post-resection. Although fecal fat content was not assessed, the absence of a compromised growth rate, coupled with the absence of diarrhea, makes this possibility unlikely in the present model of resection.

9.6. SUMMARY AND CONCLUSIONS

In this rat model of massive mid-jejuno-ileal resection, resected animals compensated for the impact of reduced absorptive surface area and exhibited a normal growth velocity by initially maintaining a greater food intake compared to both the control and sham-operated rats. In the resected group, intestinal adaptation was characterized by a significant increase in circumference, but not length of the residual intestine, and a

significant increase in the jejunal wet weight cm^{-1} without any increase in thickness of the circular or longitudinal muscle layers. The increased circumference and mass of the muscularis propria cm^{-1} were associated with increases in mg protein and μg DNA cm^{-1} , but no change in the number of cross-sectioned smooth muscle cells mm^{-1} or in the ratio of mg protein: μg DNA per unit length of muscularis propria, indicative of hyperplasia rather than hypertrophy. These morphological adaptive responses to massive resection occurred in the first ten days post-surgery.

Residual jejunal longitudinal muscle demonstrated no adaptive change in basal stress in response to stretch, optimal length for development of active tension, or tonic stress development in response to bethanechol or KCl. In contrast, phasic frequency and amplitude were significantly elevated both before and after stimulation with bethanechol, and these alterations were shown to be myogenic in origin.

Residual jejunal circular muscle displayed no alteration in basal stress in response to stretch, but did exhibit significant decreases in the development of active tonic stress and the frequency of phasic contraction following stimulation with bethanechol. While the amplitude of spontaneous phasic activity was significantly increased after resection, the increase in amplitude in response to cholinergic stimulation was significantly reduced.

Residual small intestinal longitudinal and circular muscle layers studied *in vitro* exhibit independent adaptive responses to massive resection, which for both muscle layers had occurred by day 10 post-surgery. Overall, the combination of the adaptive contractile changes in the two muscle layers observed *in vitro* in this model of massive intestinal

resection is associated with a significant reduction in the velocity of intestinal transit of luminal contents.

The depressed bethanechol-stimulated contractile response of the circular smooth muscle from the remnant jejunum is not characteristic of the response to all excitatory stimuli, cannot be attributed to a switch in the source (extracellular or intracellular) or the availability of intracellular calcium required for excitation-contraction coupling, nor can it be ascribed to a reduction in the number or affinity (additional data points might prove otherwise) of muscarinic receptors. This depressed response is not observed with 5-HT, KCl or electrical field stimulation, and is therefore unique to muscarinic receptor activation. The reduced contractility of resected tissues to bethanechol occurs despite a compensatory increase in muscarinic receptor number. It remains possible that resection induces alterations in receptor/G-protein coupling, signal transduction pathway(s) or calcium entry into the cell.

It is of interest that the two components of the contractile response, tonic and phasic activity, utilize different sources of calcium. The former relies on calcium mobilization from both intracellular and extracellular compartments, while the latter depends largely on the intracellular calcium store.

CHAPTER TEN

FUTURE PERSPECTIVES

The present investigation has demonstrated structural, contractile and functional adaptation of jejunal smooth muscle following massive intestinal resection and, in so doing, has delineated several avenues of future research.

1) Temporal aspect of adaptation

The structural adaptation of the remnant bowel, the adaptive contractile responses of longitudinal and circular muscle, and the reduction in velocity of intestinal transit were observed at the earliest time point studied, post-surgical day 10, and persisted thereafter. In the human, clinical adaptation occurs over months following resection. For this reason, the response to massive intestinal resection in the rat was studied over a forty day post-surgical period. However, the unexpectedly rapid rate of adaptation did not permit a temporal analysis. Thus, it has yet to be determined how soon after surgical manipulation these changes occur.

2) The mechanism of altered contractility

The present studies have eliminated several possible mechanisms of altered contractility, and have suggested a number of avenues for future research. Clearly, it is necessary to determine the magnitude of Ca^{2+} influx from extracellular sources in response to bethanechol stimulation of jejunal circular muscle. At the level of flux through specific ion channels, this would best be accomplished through patch-clamp experiments. In this manner, the open probability, the mean open time and the amplitude

of the current through L-type calcium channels and, possible non-specific cation channels, could be assessed. There is evidence that canine colonic circular muscle utilizes up to three sources of Ca^{2+} during excitation-contraction coupling, the major source being extracellular, with Ca^{2+} entering the cell via L-type calcium channels, release from intracellular stores, and possibly additional Ca^{2+} release and/or influx via an as yet undetermined pathway (Sato et al., 1994). It may yet be determined that conductances other than those through L-type channels contribute to the increase in intracellular Ca^{2+} following bethanechol stimulation. In addition to assessing single channel conductance characteristics, total cytosolic calcium levels, using calcium indicators such as Fura-2, could be measured spectrophotometrically in isolated smooth muscle cell suspensions subsequent to agonist stimulation. Manipulation of the external buffer; *i.e.*, \pm calcium, the addition of calcium channel blockers \pm cell permeant calcium chelators, would permit measurement of the relative magnitude of calcium fluxes from extracellular and intracellular sources.

3) Signal transduction pathways

Muscarinic receptor types on gastrointestinal smooth muscle include M2 and M3, both of which are coupled to heterotrimeric G-proteins. In the case of M2, coupling to the G_i alpha subunit leads to reduced adenylyl cyclase activity, decreased conductance through Ca^{2+} channels and increased conductance through K^+ channels. Activation of M3 receptors, coupled to G_q alpha subunit, results in the generation of the second

messenger IP_3 , with subsequent release of intracellular stores. In the present studies, resection had no effect on the contractile response generated by release of calcium from intracellular stores alone. From a purely speculative viewpoint, this might suggest that coupling of M3 receptors, which may or may not be increased in number, to G_q , and the signal transduction cascade that follows is intact. Alternatively, it is possible that the increased muscarinic receptor density, determined from the binding assays, reflects an increase in the number of muscarinic M2 receptors. Stimulation of these receptors with bethanechol may lead to an impairment in the Ca^{2+} influx from extracellular sources, perhaps through hyperpolarization of the cell (opening of K^+ channels), or perhaps via direct effects on Ca^{2+} channels. The use of molecular approaches, such as polymerase chain reaction and Western blot analysis, would permit the quantification of muscarinic receptor subtypes to assess whether massive resection alters their distribution. In addition, pharmacological techniques which selectively inactivate specific receptor subtypes (alkylation) would allow better characterization of the contractile effects associated with a single receptor subtype.

4) Generation of tonic stress versus phasic activity

The present studies suggest that the development of tonic stress and phasic activity in intestinal circular smooth muscle utilizes distinct pathways for calcium mobilization. In the literature, this hypothesis has not been well studied, and would benefit from further investigation, both at the level of smooth muscle and the enteric nervous system.

5) Neurogenic adaptation

Given that myogenic adaptation occurs post-resection, it is not unreasonable to expect that changes also occur at the level of control of the enteric nervous system. Changes in neurotransmitter content and release from the myenteric plexus have been observed following infection with *Trichinella spiralis* (Collins, 1993), a model associated with alterations in smooth muscle contractility and intestinal transit. Clearly, this possibility also exists in the model of massive intestinal resection.

6) Model of dysfunction

The present investigations have dealt with a model of adaptation. Given this groundwork, it would be of clinical relevance to develop a model which is unable to adapt to massive resection, *i.e.*, one that resembles Short Bowel Syndrome. The animal of choice might not be the rat, as its abilities for adaptation are clearly exceptional. One potential candidate is the dog, whose larger size facilitates tissue sampling and instrumentation, as well as being more amenable to stool collection and monitoring.

CHAPTER ELEVEN

BIBLIOGRAPHY

Alpert NR, Mulieri LA. Increased myothermal economy of isometric force generation in compensated cardiac hypertrophy induced by pulmonary artery constriction in the rabbit. A characterization of heat liberation in normal and hypertrophied right ventricular papillary muscles. *Circ Res* 1982;50:491-500.

Altmann GC, Leblond CF. Factors influencing villus size in the small intestine of adult rats as revealed by transposition of intestinal segments. *Am J Anat* 1970;127:15-36.

Barocelli E, Ballabeni V, Chiavarini M, Molina E, Lavezzo A, Impicciatore M. Muscarinic M1 and M3 receptor antagonist effects of a new pirenzepine analogue in isolated guinea-pig ileal longitudinal muscle-myenteric plexus. *Eur J Pharmacol* 1994;254:151-157.

Bayliss WM, Starling EH. The movements and innervation of the small intestine. *J Physiol (London)* 1899;24:99-143.

Bayliss WM, Starling EH. The movements and innervation of the large intestine. *J Physiol (London)* 1900a;26:107-118.

Bayliss WM, Starling EH. The movements and innervation of the small intestine. *J Physiol (London)* 1900b;26:125-138.

Benzonana G, Skalli O, Gabbiani G. Correlation between the distribution of smooth muscle or non smooth muscle myosins and α -smooth muscle actin in normal and pathological soft tissues. *Cell Motil Cytoskel* 1988;11:260-277.

Bitar KN, Makhoul GM. Receptors on smooth muscle cells: characterization by contraction and specific antagonists. *Am J Physiol* 1982;242:G400-G407.

Black FM, Packer SE, Parker TG, Michael LG, Roberts R, Schwartz RJ, Schneider MD. The vascular smooth muscle α -actin gene is reactivated during cardiac hypertrophy provoked by load. *J Clin Invest* 1991;88:1581-1588.

Bohane TD, Haka-Ikse K, Biggar WD, Hamilton JR, Gall DG. A clinical study of young infants after small intestinal resection. *J Pediatr* 1979;94:552-558.

Bowers RL, Eeckhout C, Weisbrodt NW. Actomyosin, collagen and cell hypertrophy in intestinal muscle after jejunoileal bypass. *Am J Physiol* 1986;250:G70-G75.

Bristol JB, Williamson RCN. Post-operative adaptation of the small intestine. *World J Surg* 1985;9:825-832.

Brookes SJH, Steele PA, Costa M. Identification and immunohistochemistry of cholinergic and non-cholinergic circular muscle motor neurons in the guinea-pig small intestine. *Neuroscience* 1991;42:863-878.

Buchheit K-H, Engel G, Mutschler E, Richardson B. Study of the contractile effect of 5-hydroxytryptamine (5-HT) in the isolated longitudinal muscle strip from guinea-pig ileum. Evidence for two distinct release mechanisms. *Naunyn-Schmiedeberg's Arch Pharmacol* 1985;329:36-41.

Bueno L, Fioramonti J. Food and gastrointestinal motility. In: *An Illustrated Guide to Gastrointestinal Motility, Second Edition*, Eds. Kumar D, Wingate D, Churchill Livingstone, New York 1993;pp130-143.

Bueno L, Fioramonti J, Rayner V, Ruckebusch Y. Effects of motilin, somatostatin and pancreatic polypeptide on the migrating myoelectric complex in pigs and dogs. *Gastroenterology*, 1982;82:1395-1402.

Bueno L, Fioramonti J, Ruckebusch Y. Rate of flow of digesta and electrical activity of the small intestine in dogs and sheep. *J Physiol (London)* 1975;249:69-85.

Bülbring E, Lin RCY. The effect of intraluminal application of 5-hydroxytryptamine and 5-hydroxytryptophan on peristalsis, the local production of 5-hydroxytryptamine and its release in relation to intraluminal pressure and propulsive activity. *J Physiol (London)* 1958;140:381-407.

Burks TF. Neurotransmission and neurotransmitters. In: *Physiology of the Gastrointestinal Tract, Third Edition*, Ed. Johnson L, 1994;pp221-242.

Castro GA, Post CA, Roy SA. Intestinal motility during the enteric phase of trichinosis in immunized rats. *J Parasitol* 1977;63:713-719.

Clatworthy HW Jr, Saleby R, Lovingood C. Extensive small bowel resection in young dogs: its effect on growth and development. *Surgery* 1952;32:3341-3349.

Code CF, Marlett JA. The interdigestive myoelectric complex of the stomach and the small bowel of dogs. *J Physiol (London)* 1975;246:298-309.

Cohen JD, Kao HW, Tan ST, Lechago J, Snape WJ Jr. Effect of acute experimental colitis on rabbit colonic smooth muscle. *Am J Physiol* 1986;251:G538-G545.

Collins SM. The immune system. In: An Illustrated Guide to Gastrointestinal Motility, Second Edition, Eds. Kumar D, Wingate D, Churchill Livingstone, New York 1993;pp 118-129.

Collins SM, Gardner JD. Cholecystokinin-induced contraction of dispersed smooth muscle cells. *Am J Physiol* 1982;243:G487-G504.

Crosthwaite AIP, Huizinga JD, Fox JET. Jejunal circular muscle motility is decreased in nematode-infected rat. *Gastroenterology* 1990;98:59-65.

Dowling RH. Small bowel adaptation and its regulation. *Scand J Gastroenterol* 1982;17:53-74.

Dowling RH, Booth CC. Structural and functional changes following small intestinal resection in the rat. *Clin Sci* 1967;32:139-149.

Eeckhout C, De Wever I, Peeters I, Hellemans J, Vantrappen G. Role of gastrin and insulin in postprandial disruption of migrating complex in dog. *Am J Physiol* 1978;235:E666-E669.

Farthing MJG. 5-hydroxytryptamine and 5-hydroxytryptamine-3 receptor antagonists. *Scand J Gastroenterol*; 1991;188:92-100.

Fatigati V, Murphy RA. Actin and tropomyosin variants in smooth muscles. Dependence on tissue type. *J Biol Chem* 1984;259:14383-14388.

Fields JZ, Roeske WR, Morkin E, Yamamura HI. Cardiac muscarinic cholinergic receptors. Biochemical identification and characterization. *J Biol Chem* 1978;253:3251-3258.

Flint JM. The effect of extensive resection of the small intestine. *Bull Johns Hopk Hosp* 1921;23:127-144.

Fox-Robichaud AE, Collins SM. Altered calcium-handling properties of jejunal smooth muscle from the nematode-infected rat. *Gastroenterology* 1986;91:1462-1469.

Fridhandler TM, Davison JS, Shaffer EA. Defective gallbladder contractility in the ground squirrel and prairie dog during the early stages of cholesterol gallstone formation. *Gastroenterology* 1983;85:803-806.

Gershon MD, Kirchgessner AL, Wade DR. Functional anatomy of the enteric nervous system. In: Physiology of the Gastrointestinal Tract, Third Edition, Ed. Johnson L, Raven Press, New York 1994;pp381-422.

Gouttebel MC, Saint Aubert B, Colette C, Astre C, Monnier LH, Joyeux H. Intestinal adaptation in patients with short bowel syndrome. Measurement by calcium absorption. Dig Dis Sci 1989;34:709-715.

Granger DN, Barrowman JA, Kvietys PR. The small intestine. In: Clinical Gastrointestinal Physiology, W.B. Saunders, Philadelphia 1985;pp141-207.

Hanson WR, Osborne JW, Sharp JS. Compensation by the residual intestine after intestinal resection in the rat. I. Influence of amount of tissue removed. Gastroenterology 1977a;72:692-700.

Hanson WR, Osborne JW, Sharp JF. Compensation by the residual intestine after intestinal resection in the rat. II. Influence of postoperative time interval. Gastroenterology 1977b;72:701-705.

Helper DJ, Lash JA, Hathaway DR. Distribution of isoelectric variants of the 17,000-Dalton myosin light chain in mammalian smooth muscle. J Biol Chem 1988;263:15748-15753.

Holgate AM, Read NW. The effect of ileal infusion on gastrointestinal transit, ileal flow rate and carbohydrate absorption in humans after a liquid meal. Gastroenterology 1985;88:1005-1011.

Huizinga JD. Action potentials in gastrointestinal smooth muscle. Can J Physiol Pharmacol 1991;69:1133-1142.

Isenberg G. Nonselective cation channels in cardiac and smooth muscle cells. EXS 1993;66:247-260.

Izumo S, Nadal-Ginard B, Mahdavi V. Protooncogene induction and reprogramming of cardiac gene expression produced by pressure overload. Proc Natl Acad Sci USA 1988;85:339-343.

Johnson LR. Regulation of gastrointestinal mucosal growth. Physiol Rev 1988;68:456-498.

Kalser MH, Roth JLA, Tumen H, Johnson TA. Relation of small bowel resection to nutrition in man. Gastroenterology 1960;38:605.

Kimura H, Ito S, Ohta T, Asano T, Nakazato Y. Vasoactive intestinal peptide released by acetylcholine in the dog ileum. *J Autonomic Nerv Sys* 1994;48:167-174.

Kloog Y, Sokolovsky M. Muscarinic acetylcholine receptor interactions: competition binding studies with agonists and antagonists. *Brain Res* 1977;134:167-172.

Kuemmerle JF, Murthy KS, Makhlof GM. Agonist-activated, ryanodine-sensitive, IP₃-insensitive Ca²⁺ release channels in longitudinal muscle of intestine. *Am J Physiol* 1994;266:C1421-C1431.

Lai M, Thomason DB, Weisbrodt NW. Effect of intestinal bypass on the expression of actin mRNA in ileal smooth muscle. *Am J Physiol* 1990;258:R39-R43.

Lee KY, Kim PS, Chey WY. Effects of a meal and gut hormones on plasma motility and duodenal motility in dog. *Am J Physiol* 1980;238:G280-G283.

Lessard JL. Two monoclonal antibodies to actin: one muscle selective and one generally reactive. *Cell Motil Cytoskel* 1988;10:349-362.

Li YF, Bowers RL, Haley-Russell D., Moody FG, Weisbrodt NW. Actin and myosin isoforms in gallbladder smooth muscle following cholesterol feeding in prairie dogs. *Gastroenterology* 1990;99:1460-1466.

Li YF, Weisbrodt NW, Moody FG, Coelho JU, Gouma DJ. Calcium-induced contraction and contractile protein content of gallbladder smooth muscle after high-cholesterol feeding of prairie dogs. *Gastroenterology* 1987;92:746-750.

Lompre A-M, Schwartz K, d'Albis A, Lacombe G, Van Thiem N, Swynghedauw B. Myosin isoenzyme redistribution in chronic heart overload. *Nature* 1979;282:105-107.

Longtine JA, Pinkus GS, Fujiwara K, Corson JN. Immunohistochemical localization of smooth muscle myosin in normal human tissues. *J Histochem Cytochem* 1985;33:179-184.

Loran MR, Althausen TL. Hypertrophy and changes in cholinesterase activities of the intestine, erythrocytes and plasma after "partial" resection of the small intestine of the rat. *Am J Physiol* 1958;193:516-520.

Lowry OH, Rosebrough NJ, Farr AL, Randall RJ. Protein measurement with Folin phenol reagent. *J Biol Chem* 1951;193:265-275.

- Marzio L, Blennerhassett P, Chiverton S, Vermillion DL, Langer J, Collins SM. Altered smooth muscle function in worm-free gut regions of *Trichinella*-infected rats. *Am J Physiol* 1990;259:G306-G313.
- McHugh KM, Crawford K, Lessard JL. A comprehensive analysis of the developmental and tissue-specific expression of the isoactin multigene family in the rat. *Dev Biol* 1991;148:442-458.
- Meddings JB, Scott RB, Fick GH. Analysis and comparison of sigmoidal curves: application to dose-response data. *Am J Physiol* 1989;257:G982-G989.
- Mendenhall W. Introduction to linear models and the design and analysis of experiments. Belmont, CA: Wadsworth, 1968.
- Mercadier J-J, Lompre A-M, Wisnewsky C, Samuel JL, Bercovici J, Swynghedauw B, Schwartz K. Myosin isoenzymic changes in several models of rat cardiac hypertrophy. *Circ Res* 1981;49:525-532.
- Minocha A, Galligan JJ. Erythromycin inhibits contraction of nerve-muscle preparations of the guinea pig small intestine. *J Pharmacol Exp Ther* 1991;257:1248-1252.
- Mukhopadhyay AK, Thor PJ, Copeland EM, Johnson LR, Weisbrodt NW. Effect of cholecystokinin on myoelectric activity of small bowel of the dog. *Am J Physiol* 1977;232:E44-E47.
- Murthy KS, Grider JR, Makhlof GM. Receptor-coupled G proteins mediate contraction and Ca^{2+} mobilization in isolated intestinal muscle cells. *J Pharmacol Exp Ther* 1992;260:90-97.
- Nemeth PR, Kwee DJ, Weisbrodt NW. Adaptation of intestinal muscle in continuity after jejunoileal bypass in the rat. *Am J Physiol* 1981;241:G259-G263.
- Nemeth PR, Kwee DJ, Weisbrodt NW. Adaptation of intestinal muscle in bypassed loops after jejunoileal bypass in rat. *Am J Physiol* 1983;244:G599-G603.
- Nightingale JMD, Lennard-Jones JE. The short bowel syndrome: what's new and old? *Dig Dis* 1993;11:12-31.
- Nygaard K. Resection of the small intestine in rats. I. Nutritional status and adaptation of fat and protein absorption. *Acta Chir Scand* 1966a;132:731-742.

Nygaard K. Resection of the small intestine in rats. II. Absorption of vitamin B₁₂, with special regard to adaptation of absorption. Acta Chir Scand 1966b;132:743-750.

Nygaard K. Resection of the small intestine in rats. III. Morphological changes in the intestinal tract. Acta Chir Scand 1967a;133:233-248.

Nygaard K. Resection of the small intestine in rats. IV. Adaptation of gastrointestinal motility. Acta Chir Scand 1967b;133:407-416.

Oigaard A, Dorph S. The relative significance of electrical spike potentials and intraluminal pressure waves as quantitative indicators of motility. Am J Dig Dis 1974;19:797-803.

Owens GK, Schwartz SM. Vascular smooth muscle cell hypertrophy and hyperploidy in the Goldblatt hypertensive rat. Circ Res 1983;53:491-501.

Palmer JM, Weisbrodt NM, Castro GA. *Trichinella spiralis*: intestinal myoelectrical activity during enteric infusion in the rat. Exp Parasitol 1984;57:132-141.

Pascaud X, Ferre JP, Genton M, Roger A, Ruckebusch M, Bueno L. Intestinal motility response to insulin and glucagon in streptozotocin diabetic rats. Can J Physiol Pharmacol 1982;60:960-967.

Porus RL. Epithelial hyperplasia following massive small bowel resection in man. Gastroenterology 1965;48:753-759.

Prestwich SA, Bolton TB. G-protein involvement in muscarinic receptor-stimulation of inositol phosphates in longitudinal smooth muscle from the small intestine of the guinea-pig. Br J Pharmacol 1995;114:119-126.

Quigley EMM, Thompson JS. The motor response to intestinal resection: motor activity in the canine small intestine following distal resection. Gastroenterology 1993;105:791-798.

Read NW. Speculations on the role of motility in the pathogenesis and treatment of diarrhoea. Scand J Gastroenterol Suppl 1983;84:45-63.

Read NW. Diarrhée Motrice. Clinic in Gastroenterology 1986;15:657-686.

Rembold CM. Regulation of contraction and relaxation in arterial smooth muscle. Hypertension 1992;20:129-137.

- Rimele TJ, Rogers WA, Gaginella TS. Characterization of muscarinic cholinergic receptors in the lower esophageal sphincter of the cat: binding of [³H]Quinuclidinylbenzilate. *Gastroenterology* 1979;77:1225-1234.
- Rovner AS, Thompson MM, Murphy RA. Two different heavy chains are found in smooth muscle myosin. *Am J Physiol* 1986;250:C861-C870.
- Sarna SK. Gastrointestinal longitudinal muscle contractions. *Am J Physiol* 1993;265:G156-G164.
- Sato K, Sanders KM, Gerthoffer WT, Publicover NG. Sources of calcium utilized in cholinergic responses in canine colonic smooth muscle. *Am J Physiol* 1994;267:C1666-C1673.
- Sawtell NM, Lessard JL. Cellular distribution of smooth muscle actins during mammalian embryogenesis: expression of the α -vascular but not the γ -enteric isoform in differentiating striated myocytes. *J Cell Biol* 1989;109:2929-2937.
- Schiaffino S, Samuel JL, Sassoon D, Lompre A-M, Garner I, Marotte F, Buckingham M, Rappaport L, Schwartz K. Nonsynchronous accumulation of α -skeletal actin and β -myosin heavy chain mRNAs during early stages of pressure-overload-induced cardiac hypertrophy demonstrated by in situ hybridization. *Circ Res* 1989;64:937-948.
- Schmid P, Schmid C, Brodie D. The determination of total deoxyribose of deoxyribonucleic acid. *J Biol Chem* 1963;238:1068-1072.
- Schneider MD, Roberts R, Parker TG. Modulation of cardiac genes by mechanical stress. The oncogene signalling hypothesis. *Mol Biol Med* 1991;8:167-183.
- Schulzke J-D, Fromm M, Bentzel CJ, Zeitz M, Menge H, Riecken E-O. Ion transport in the experimental short bowel syndrome of the rat. *Gastroenterology* 1992;102:497-504.
- Schwartz K, Lecarpentier Y, Martin JL, Lompre A-M, Mercadier J-J, Swynghedauw B. Myosin isoenzymic distribution correlates with speed of myocardial contraction. *J Mol Cell Cardiol* 1981;13:1071-1075.
- Scott RB, Gall DG, Diamant SC. Intestinal motility during acute *Yersinia enterocolitica* enteritis in rabbits. *Can J Physiol Pharmacol* 1989;67:553-560.
- Scott RB, Tan DTM. Differences in longitudinal smooth muscle response along the length of the rabbit small intestine. *J Gastrointest Mot* 1992;4:253-259.

Skalli O, Ropraz P, Trzeciak A, Benzonana G, Gillesen D, Gabbiani G. A monoclonal antibody against α -smooth muscle actin: a new probe for smooth muscle differentiation. *J Cell Biol* 1986;103:2787-2796.

Spiller RC, Trotman IF, Higgins BE, Ghatei M, Grimble GK, Lee YC, Bloom SR, Misiewicz JJ, Silk DB. The ileal brake-inhibition of jejunal motility after ileal fat perfusion in man. *Gut* 1984;25:365-374.

Szurszewski JH. A migrating electric complex of the canine small intestine. *Am J Physiol* 1969;217:1757-1763.

Tepperman J, Brobeck JR, Long CNH. Effects of hypothalamic hyperphagia and of alteration in feeding habits on metabolism of albino rats. *Yale J Biol Med* 1942;15:855-874.

Thompson JS. Management of the short bowel syndrome. *Gastroenterology Clinics of North America* 1994;23:403-420

Thompson JS, Pinch LW, Murray N, Vanderhoof JA, Schultz LR. Experience with intestinal lengthening for the short-bowel syndrome. *J Pediatr Surg* 1991;25:721-724.

Thompson JS, Quigley EMM, Nguyen BL, Meyer S. Intestinal muscle response to intestinal resection and restorative procedures. *Transplant Proc* 1994;26:1453-1454.

Touloukian RJ, Walker-Smith GJ. Normal intestinal length in preterm infants. *J Pediatr Surg* 1983;18:720-723.

Trendelenburg P. Physiologische und pharmackologische Versuche uber die Duundarm Perisaltick. *Naunyn Schmiedeberg's Arch Exp Pathol Pharmackol* 1917;81:55-129.

Van Der Heijden FL, James J. Polyploidy in the human myometrium. *Z. Mikrosk. Anat. Forsch. Leipzig* 1975;89:18-26.

Vandekerckhove N, Weber K. At least six different actins are expressed in a higher mammal: an analysis based on the amino acid sequence of the amino-terminal tryptic peptide. *J Mol Biol* 1978;126:783-802.

Vandekerckhove N, Weber K. Actin typing on total cellular extracts. A highly sensitive protein-chemical procedure able to distinguish different actins. *Eur J Biochem* 1981;113:595-603.

Vanderhoof JA, Langnas AN, Pinch LW, Thompson JS, Kaufman SS. Short bowel syndrome. *J Pediatr Gastroenterol Nutr* 1992;14:359-370.

Vermillion DL, Collins SM. Increased responsiveness of jejunal longitudinal muscle in *Trichinella*-infected rats. *Am J Physiol* 1988;254:G124-G129.

Vermillion DL, Huizinga JD, Riddell RH, Collins SM. Altered small intestinal smooth muscle function in Crohn's disease. *Gastroenterology* 1993;104:1692-1699.

Villarreal FJ, Dillman WH. Cardiac hypertrophy-induced changes in mRNA levels for TGF- β_1 , fibronectin, and collagen. *Am J Physiol* 1992;262:H1861-H1866.

Walsh MP. Calcium-dependent mechanisms of regulation of smooth muscle contraction. *Biochem Cell Biol* 1991;69:771-800.

Walsh MP. Regulation of vascular smooth muscle tone. *Can J Physiol Pharmacol* 1994;72:919-936.

Weems WA. Intestinal fluid flow: Its production and control. In: *Physiology of the Gastrointestinal Tract*, Second Edition, Ed. Johnson LR, Raven Press, New York, 1987; pp371-393.

Weinstein LD, Shoemaker CP, Hersh T, Wright HK. Enhanced intestinal absorption after small bowel resection in man. *Arch Surg* 1969;99:560-562.

Weisbrodt NW, Copeland EM, Thor PJ, Dudrick SJ. The myoelectric activity of the small intestine of the dog during total parental nutrition. *Proc Soc Exp Biol Med* 1976; 153:121-124.

Weisbrodt NW, Nemeth PR, Bowers RI, Weems WA. Functional and structural changes in intestinal smooth muscle after jejunoileal bypass in rats. *Gastroenterology* 1985;88:958-963.

Weser E, Hernandez MH. Studies of small bowel adaptation after intestinal resection in the rat. *Gastroenterology* 1971;60:69-75.

Williamson RCN. Intestinal adaptation: structural, functional and cytokinetic changes. *N Engl J Med* 1978;298:1393-1402.

Williamson RCN. Adaptive intestinal hyperplasia. In: *Function and dysfunction of the small intestine*. Eds. Batt R, Lawrence TLS. Liverpool: Liverpool University Press, 1984;55-76.

Wilmore DW, Dudrick SJ, Daly JM, Vars H. The role of nutrition in the adaptation of the small intestine after massive resection. *Surg Gynecol Obstet* 1971;132:673-680.

Wilmore DW. Factors correlating with a successful outcome following extensive intestinal resection in newborn infants. *J Pediatr* 1972;80:88-95.

Wingate DL. Intrinsic and extrinsic neural control. In: *An Illustrated Guide to Gastrointestinal Motility*, Second Edition, Eds. Kumar D, Wingate D, Churchill Livingstone, New York 1993; pp64-77.

Wingate DL, Pearce EA, Hutton M, Dand A, Thompson HH, Wunsch E. Quantitative comparison of the effects of cholecystokinin, secretin and pentagastrin on gastrointestinal myoelectric activity in the conscious fasted dog. *Gut* 1978;19:593-601.

Wittman T, Crenner F, Grenier JF. Cyclic motor activity and trophicity after jejunal resection and bypass in rats. *Dig Dis Sci* 1986;31:65-72.

Wittman T, Crenner F, Koenig M, Grenier JF. Adaptive changes in postprandial motility after intestinal resection and bypass. Electromyographic study in rats. *Dig Dis Sci* 1988;33:1370-1376.

Wood JD. Physiology of the enteric nervous system. In: *Physiology of the Gastrointestinal Tract*, Third Edition, Ed. Johnson LR, Raven Press, New York 1994;pp423-482.

Xu H, Gintzler AR. Opioid enhancement of evoked [Met5]enkephalin release requires activation of cholinergic receptors: possible involvement of intracellular calcium. *Proc Natl Acad Sci USA* 1992;89:1978-1982.

Yamamura HI, Snyder SH. Muscarinic cholinergic receptor binding in the longitudinal muscle of the guinea pig ileum with [³H]-quinuclidinyl benzilate. *Mol Pharmacol* 1974;10:861-867.

CHAPTER TWELVE

APPENDICES

APPENDIX I.

The effect of time on the phasic frequency of bethanechol-stimulated longitudinal muscle from the sham-operated group.

log [B], M	Day 10	Day 20	Day 30	Day 40
-6	27.8 \pm 1.5	25.6 \pm 1.0	25.0 \pm 1.2	27.4 \pm 1.8
-4	25.0 \pm 2.0	24.9 \pm 4.0	22.3 \pm 1.2	28.5 \pm 6.6

The table shows the bethanechol-stimulated frequency (cycles min⁻¹) of phasic contractile activity of jejunal longitudinal muscle obtained from sham-operated rats on post-surgical days 10, 20, 30 and 40. Within the treatment group, there was no significant effect of the length of time after surgery with respect to phasic frequency and, therefore, data were pooled. n=7 per time point per concentration of bethanechol, [B].

APPENDIX II.

The effect of time on the phasic frequency of bethanechol-stimulated longitudinal muscle from the resected group.

log [B], M	Day 10	Day 20	Day 30	Day 40
-6	31.3 \pm 3.6	29.3 \pm 2.6	35.0 \pm 3.6	34.1 \pm 2.7
-4	29.2 \pm 3.2	29.3 \pm 2.8	26.2 \pm 2.5	32.0 \pm 4.2

The table shows the bethanechol-stimulated frequency (cycles min⁻¹) of phasic contractile activity of jejunal longitudinal muscle obtained from resected rats on post-surgical days 10, 20, 30 and 40. Within the treatment group, there was no significant effect of the length of time after surgery with respect to phasic frequency and, therefore, data were pooled. n=7 per time point per concentration of bethanechol, [B].

APPENDIX III.

The effect of time on the phasic amplitude of bethanechol-stimulated longitudinal muscle from the sham-operated group.

log [B], M	Day 10	Day 20	Day 30	Day 40
-6	7.3 \pm 3.1	3.5 \pm 1.2	2.9 \pm 0.7	2.7 \pm 0.5
-4	4.5 \pm 1.9	4.8 \pm 1.7	1.7 \pm 0.4	3.5 \pm 0.5

The table shows the bethanechol-stimulated amplitude (mN mm⁻²) of phasic contractile activity of jejunal longitudinal muscle obtained from sham-operated rats on post-surgical days 10, 20, 30 and 40. Within the treatment group, there was no significant effect of the length of time after surgery with respect to phasic amplitude and, therefore, data were pooled. n=7 per time point per concentration of bethanechol, [B].

APPENDIX IV.

The effect of time on the phasic amplitude of bethanechol-stimulated longitudinal muscle from the resected group.

log [B], M	Day 10	Day 20	Day 30	Day 40
-6	7.5 ± 2.0	9.1 ± 1.9*	6.7 ± 1.2	3.3 ± 0.6*
-4	5.8 ± 1.8	5.5 ± 0.9	3.0 ± 1.0	4.5 ± 1.5

The table shows the bethanechol-stimulated amplitude (mN mm⁻²) of phasic contractile activity of jejunal longitudinal muscle obtained from resected rats on post-surgical days 10, 20, 30 and 40. Within the treatment group, there was a significant difference between the responses of day 20 and day 40, at the 10⁻⁶ M concentration of bethanechol. To assess the physiological relevance of this difference, the data were also compared to the unoperated control group (day 0), and revealed no significant differences among the five time points (unoperated control, day 0; resected, days 10-20; ANOVA, Tukey's post-hoc test). All other comparisons at both bethanechol concentrations revealed no significant differences in the amplitude response over time. For these reasons, data were pooled. n=7 per time point per concentration of bethanechol, [B]. ★, p<0.05.

APPENDIX V.

The effect of time on the tonic stress response of bethanechol-stimulated circular muscle from the sham-operated group.

log [B], M	Day 10	Day 20	Day 30	Day 40
-9	0.6 ± 0.6	0 ± 0	-0.2 ± 0.2	-0.3 ± 0.4
-8	0.7 ± 0.7	0.4 ± 0.4	0.2 ± 0.2	0.8 ± 0.4
-7	0.7 ± 0.4	0.5 ± 0.2	0.7 ± 0.5	0.4 ± 0.5
-6	2.0 ± 0.7	1.7 ± 0.8	1.5 ± 0.6	2.3 ± 0.8
-5.3	8.2 ± 2.6	4.9 ± 0.8	8.3 ± 2.3	8.5 ± 2.5
-5	9.8 ± 2.5	8.9 ± 3.3	12.4 ± 4.7	9.4 ± 3.0
-4.3	25.1 ± 6.3	26.5 ± 5.1	21.2 ± 5.6	16.3 ± 3.9
-4	24.3 ± 6.8	25.3 ± 6.0	18.0 ± 5.2	21.5 ± 6.0

The table shows the bethanechol-stimulated tonic stress response (mN mm^{-2}) of jejunal circular muscle obtained from sham-operated rats on post-surgical days 10, 20, 30 and 40. Within the treatment group, there was no significant effect of the length of time after surgery with respect to tonic stress and, therefore, data were pooled. $n=6$ per time point per concentration of bethanechol, [B].

APPENDIX VI.

The effect of time on the tonic stress response of bethanechol-stimulated circular muscle from the resected group.

log [B], M	Day 10	Day 20	Day 30	Day 40
-9	0.4 ± 0.5	0.2 ± 0.2	0 ± 0	-0.1 ± 0.1
-8	0.2 ± 0.2	0.9 ± 0.6	0.3 ± 0.3	0.1 ± 0.1
-7	0.5 ± 0.5	0.1 ± 0.1	1.5 ± 1.0	2.5 ± 0.9
-6	3.0 ± 1.2	1.8 ± 0.6	12.1 ± 2.0	6.7 ± 1.7
-5.3	7.0 ± 1.8	8.8 ± 2.9	15.6 ± 4.6	7.5 ± 1.1
-5	5.7 ± 1.3	10.8 ± 3.1	16.0 ± 2.7	15.9 ± 4.0
-4.3	14.1 ± 3.2	15.6 ± 4.3	10.8 ± 1.1	8.45 ± 1.7
-4	12.3 ± 2.7	15.0 ± 3.1	18.0 ± 5.2	21.5 ± 6.0

The table shows the bethanechol-stimulated tonic stress response (mN mm^{-2}) of jejunal circular muscle obtained from resected rats on post-surgical days 10, 20, 30 and 40. Within the treatment group, there was no significant effect of the length of time after surgery with respect to tonic stress and, therefore, data were pooled. $n=6$ per time point per concentration of bethanechol, [B].

APPENDIX VII.

The effect of time on the phasic frequency of bethanechol-stimulated circular muscle from the sham-operated group.

log [B], M	Day 10	Day 20	Day 30	Day 40
-9	27.8 \pm 2.6	31.0 \pm 0.9	30.3 \pm 0.4	30.5 \pm 0.7
-8	29.7 \pm 1.8	32.2 \pm 1.0	31.5 \pm 0.7	29.7 \pm 1.0
-7	30.2 \pm 2.1	30.8 \pm 0.3	32.0 \pm 0.7	29.5 \pm 1.0
-6	28.5 \pm 2.1	30.3 \pm 0.6	30.5 \pm 0.6	30.0 \pm 0.6
-5.3	28.7 \pm 1.7	29.5 \pm 0.6	31.2 \pm 0.4	28.5 \pm 0.8
-5	29.3 \pm 1.4	31.2 \pm 1.4	30.3 \pm 2.8	28.2 \pm 2.7
-4.3	35.7 \pm 3.2	36.25 \pm 4.3	32.3 \pm 3.8	27.8 \pm 3.0
-4	31.0 \pm 3.6	37.5 \pm 4.9	26.8 \pm 5.4	23.7 \pm 4.7

The table shows the bethanechol-stimulated frequency (cycles min⁻¹) of phasic contractile activity of jejunal circular muscle obtained from sham-operated rats on post-surgical days 10, 20, 30 and 40. Within the treatment group, there was no significant effect of the length of time after surgery with respect to phasic frequency and, therefore, data were pooled. n=6 per time point per concentration of bethanechol, [B].

APPENDIX VIII.

The effect of time on the phasic frequency of bethanechol-stimulated circular muscle from the resected group.

log [B], M	Day 10	Day 20	Day 30	Day 40
-9	28.2 \pm 1.4	29.2 \pm 0.6	26.3 \pm 1.4	25.7 \pm 1.4
-8	29.7 \pm 0.6	27.3 \pm 0.8	26.7 \pm 0.8	28.5 \pm 0.7
-7	29.3 \pm 1.0	27.0 \pm 0.9	27.5 \pm 1.2	28.5 \pm 0.6
-6	28.8 \pm 1.0	27.5 \pm 1.2	29.2 \pm 0.5	28.0 \pm 0.8
-5.3	26.8 \pm 0.9	28.7 \pm 2.4	28.0 \pm 1.2	25.8 \pm 0.8
-5	26.0 \pm 0.8	26.5 \pm 0.6	26.0 \pm 1.6	23.7 \pm 0.8
-4.3	25.5 \pm 1.8	25.5 \pm 1.0	22.5 \pm 2.3	22.0 \pm 0.9
-4	25.3 \pm 1.4	25.0 \pm 1.4	21.3 \pm 3.6	23.2 \pm 1.4

The table shows the bethanechol-stimulated frequency (cycles min⁻¹) of phasic contractile activity of jejunal circular muscle obtained from resected rats on post-surgical days 10, 20, 30 and 40. Within the treatment group, there was no significant effect of the length of time after surgery with respect to phasic frequency and, therefore, data were pooled. n=6 per time point per concentration of bethanechol, [B].

APPENDIX IX

The effect of time on the phasic amplitude of bethanechol-stimulated circular muscle from the sham-operated group.

log [B], M	Day 10	Day 20	Day 30	Day 40
-9	8.9 ± 5.5	3.4 ± 0.7	4.1 ± 1.7	2.8 ± 0.8
-8	8.5 ± 4.5	3.1 ± 0.8	2.5 ± 0.8	1.8 ± 0.1
-7	6.5 ± 2.8	2.3 ± 0.5	2.9 ± 1.3	2.0 ± 0.3
-6	8.5 ± 2.9	3.6 ± 1.1	5.5 ± 2.8	2.9 ± 0.6
-5.3	14.0 ± 5.3	9.4 ± 2.0	12.5 ± 5.0	7.1 ± 1.8
-5	22.9 ± 6.8	16.7 ± 1.2	18.6 ± 5.1	17.5 ± 4.6
-4.3	34.6 ± 6.2	30.0 ± 4.1	28.8 ± 3.4	35.9 ± 2.4
-4	46.5 ± 8.5	37.1 ± 7.2	40.4 ± 3.7	47.5 ± 3.0

The table shows the bethanechol-stimulated amplitude (mN mm⁻²) of phasic contractile activity of jejunal circular muscle obtained from sham-operated rats on post-surgical days 10, 20, 30 and 40. Within the treatment group, there was no significant effect of the length of time after surgery with respect to phasic amplitude and, therefore, data were pooled. n=6 per time point per concentration of bethanechol, [B].

APPENDIX X

The effect of time on the phasic amplitude of bethanechol-stimulated circular muscle from the resected group.

log [B], M	Day 10	Day 20	Day 30	Day 40
-9	8.6 ± 3.2	6.2 ± 1.4	7.5 ± 1.6	10.2 ± 3.2
-8	8.0 ± 3.4	6.7 ± 1.3	5.9 ± 1.6	9.3 ± 2.8
-7	8.5 ± 2.6	6.4 ± 1.7	4.0 ± 0.9	8.7 ± 2.2
-6	10.9 ± 3.1	6.9 ± 1.2	4.5 ± 1.3	7.9 ± 2.6
-5.3	14.0 ± 2.8	11.7 ± 2.9	10.2 ± 3.7	8.5 ± 1.7
-5	14.4 ± 2.4	11.7 ± 2.8	13.1 ± 3.2	12.1 ± 2.5
-4.3	14.1 ± 2.3	10.6 ± 2.3	15.4 ± 5.3	10.7 ± 1.9
-4	19.3 ± 3.2	13.8 ± 3.5	21.8 ± 6.5	15.9 ± 3.5

The table shows the bethanechol-stimulated amplitude (mN mm^{-2}) of phasic contractile activity of jejunal circular muscle obtained from resected rats on post-surgical days 10, 20, 30 and 40. Within the treatment group, there was no significant effect of the length of time after surgery with respect to phasic amplitude and, therefore, data were pooled. $n=6$ per time point per concentration of bethanechol, [B].

APPENDIX XI

Manuscripts

In addition to this doctoral dissertation, the investigations described herein have culminated in the authorship of five manuscripts: published, in press or in preparation.

Scott RB, Sheehan A, Chin BC, Tan DTM. Hyperplasia of the muscularis propria in response to massive intestinal resection in rat. *J Pediatr Gastroenterol Nutr* 1995;21:399-409.

Chin BC, Tan DTM, Scott RB. Massive intestinal resection depresses circular smooth muscle contractility in the rat. *Can J Physiol Pharmacol* 1995;73:1443-1450.

Chin BC, Tan DTM, Scott RB. Contractility of longitudinal smooth muscle after massive intestinal resection in rat. *J Clin Invest Med*. In press.

Chin BC, Tan DTM, Scott RB. Altered intestinal smooth muscle contractility after *Yersinia enterocolitica* enteritis in rabbit is not due to changes in contractile protein content or calcium source. In preparation.

Chin BC, Tan DTM, Scott RB. Depressed smooth muscle contractility after massive intestinal resection in the rat is not a function of muscarinic receptor status or changes in the contractile source of calcium. In preparation.